

DOCKETED	
Docket Number:	21-BSTD-01
Project Title:	2022 Energy Code Update Rulemaking
TN #:	238048
Document Title:	Analysis of Duct Insulation Requirements for Ducts in Conditioned and Indirectly Conditioned Spaces
Description:	This report describes a study of issues associated with running uninsulated ductwork through conditioned spaces in houses.
Filer:	Peter Strait
Organization:	California Energy Commission
Submitter Role:	Commission Staff
Submission Date:	5/28/2021 3:08:31 PM
Docketed Date:	5/28/2021

**Analysis of Duct Insulation Requirements for Ducts in Conditioned
and Indirectly Conditioned Spaces**

March 5, 2021

Mark Modera
Antash Najib
Curtis Harington

Western Cooling Efficiency Center
University of California – Davis

Submitted to:

Kelly Cunningham
Pacific Gas and Electric Company

Executive Summary

This report describes a study of issues associated with running uninsulated ductwork through conditioned spaces in houses. The primary focus of the analysis is uninsulated ducts that pass through vertical stud cavities, however other duct installations are also investigated. The two key issues are: a) the potential for condensation on cool duct surfaces, and b) non-uniformity in grille delivery temperatures due to thermal conduction losses through the duct walls. The two objectives of this report are: 1) to investigate both of these effects, and 2) to provide some guidance to the California Energy Commission on how to address the insulation level of ductwork running through conditioned and indirectly conditioned spaces. The research performed included: a) modelling of indoor dew points with CBECC-RES simulations, including comparison with existing measurements, b) comparison of indoor versus outdoor dew point temperatures, c) modelling of condensation/evaporation in building cavities with uninsulated ducts, d) modelling of condensation/evaporation for insulated and uninsulated ducts located in rooms and in cavities for different surface emissivities, and e) modelling of thermal losses from uninsulated ducts.

Based on the analyses performed the authors conclude that condensation of water on duct surfaces is not likely to be a major issue for uninsulated ducts located in wall cavities in California homes. The worst-case maximum condensation of water on a duct in a relatively leaky vertical stud cavity (5/8th inch diameter holes top and bottom) was 3.4 cubic centimeters of water in Burbank, California for a duct surface emissivity of 0.1. This condensation corresponds to 0.0076 lbs of water (0.7 teaspoons) in a vertical stud cavity, or a 0.06% change in the moisture content of the wood in that stud cavity, whose moisture content typically ranges between 7% and 15%. Putting this into perspective, the maximum thickness of condensation on the duct surface is 0.2 thousandths of an inch, and all condensation evaporates within 5 hours. Another way to put this amount of condensation in perspective is to compare it to condensation on windows in the winter. Yet another relevant comparison is with the interior surfaces of uninsulated exterior walls in the winter, which would also be exposed to warm humid indoor air. These surfaces are likely to be considerably colder than the 55°F temperatures in the ducts, and therefore experience as much or more condensation.

Turning to our sensitivity analysis, simply using ducts with a standard emissivity of 0.9 reduces this maximum condensation by 30%. In addition, this condensation is reduced by roughly another factor of two for horizontal cavities (due to less height for driving room air through the cavity). Finally, since the moisture available for condensation comes from air being brought into the cavity from the room, the total condensation is controlled by the flowrate of room air into the cavity, which means that there will be less condensation in tighter cavities. In the limit, for an airtight cavity the maximum 0.0076 lbs of water condensation is reduced by roughly 90%. One recommendation might be to forbid low-emissivity surfaces on ducts in cavities.

Relative to the condensation issue, the impact of locating the ducts in the occupied space rather than in cavities was also examined. The simulations indicate that the quantity of water condensed on uninsulated in-space ducts with low emissivity surfaces ($e=0.1$) was five times higher than that for cavity ducts. For ducts with standard emissivity surfaces ($e=0.9$) the condensation was only twice as high in-space, suggesting that emissivity has a larger impact on in-space ducts. This level of condensation might or might not be acceptable, as it might be visible and/or dripping might occur in wetter climates (e.g. Burbank). That said, simply avoiding low-emissivity surfaces eliminated the

possibility of condensation in Climate Zone 13 (Fresno). Going to R-3.1 insulation for low-emissivity ducts ($\epsilon=0.1$), or going to R-0.8 insulation for normal-emissivity ducts ($\epsilon=0.9$) in the occupied space avoids the possibility of condensation in any climate zone (including Burbank), due to duct surfaces never being cooler than 70°F.

Turning to the thermal performance of uninsulated ducts in conditioned spaces, it appears that they exhibit thermal-distribution inefficiencies similar to insulated ducts running through an attic, although the performance of uninsulated interior ducts is somewhat worse at full cooling capacity. In both cases, slowing down the fan and reducing cooling capacity result in significant degradation of distribution performance. It should be noted however that the losses for the interior ducts wind up in the conditioned space, although not necessarily where intended.

Keywords

Indoor dew point temperature, Condensation, Duct insulation, Heat and mass transfer.

1. Introduction

Existing requirements for duct insulation are typically based upon the conditions in the spaces surrounding the ductwork, focusing principally on energy-use concerns (see Table 3 below from ASHRAE 2017 Handbook of Fundamentals).

Insulation for Mechanical Systems

23.3

Table 3 Minimum Duct Insulation R-Value,^a Combined Heating and Cooling Supply Ducts and Return Ducts

Climate Zone	Duct Location						Buried
	Exterior	Ventilated Attic	Unvented Attic Above Insulated Ceiling	Unvented Attic with Roof Insulation ^a	Unconditioned Space ^b	Indirectly Conditioned Space ^c	
Supply Ducts							
1	R-4	R-6	R-8	R-3.5	R-3.5	none	R-3.5
2	R-6	R-6	R-6	R-3.5	R-3.5	none	R-3.5
3	R-6	R-6	R-6	R-3.5	R-3.5	none	R-3.5
4	R-6	R-6	R-6	R-3.5	R-3.5	none	R-3.5
5	R-6	R-6	R-6	R-1.9	R-3.5	none	R-3.5
6	R-6	R-6	R-6	R-1.9	R-3.5	none	R-3.5
7	R-6	R-6	R-6	R-1.9	R-3.5	none	R-3.5
8	R-8	R-8	R-8	R-1.9	R-6	none	R-6
Return Ducts							
1 to 8	R-3.5	R-3.5	R-3.5	none	none	none	none

^aInsulation R-values, measured in h·ft²·°F/Btu, are for the insulation as installed and do not include film resistance. The required minimum thicknesses do not consider water vapor transmission and possible surface condensation. Where exterior walls are used as plenum walls, wall insulation must be as required by the most restrictive condition of Section 6.4.4.2 or Section 5 of 90.1-2010. Insulation resistance measured on a horizontal plane in accordance with ASTM C518 at a mean temperature of 75°F at the installed thickness.

^bIncludes crawlspaces, both ventilated and nonventilated.

^cIncludes return air plenums with or without exposed roofs above.

There are two concerns other than energy use that are associated with choosing appropriate minimum duct insulation requirements for ducts located in conditioned and indirectly conditioned spaces. These are:

1. Exterior surfaces of such ducts should not be allowed to experience temperatures lower than the dew point of the surrounding air, which would result in condensation on those surfaces,
2. Duct system design insulation levels should ensure that grille delivery temperatures are uniform, meaning that the temperature of the air leaving a grille should not vary depending upon the distance between the grille and the supply plenum. Supply temperatures at the grilles that are not the same in all rooms may potentially result in unsatisfactory comfort issues.

The two objectives of this report are: 1) to investigate both of these effects, and 2) to provide recommendations to the California Energy Commission on how to address the insulation level of ductwork running through conditioned and indirectly conditioned spaces.

In order to assess the condensation question, simulation results from the California Building Energy Code Compliance-Residential (CBECC-Res) [1] simulation program were used. The CBECC-Res parameters and results are presented in section 2. For all sixteen climate zones, the following parameters were analyzed in detail:

1. Indoor dew point temperatures for a typical house
2. Outdoor dew point temperatures (from weather files)
3. Time duration of the air conditioner providing cooling to the house

The combination of these three parameters are analyzed to identify the hours of the year for which the mass of water condensed on the duct would be expected to be maximum for each climate zone.

To analyze the condensation problem, precise duct location is important. Ducts in the middle of an occupied indoor space are not the same as ducts inside the thermal envelope of the house but separated from occupied space by a wall (e.g. in a soffit or vertical stud cavity). This is because the amount of condensation on a duct is limited by the condition of the local air surrounding the duct.

Although the air in a soffit or cavity starts out at the same condition as the air in the occupied space, the air supply to such spaces is limited, which means that as condensation occurs, the condition of the air in the cavity changes, and becomes limited by the flow rate of additional room air into the cavity. This report analyzes the performance of ducts located in vertical stud cavities, and should not be used to evaluate uninsulated ducts located in the occupied space (although a limited analysis of such ducts is presented below).

A detailed heat and mass transfer model was developed to simulate the condensation-evaporation process in vertical stud cavities containing uninsulated ducts. The model details and results are presented in section 3. The implications of the condensation results are discussed in section 4.

To address the grille-temperature non-uniformity question, a model developed in an earlier CEC project to analyze the performance of next-generation heat pumps (EPRI project with UC Davis responsibility for the duct performance analysis) was utilized. The analysis in this report applies that model to uninsulated and minimally insulated ducts, both for single-capacity and variable capacity equipment. Section 5 presents the modelling of duct thermal losses and delivery effectiveness for different duct insulation levels while the results and implications are discussed in section 6.

Finally, the conclusions are presented in section 7.

2. Indoor and outdoor dew point temperatures

2.1. CBECC-Res simulation

The CBECC-Res energy simulation tool [1] was used to calculate the cooling and heating load of a detached, single-family, two story home for the two locations. The total conditioned area was 251 m² (2700 ft²), not including an attached garage. The house construction was based on the 2013 California Residential Alternative Calculation Method (ACM) [2] reference manual prototype house. Table 1 lists the main characteristics of the home model.

Table 1 – Basic characteristics of the home used for in CBECC-Res.

House Characteristic	Value
General house dimensions	
- Conditioned floor area	251 m ² (2700 ft ²)
- Roof area	135 m ² (1450 ft ²)
- Number of stories	2
- Number of zones	4
- Window-to-Wall Ratio	0.20
Wall Area by Orientation	
- North, East, South and West	62.5 m ² (673 ft ²)
Overall heat transfer coefficient, or U-value	
- Walls	0.37 Wm ⁻² K ⁻¹ (0.065 BTU h ⁻¹ ft ⁻² F ⁻¹)
- Windows	1.82 Wm ⁻² K ⁻¹ (0.32 BTU h ⁻¹ ft ⁻² F ⁻¹)
Exterior shade	None
Foundation type	Slab-on-grade
House Air Flow Parameters	
- Living space	0.5 ACH @ 50Pa (very tight)
- Attic	N/A (Ventilated)
- Ventilation rate	118 CFM (constant)

The model utilized the following assumptions:

1. Hour by hour default internal sensible and latent loads of the house were used.
2. Internal loads were the same for all climate zones. Infiltration load was neglected based upon using a very tight envelope and mechanical ventilation.
3. The number of occupants varied based on the default schedule (time of day, weekend or weekday, day of the year). Occupancy varied between two and six people.
4. Default temperature set-points were used. These set-points determined when the heating and cooling systems cycle on or off.
5. The set-point for heating (winter load) for each hour of the day is as follows:
 - a. From 11 PM to 6 AM: 65°F
 - b. 7 AM: 65°F
 - c. 8 AM to 10 PM: 68°F
6. The set-point for cooling (summer load) for each hour of the day is as follows:
 - a. From 5 PM to 6 AM: 78°F
 - b. From 7 AM to 12 PM: 83°F
 - c. For 1 PM, 2 PM, 3 PM, 4 PM: 82°F, 81°F, 80°F, 79°F respectively.

The next section presents the results of the CBECC-Res simulations for different climate zones.

2.2. Dew point temperature analysis

Based on the CBECC-Res simulation results, the climate zones were divided into the following three categories:

- 1) Climate zones where the house does not need cooling from the air conditioner at any hour of the year (i.e., air conditioning remains off throughout the year). These are Climate Zones 1, 3 and 5.

- 2) Climate zones where the house requires cooling for a less than 100 hours (cumulative) of the year. These are Climate Zones 2, 4, 6 and 7.
- 3) Climate zones where the house requires cooling for more than 100 hours (cumulative) of the year. All other Climate Zones fall under this category.

Measured indoor humidity from a large number of southern California homes in previous report (prepared by Proctor Engineering) was used as a reference. The geographical distribution of the homes represented in that sample was:

1. CZ 6, Los Angeles 68%
2. CZ 13, Fresno 27% (Central Valley)
3. CZ 15, Palm Springs 5% (Imperial Valley)

Out of these three climate zones, CZ 13 does not require as much cooling as CZ 15, yet it still requires considerable cooling, is more representative of the state, and is a reasonable fraction of the field-testing data set. Therefore, CZ 13 was selected as our reference climate. The results for CZ 13 are presented first and are discussed most extensively.

The indoor dew point temperature is the key parameter for condensation. A high indoor dew point also makes it likely that the air in the stud bay cavity has a high dew point. This would lead to condensation when the air conditioner cycles on and cold air starts to flow inside the duct.

If the air conditioner is off and there are internal latent loads in the house, the indoor dew point temperature would be higher than the outdoor dew point temperature. In the subsequent sections, the outdoor air dew point is presented alongside the indoor dew point temperature to understand how much moisture is being added to the indoor air due to latent loads and how much of this moisture is being removed by the air conditioner. It should be noted that the air conditioner cycles on or off based on the dry bulb temperature set-point (not the indoor dew point or wet bulb temperature).

2.2.1. Reference Climate Zone 13 - Fresno

For Climate Zone 13, based on the CBECC-Res simulation results, in a Typical Meteorological Year the air conditioner operates for the first time on May 21 at 6:09 PM. The air conditioner provides cooling for the last time on September 27 at 1:33 AM.

Figure 1 shows the seven-day moving average of the room (or indoor air-conditioned space) dew point temperature over the summer. The seven-day moving average of outdoor air temperature is also shown. Air conditioner operation (on or off) is shown on the secondary axis. The temperatures are plotted against the halfway point of the week. The maximum indoor dew point temperature is 55.24°F and occurs in the week that starts on June 26, 3:30 PM and ends on July 3, 3:30 PM. The halfway point for the week corresponds to June 29, 3:30 PM. There is another peak of 55.11°F (with halfway point on September 21). It should be noted that the air conditioner cycles on and off during this period.

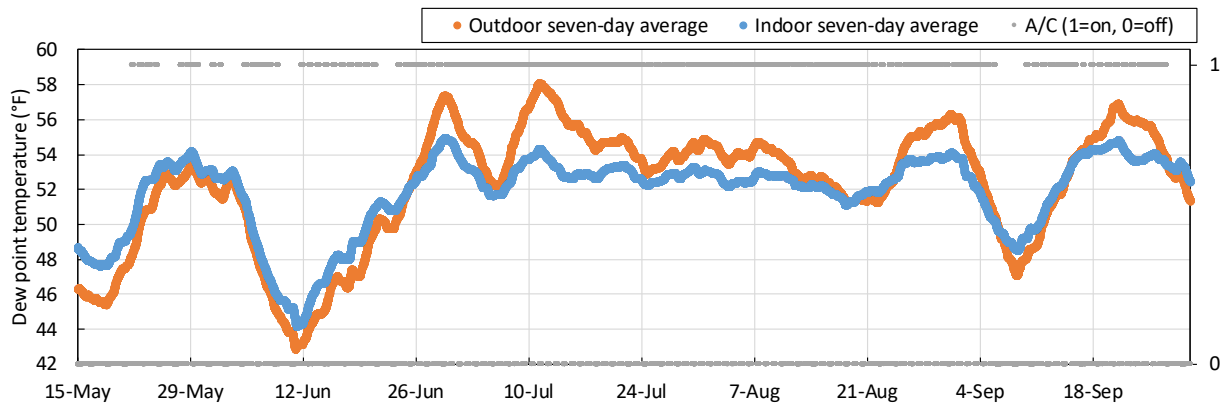


Figure 1: Seven-day moving average indoor (room) and outdoor dew point temperatures for CZ 13 Fresno. Air conditioner operation (on or off) is shown on the secondary axis.

Figure 2 shows the indoor and outdoor dew point temperatures from June 26 to July 3. This period includes the week with the highest seven-day average indoor dew point temperature. Air conditioner operation (on or off) is shown on the secondary axis. It can be seen that as the air conditioner turns on, the indoor dew point temperature falls. Once the air conditioner turns off, the indoor dew point temperature increases rapidly, and in many cases increases above the outdoor dew point temperature. This is caused by moisture generation due to internal latent loads.

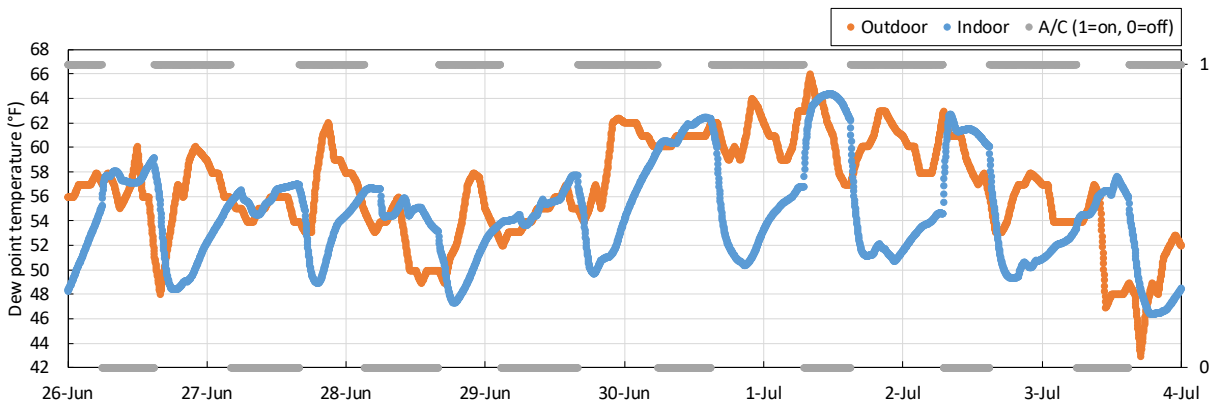


Figure 2: Indoor and outdoor dew point temperatures for CZ 13 Fresno from June 26 to July 4.

Figure 3 through Figure 7 show the distribution of hours in a given month corresponding to dew point temperature intervals of 2.5°F starting from 22.5°F up to 75°F from May to September for climate zone 13. Each range represents temperatures equal to or above the lower value and below the upper value. Both indoor and outdoor temperature distributions are shown, including the number of hours in in each bin for indoor and outdoor dew point temperatures during periods when the air conditioner is on.

For May, the indoor dew point temperature distribution for higher ranges is similar to that for outdoors. However, in the range 47.5°F to 50°F indoors has 60 more hours than outdoors. The result is that the indoor dew point temperature is on average higher than the outdoor dew point temperature. However, when the air conditioner is on the indoor dew point temperature is on average lower than

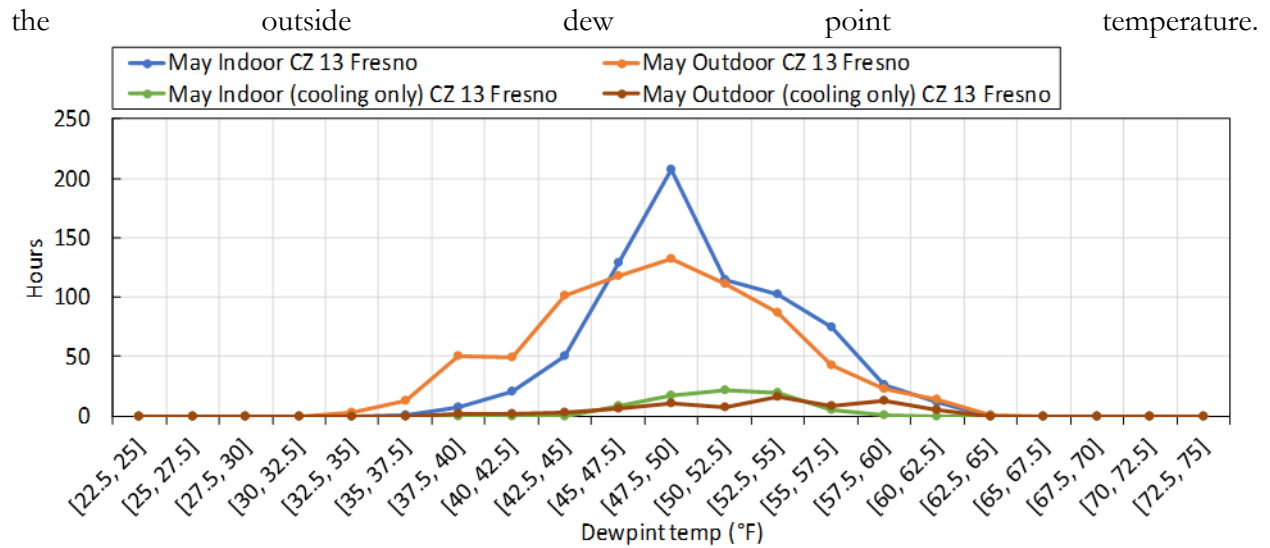


Figure 3: Distribution of hours for indoor and outdoor dew point temperatures for CZ 13 Fresno for May, including hours during periods when air conditioner is on.

For June, the indoor dew point temperature trend is more comparable to the outdoor trend, although the indoor temperature is still more likely to be higher than outdoors. The air conditioner is on for considerably longer periods than May. This is reflected in the number of cooling-only hours. As expected, when the A.C. is on the indoor dew point temperature is generally lower than outdoors.

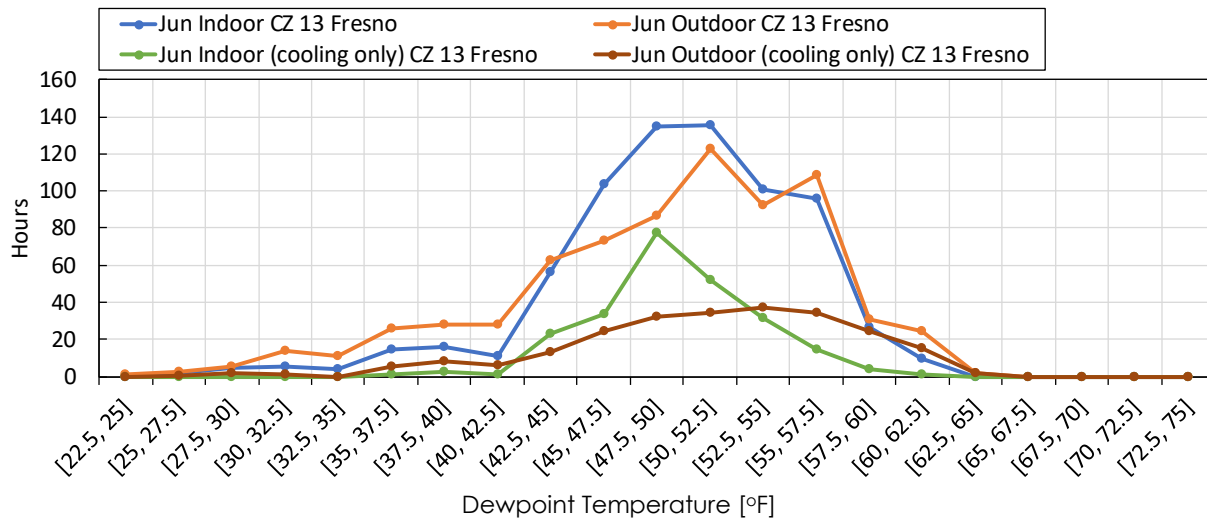


Figure 4: Distribution of hours for indoor and outdoor dew point temperatures for CZ 13 Fresno, for June, including hours during periods when air conditioner is on.

For July, the air conditioner is on for significantly more time. As a result, the indoor dew point temperature is lower than the outdoor dew point. For August, the extensive use of air conditioning causes the indoor dew point distribution to be somewhat bimodal.

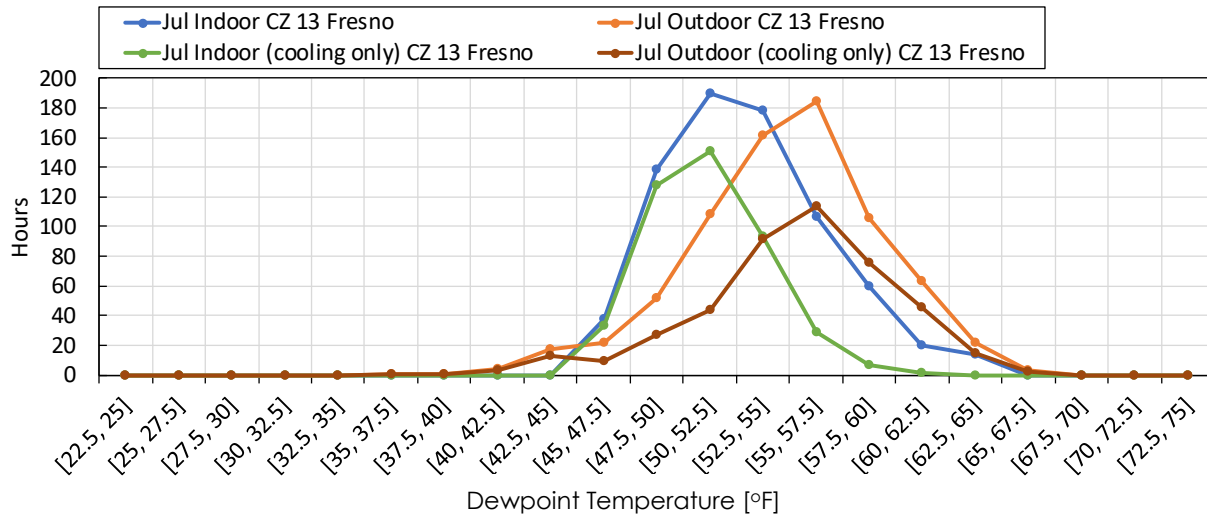


Figure 5: Distribution of hours for indoor and outdoor dew point temperatures for CZ 13 Fresno, for July, including hours during periods when air conditioner is on.

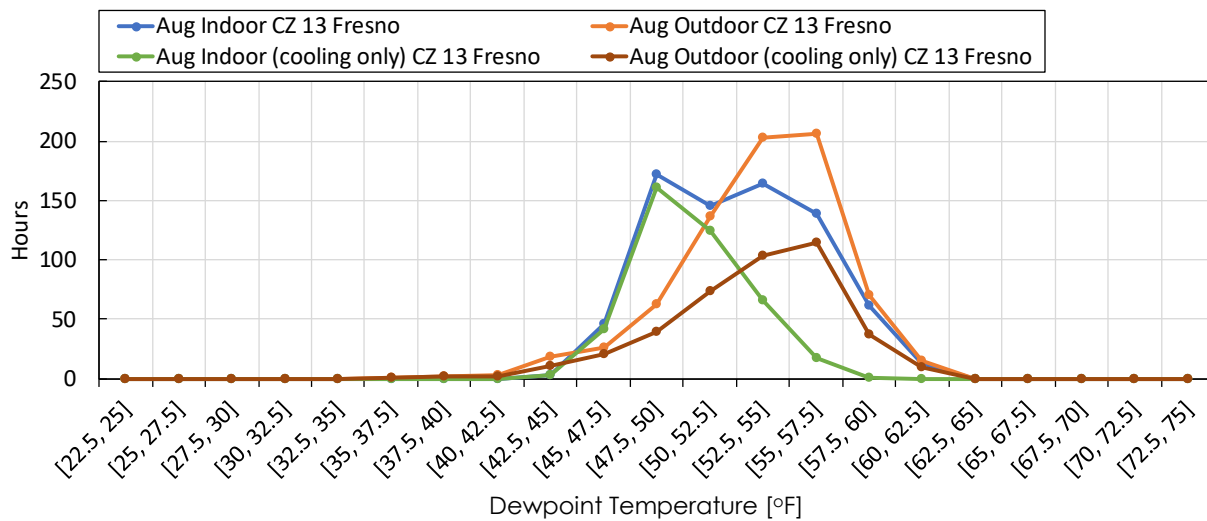


Figure 6: Distribution of hours for indoor and outdoor dew point temperatures for CZ 13 Fresno, for August, including hours during periods when air conditioner is on.

For the month of September, the air conditioner on for shorter periods of time (compared to July and August). Interestingly, the indoor dew point temperature is similar to the outdoor dew point temperature, indicating a balance between periods when internal latent loads cause the indoor dew point to be higher, and periods with air conditioning when the indoor dew point is lower than the outdoor dew point.

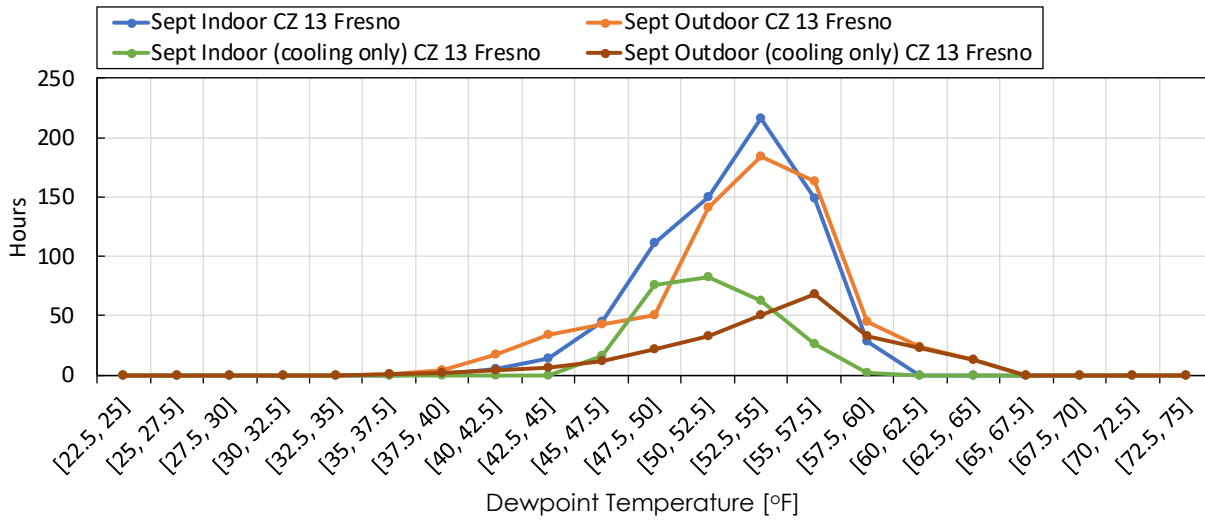


Figure 7: Distribution of hours for indoor and outdoor dew point temperatures for CZ 13 Fresno, for September, including hours during periods when air conditioner is on.

CLIMATE ZONE WITH NO COOLING REQUIRED

2.2.2. Climate Zone 1 - Arcata

The CBECC-Res simulation results for climate zone 1 indicate that the air conditioner does not operate in cooling mode for any hour of the year. The maximum seven-day average indoor dew point temperature is 57.4°F and occurs on August 5 at 7:03 PM (week: August 2 to August 9 at 7:03 AM). Figure 8 shows the indoor and outdoor dew point temperatures for CZ 1 Arcata from August 2 to August 10. The indoor dew point temperature exceeds 61°F once during this period. It can be seen that the indoor dew point temperatures are higher than the outdoor dew point temperatures. This is because of internal latent loads in the house. In the absence of air-conditioning, the internal loads cause indoor moisture to build-up which leads to a higher indoor dew point temperature.

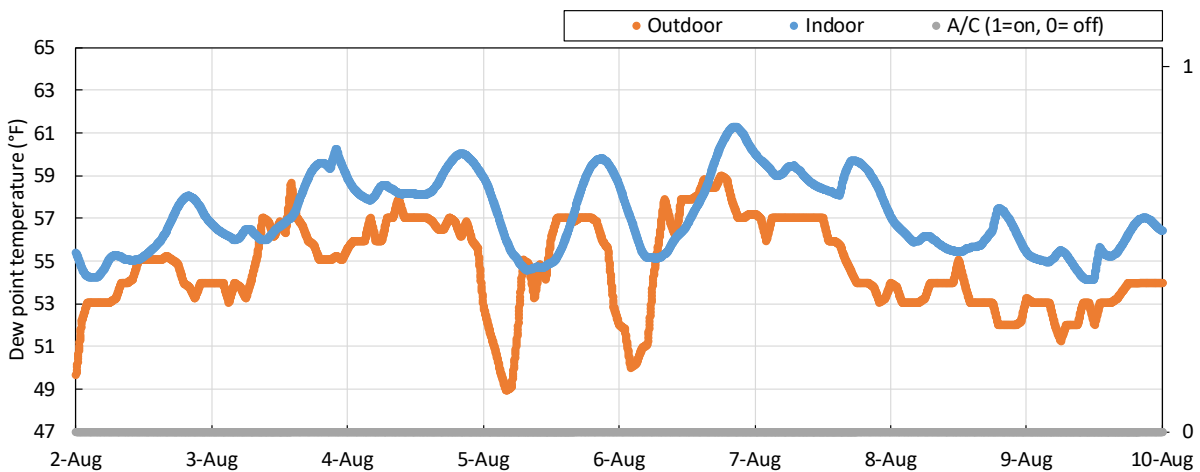


Figure 8: Indoor and outdoor dew point temperatures for CZ 1 Arcata from August 2 to August 10.

Figure 9 shows the distribution of hours for indoor and outdoor dew point temperatures for the month of August. The indoor temperature hourly distribution follows a very similar pattern to that for outdoors, however, the indoor distribution is shifted 2.5°F higher than outdoors.

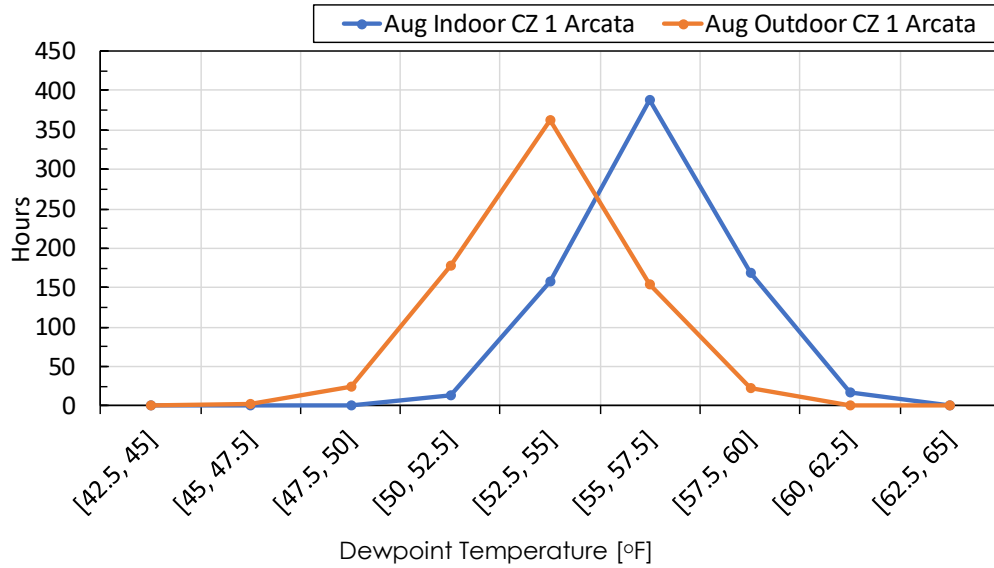


Figure 9: Distribution of hours for indoor and outdoor dew point temperatures for CZ 1 Arcata, for August.

2.2.3. Climate Zone 3 - Oakland

The CBECC-Res simulation results for climate zone 3 indicate that the maximum seven-day average indoor dew point temperature is 57.8°F and occurs on September 20 at 6:33 AM (week: September 16 to September 23 at 6:33 PM).

Figure 10 shows the indoor and outdoor dew point temperatures from September 16 to 24. It can be seen that with a few exceptions, the indoor dew point temperature is higher than the outdoor dew point temperature. During the period shown, the indoor dew point temperature exceeds 61°F on three occasions. As noted earlier, the air conditioner is off throughout.

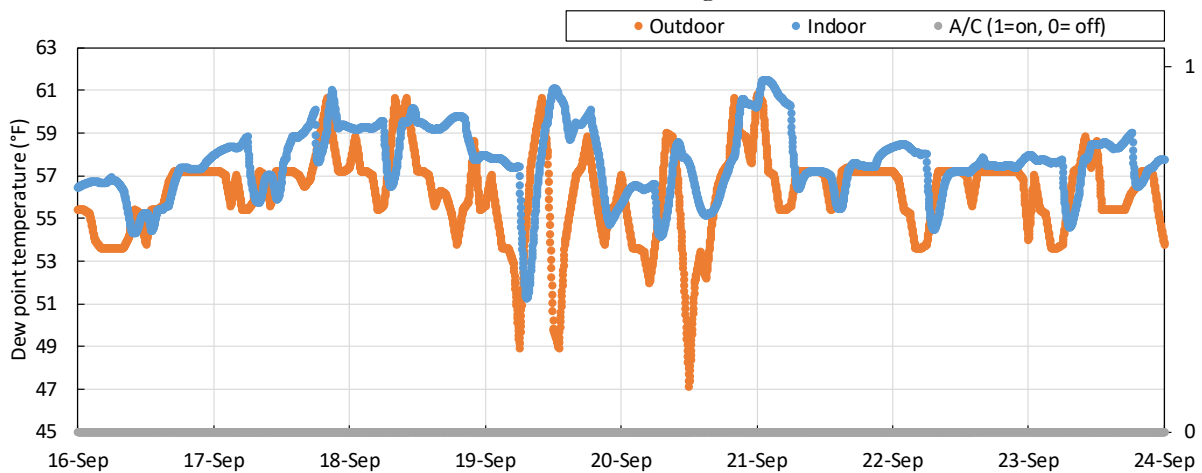


Figure 10: Indoor and outdoor dew point temperatures for CZ 3 Oakland from September 16 to 24.

Figure 11 shows the distribution of hours for indoor and outdoor dew point temperatures for the month of September. It can be seen that there are more hours with high dew point range for indoor compared to outdoor conditions.

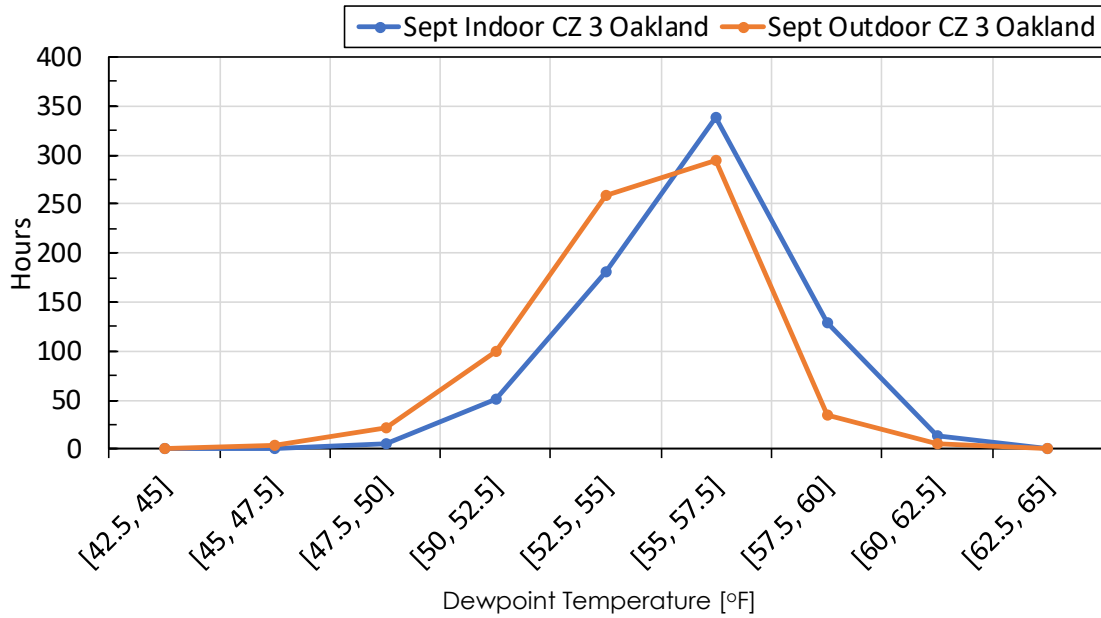


Figure 11: Distribution of hours for indoor and outdoor dew point temperatures for CZ 3 Oakland, for September.

2.2.4. Climate Zone 5 - Santa Maria

The climate zone 5 CBECC-Res simulation results indicate that the maximum seven-day average indoor dew point temperature is 57.2°F and occurs on July 11 at 4:06 AM (week: July 7 to July 14 at 4:06 PM).

Figure 12 shows the distribution of hours for indoor and outdoor dew point temperatures for the month of July. As expected, the indoor dew point distribution corresponds to higher temperatures compared to that of the outdoor condition.

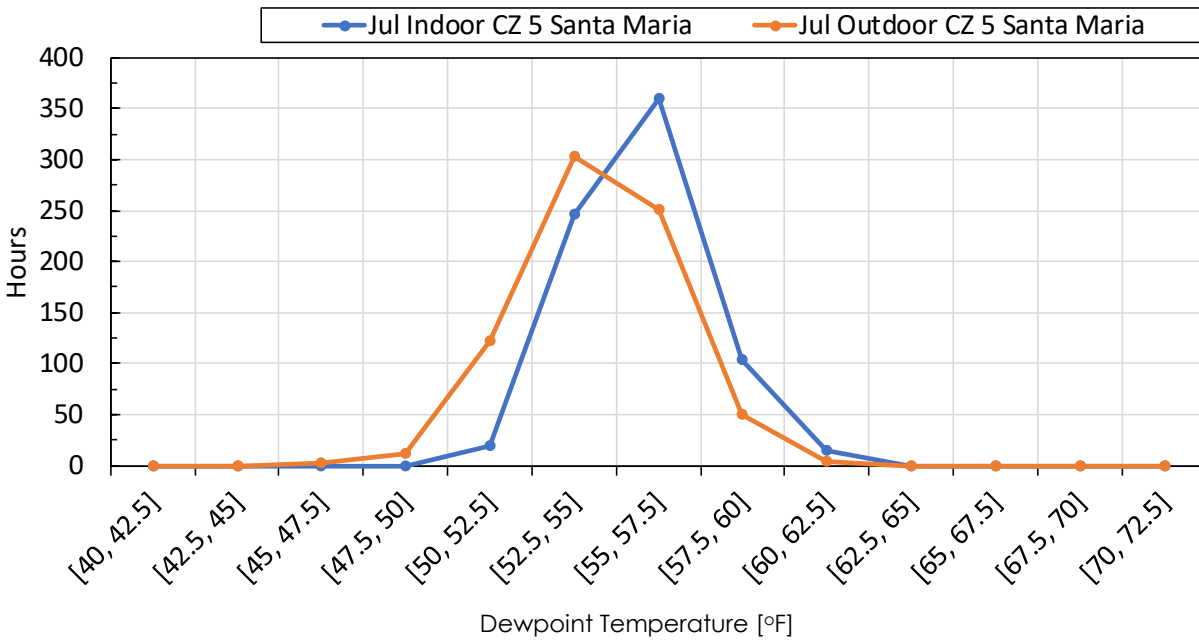


Figure 12: Distribution of hours for indoor and outdoor dew point temperatures for CZ 5 Santa Maria for July.

CLIMATE ZONES WITH LESS THAN 100 HOURS OF COOLING

2.2.5. Climate Zone 2 - Santa Rosa

The climate zone 2 CBECC-Res simulation results indicate that the air-conditioner cooling period is from June 5, 6:06 PM to Aug 28, 8:54 PM. The total number of hours for which the air conditioning provides cooling is 35.5 which is relatively small. Figure 13 shows the seven-day moving average indoor and outdoor dew point temperatures for summer. The indoor is always higher than the outdoor dew point temperature average.

The maximum seven-day average indoor dew point temperature is 57.4°F and occurs on August 8 at 7:03 PM (week: August 2 to 9 at 7:03 AM). However, the air conditioning is off during this period.

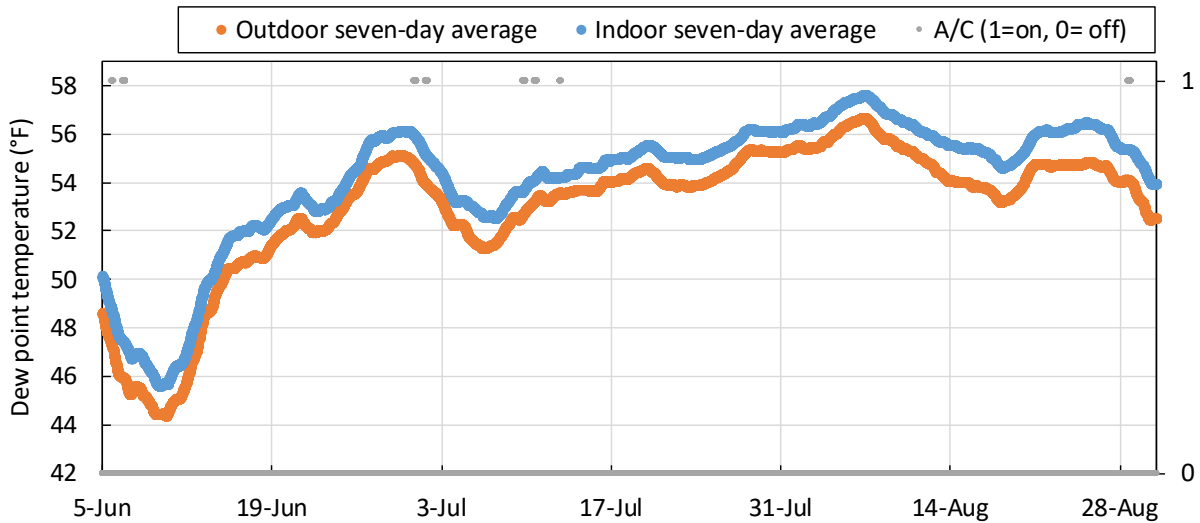


Figure 13: Seven-day moving average indoor (room) and outdoor dew point temperatures for CZ 2 Santa Rosa for summer. Air conditioner operation (on or off) is shown on the secondary axis.

Figure 14 shows the indoor and outdoor dew point temperatures from June 30 to July 5. This includes the period during which the indoor dew point temperature is high and the air conditioning is on. It can be seen that the indoor dew point is generally higher than that of the outdoor. When the air conditioner cycles on, the indoor dew point temperatures decrease below the outdoor dew point on both occasions.

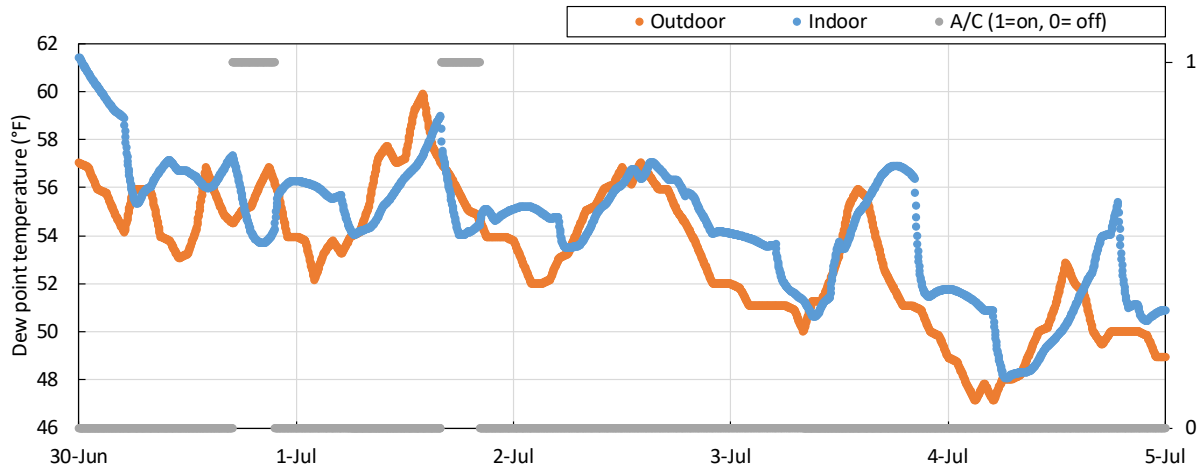


Figure 14: Indoor and outdoor dew point temperatures for CZ 2 Santa Rosa from June 30 to July 5.

Figure 15 shows the distribution of hours for indoor and outdoor dew point temperatures for the month of July. The distributions are similar, with indoor dew point distribution being slightly higher than that of the outdoor condition. Since the air conditioning is off most of the month, the hours for cooling only period are much lower. When cooling is on, the indoor has a dew point that is lower than that of the outdoor environment.

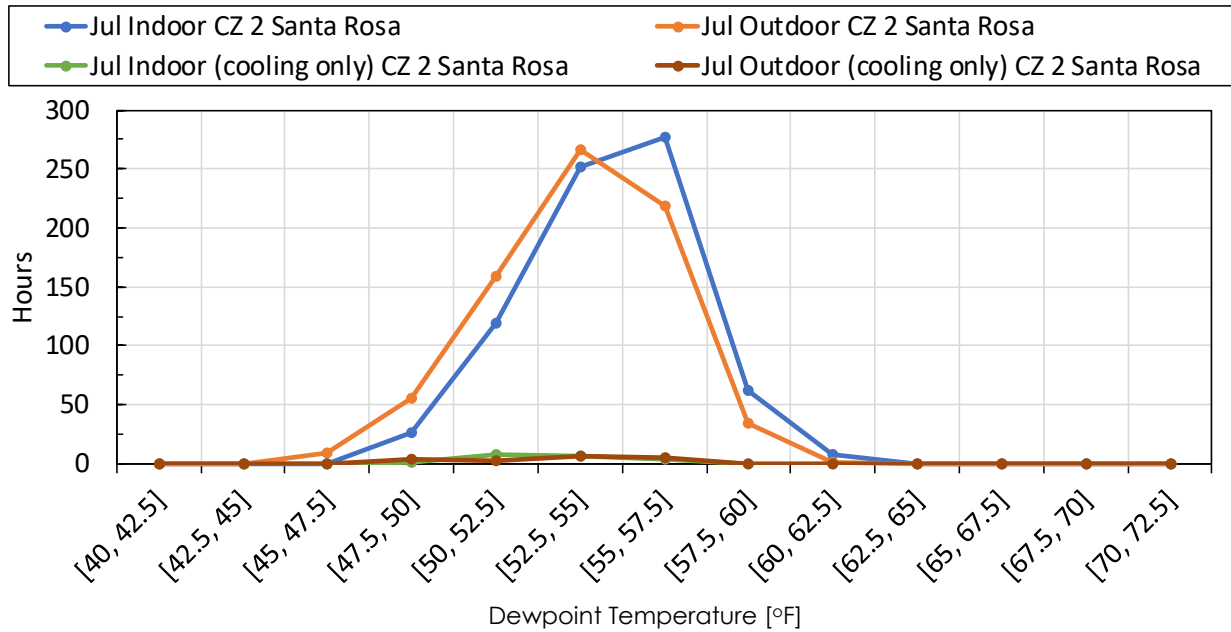


Figure 15: Distribution of hours for indoor and outdoor dew point temperatures for CZ 2 Santa Rosa for July. Distribution for periods with cooling only also shown.

2.2.6. Climate Zone 4 - San Jose

The climate zone 4 CBECC-Res simulation results indicate that the air conditioner cooling period is from July 11, 5:45 PM to September 25, 7:45 PM. The air conditioner provides cooling for less than 62 hours. Figure 16 shows the seven-day moving average indoor and outdoor dew point temperatures for summer. The indoor is always higher than the outdoor dew point temperature average.

The maximum seven-day average indoor dew point temperature is 57.9°F and occurs on August 7 at 6:06 AM (week: August 3 to 10 at 6:06 PM). The air conditioner cycles on briefly during this period.

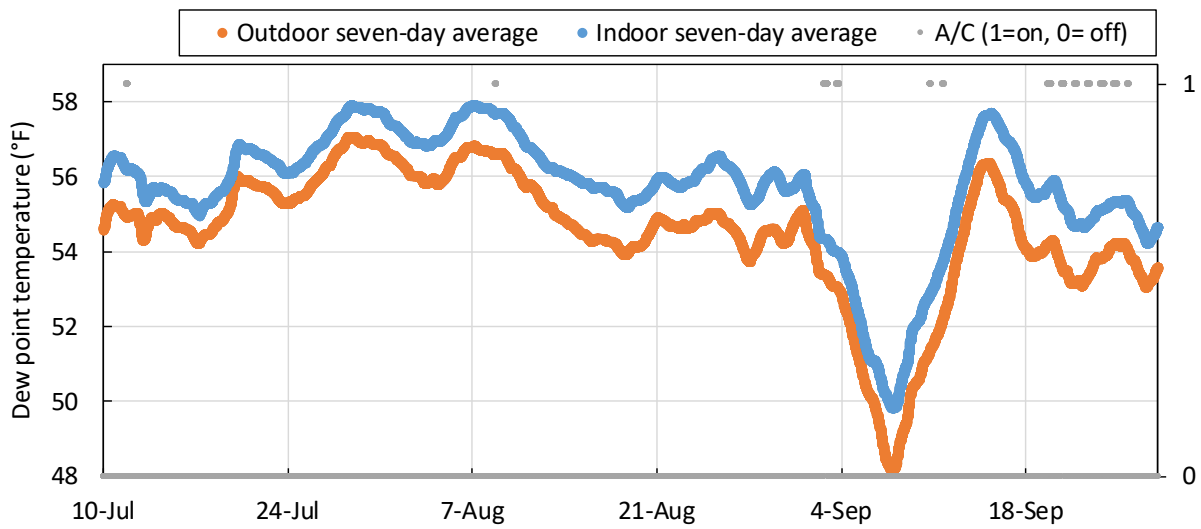


Figure 16: Seven-day moving average indoor (room) and outdoor dew point temperatures for CZ 4 San Jose for summer. Air conditioner operation (on or off) is shown on the secondary axis.

Figure 17 shows the indoor and outdoor dew point temperatures from August 6 to 11. This includes the period during which the indoor dew point temperature is high and the air conditioner is on. The unique feature is that the dew point temperature continues to rise even when the air conditioner cycles on although the rate of increases decreases. The outdoor environment is generally at a lower dew point temperature than the indoor conditions.

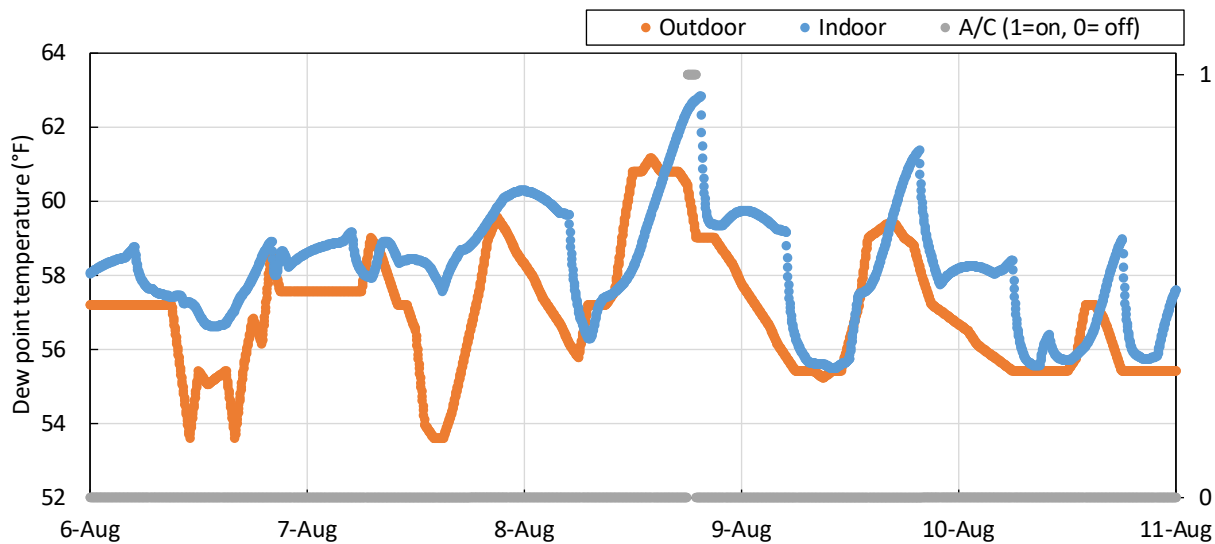


Figure 17: Indoor and outdoor dew point temperatures for CZ 4 San Jose from August 6 to 11.

Figure 18 shows the distribution of hours for indoor and outdoor dew point temperatures for the month of August. The indoor dew point distribution is higher than that of the outdoor condition. Since the air conditioner is on for only one hour during this month, the hours for cooling only period appear to be zero.

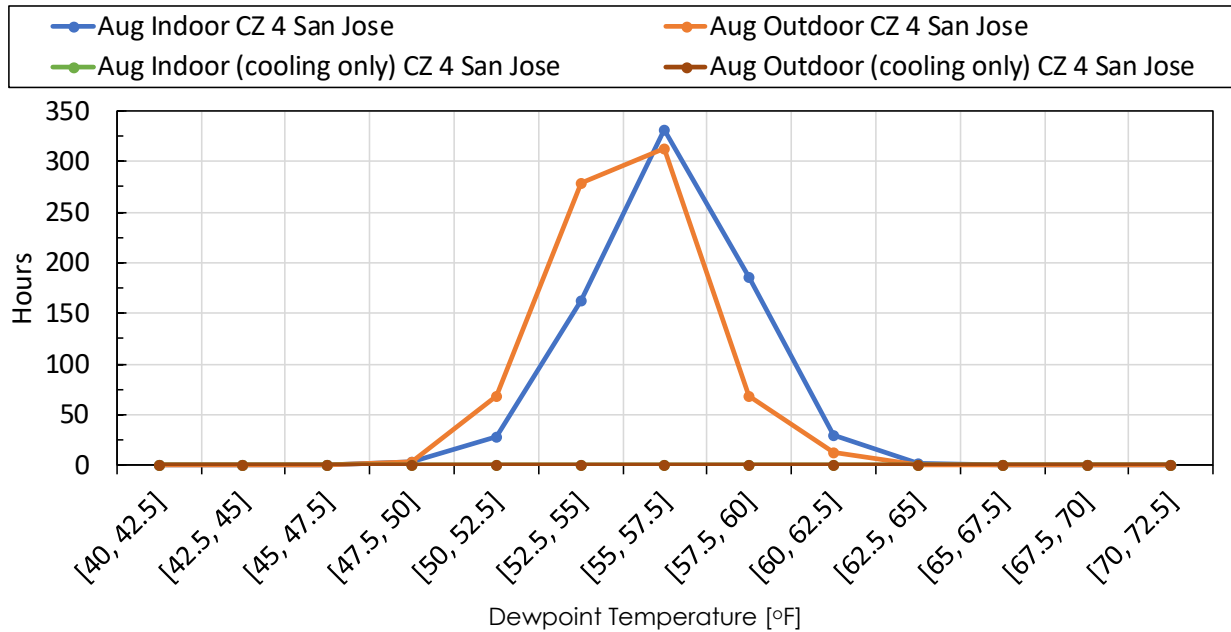


Figure 18: Distribution of hours for indoor and outdoor dew point temperatures for CZ 4 San Jose for August. Distribution for periods with cooling also shown.

2.2.7. Climate Zone 6 - Los Angeles/Torrance

The climate zone 6 CBECC-Res simulation results indicate that the air conditioner operates in cooling mode for the first time on July 7 at 5:00 PM. The air conditioner provides cooling for the last time on October 6 at 9:18 PM. However, the air conditioner is on for only 48.5 hours. (In contrast, the air conditioner provides cooling for 1436 hours in climate zone 13).

Figure 19 shows the seven-day moving average of the room (or indoor air-conditioned space) dew point temperature over the summer. The seven-day moving average of outdoor air temperature is also shown. Air conditioner operation (on or off) is shown on the secondary axis. It can be seen that the indoor and outdoor temperatures are very similar. The maximum average indoor dew point temperature is 63.8°F and occurs in the week that starts from July 8, 10:57 AM and ends on July 15, 10:57 AM. The halfway point for the week corresponds to July 11, 10:57 PM. The figure also shows the rapid decrease in dew point temperatures towards the start of October, which is likely caused by the extremely dry winds, called Santa Ana winds that prevail during this period.

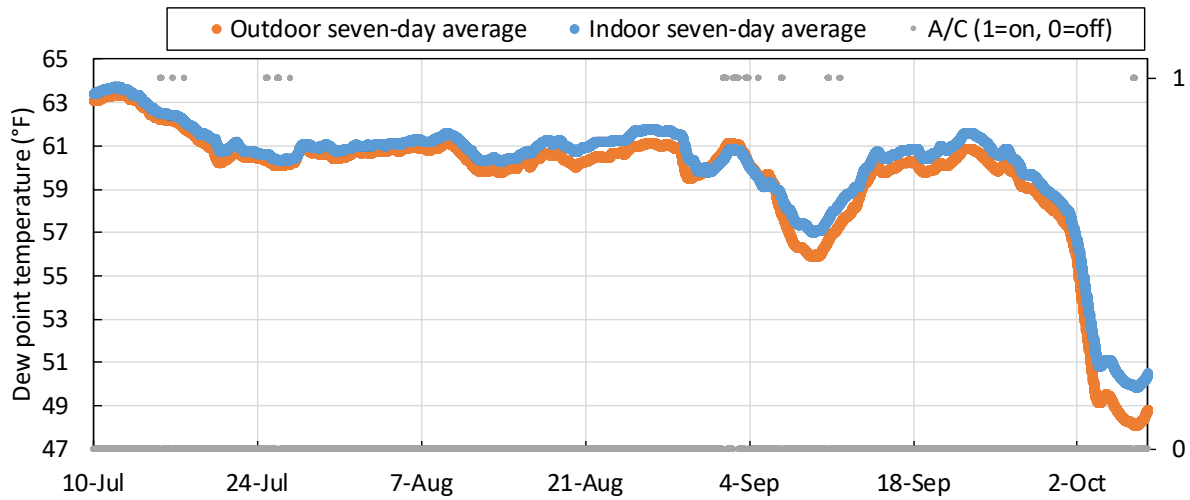


Figure 19: Seven-day moving average indoor (room) and outdoor dew point temperatures for CZ 6 LA. Air conditioner operation (on or off) is shown on the secondary axis.

Figure 20 shows the indoor and outdoor dew point temperatures from July 15 to July 19. This period includes the week with the highest indoor seven-day average dew point temperature when cooling is on. It can be seen that the indoor dew point temperature is slightly higher than the outdoor dew point temperature but it rapidly decreases when the air conditioner is turned on. Once the air conditioner is turned off, it rapidly increases to its original value. Since there is a high indoor dew point temperature and the air conditioner also turns on during these periods, in the subsequent sections, these periods shall be analyzed to assess condensation.

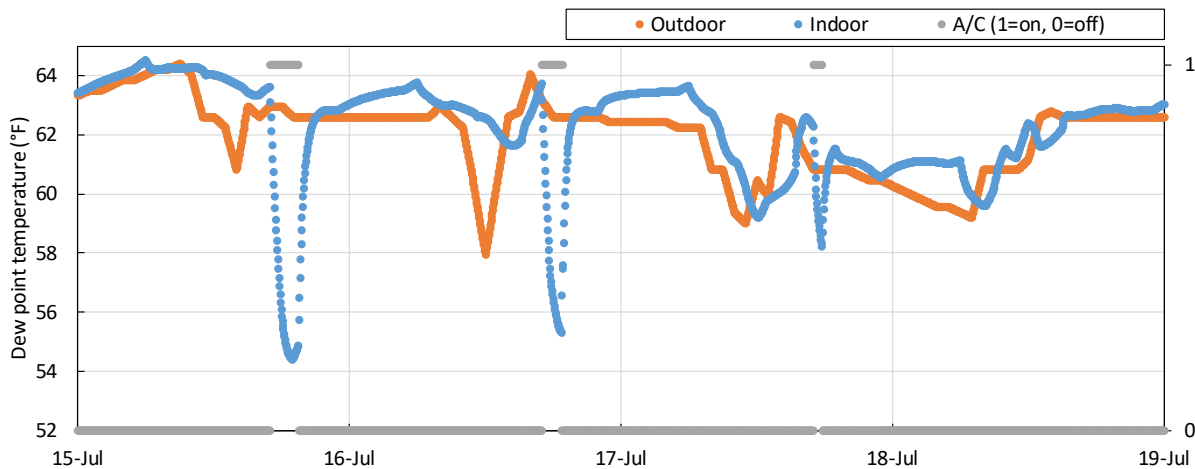


Figure 20: Indoor and outdoor dew point temperatures for CZ 6 LA from July 15 to 19.

Figure 21 shows the distribution of hours corresponding to different dew point temperature ranges for indoor and outdoor conditions for the month of July. It can be seen that indoor and outdoor distribution is very similar.

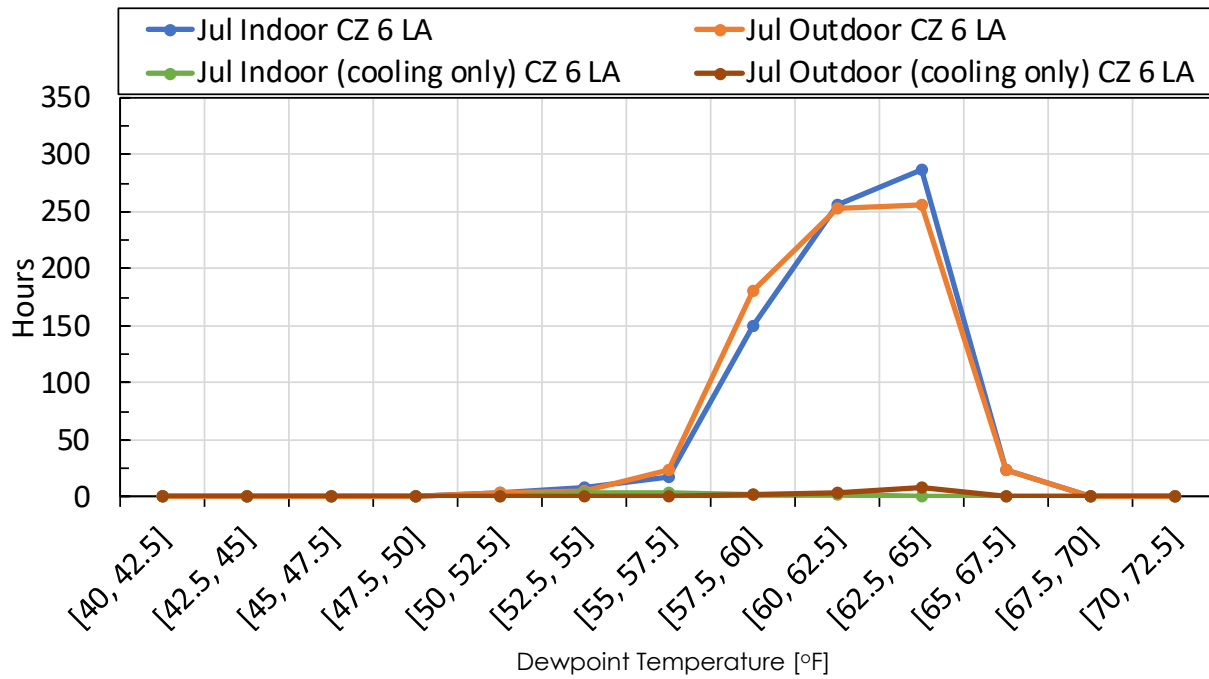


Figure 21: Distribution of hours for indoor and outdoor dew point temperatures for CZ 6 LA, for July. Hours during periods when air conditioner is on also shown.

2.2.8. Climate Zone 7 - San Diego

The results indicate that the air conditioner cooling period is from September 2, 4:03 PM to September 11, 5:09 PM. The air conditioner provides cooling for less than 6.5 hours.

Figure 22 shows the indoor and outdoor dew point temperatures from September 2 to 11. This includes the two occasions during which the air conditioner cycles on. The indoor dew point temperature rapidly falls on both occasions.

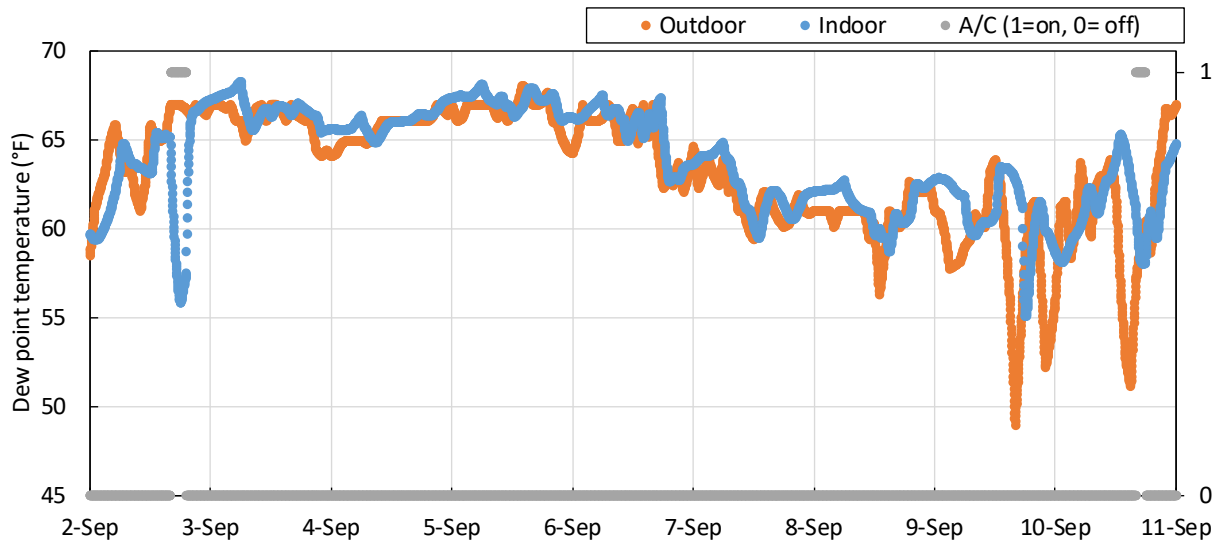


Figure 22: Indoor and outdoor dew point temperatures for CZ 7 San Diego from September 2 to 11.

Figure 23 shows the distribution of hours for indoor and outdoor dew point temperatures for the month of August. The indoor dew point distribution very similar to that of the outdoor condition. Since the air conditioner is on for less than 6.5 hours, the hours for cooling only period appear to be zero.

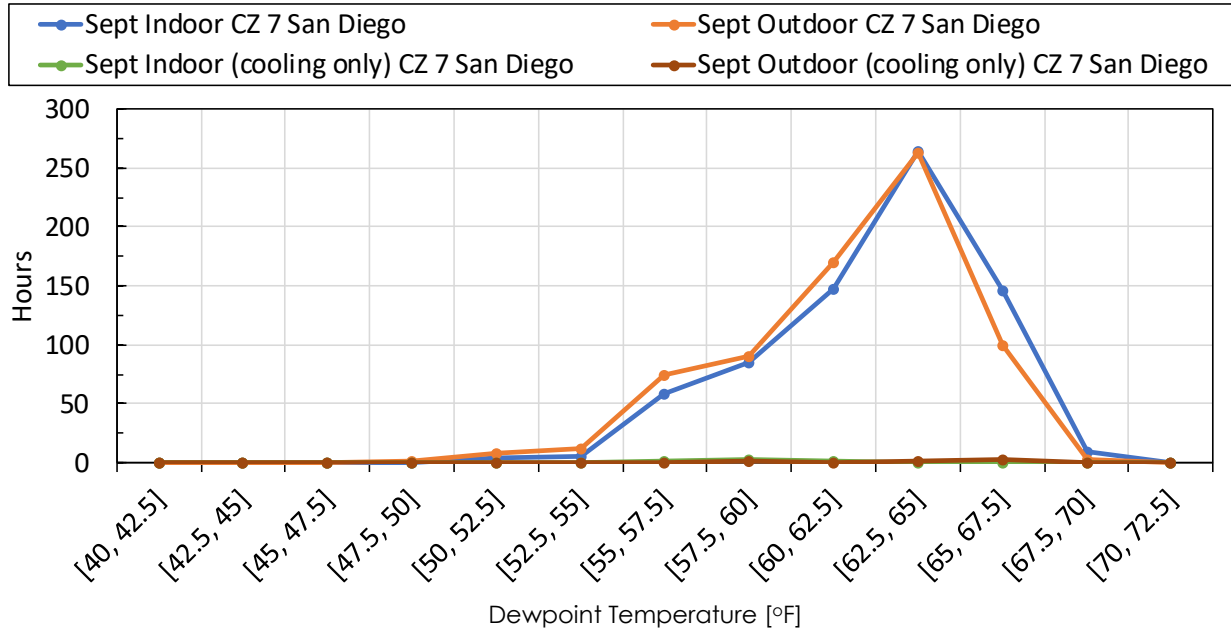


Figure 23: Distribution of hours for indoor and outdoor dew point temperatures for CZ 7 San Diego for September. Distribution for periods with cooling also shown.

CLIMATE ZONES WITH MORE THAN 100 HOURS OF COOLING

2.2.9. Climate Zone 12 - Sacramento

The climate zone 12 CBECC-Res simulation results indicate that the air conditioner operates in cooling mode for the first time on May 23 at 5:00 PM and for the last time on September 25 at 11:36 PM. The air conditioner is on for 347 hours.

Figure 24 shows the seven-day moving average of the room (or indoor air-conditioned space) dew point temperature over the summer. The maximum seven-day average indoor dew point temperature is 57.8°F and occurs on May 28 at 4:03 PM (week: May 24, 4:03 PM to July 1, 4:03 PM).

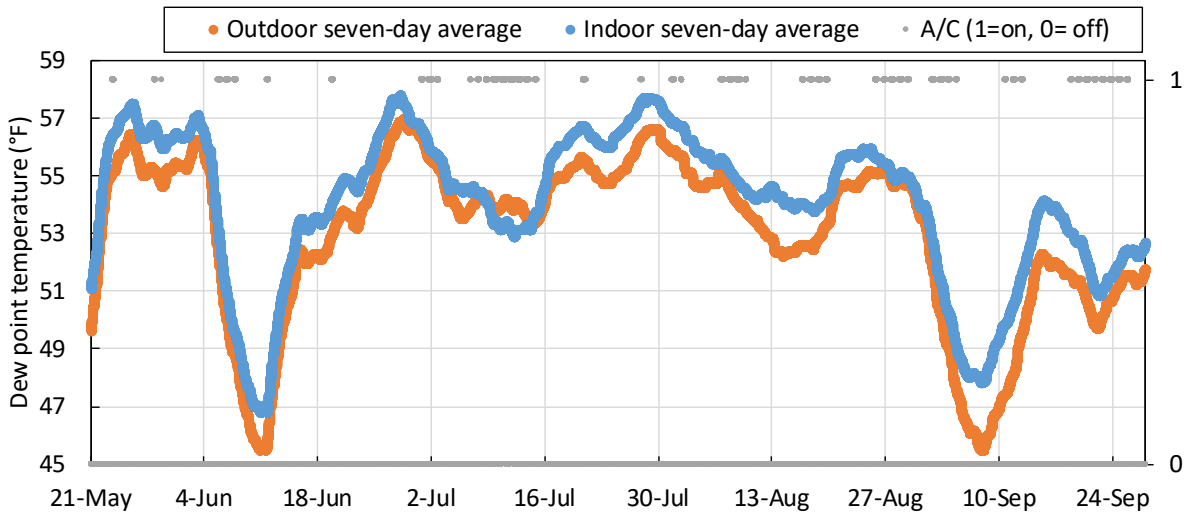


Figure 24: Seven-day moving average indoor (room) and outdoor dew point temperatures for CZ 12 Sacramento. Air conditioner operation (on or off) is shown on the secondary axis.

Figure 25 shows the indoor and outdoor dew point temperatures for from July 25 to August 4. Based on the condensation model results, this period would be shown to have the maximum water condensed on the duct (July 27 to July 28).

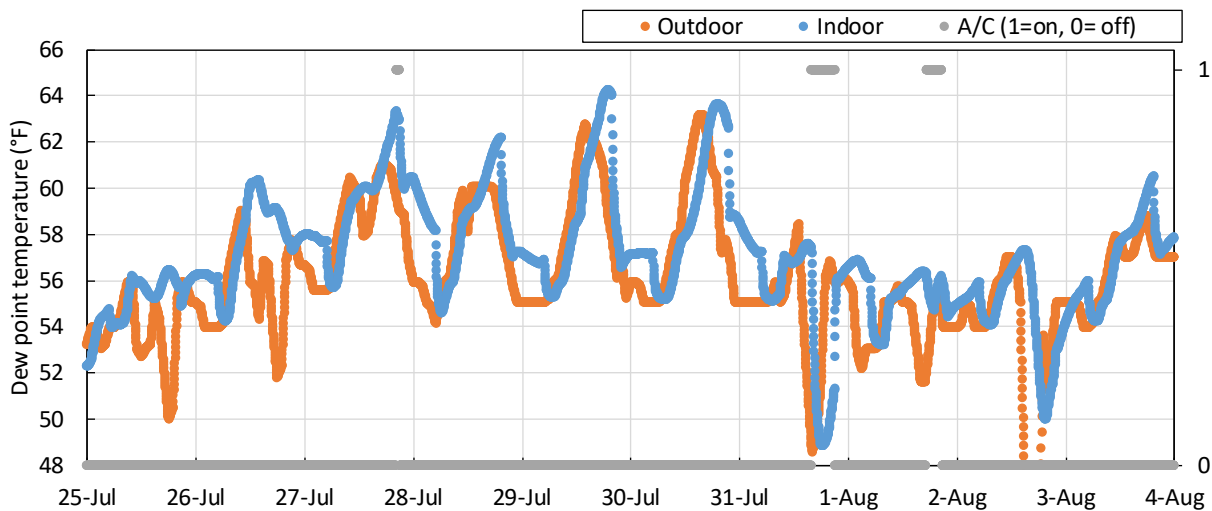


Figure 25: Indoor and outdoor dew point temperatures for CZ 12 Sacramento from July 25 to Aug 4.

Figure 26 shows the distribution of hours for indoor and outdoor dew point temperatures for the month of July. The indoor dew point distribution is very similar to that of the outdoor condition. When the air conditioner is on, the indoor dew point temperature is lower than the outdoor dew point temperature.

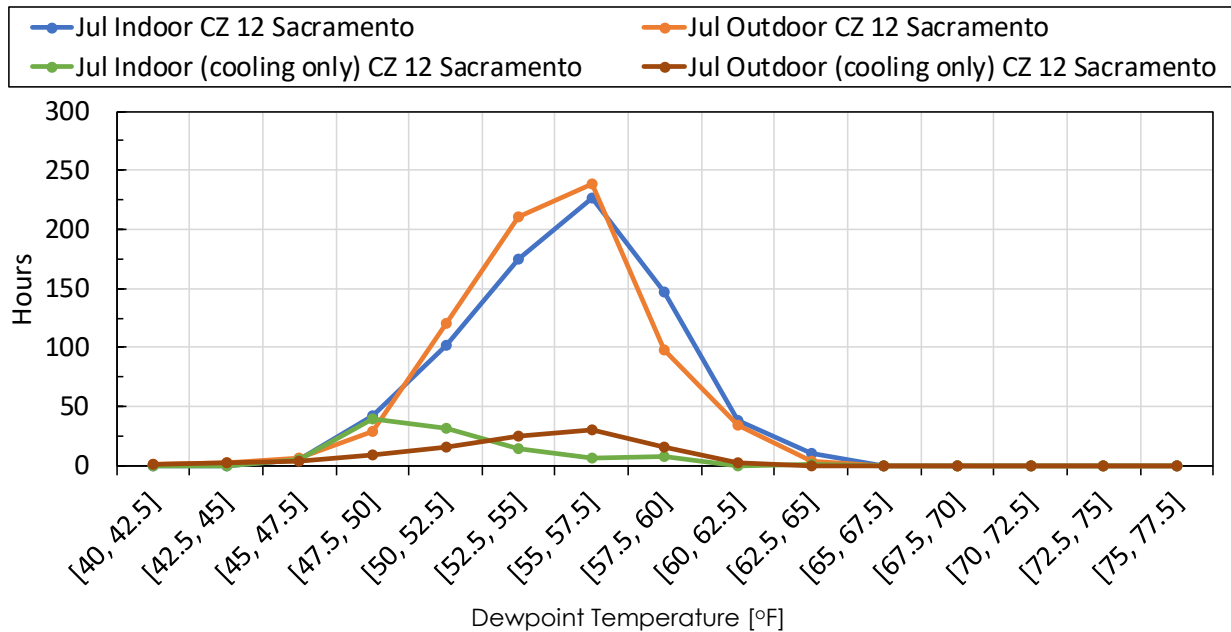


Figure 26: Distribution of hours for indoor and outdoor dew point temperatures for CZ 12 Sacramento for July. Hours during periods when air conditioner is on also shown.

2.2.10. Climate Zone 8 - Fullerton

The climate zone 8 CBECC-Res simulation results indicate that the air conditioner cooling period is from July 12, 4:00 PM to October 7, 6:06 PM. The air conditioner provides cooling for 220 hours. Figure 27 shows the seven-day moving average indoor and outdoor dew point temperatures for summer. The indoor is usually higher than the outdoor dew point temperature average although both have a very similar trend. The dew point temperatures become very low towards the end of September. Since condensation requires high dew point temperatures, this period is not shown. The maximum seven-day average indoor dew point temperature is 63.8°F and occurs on July 9 at 4:39 AM (week: July 5 to 12 at 4:39 PM). The air conditioner cycles on close to this period.

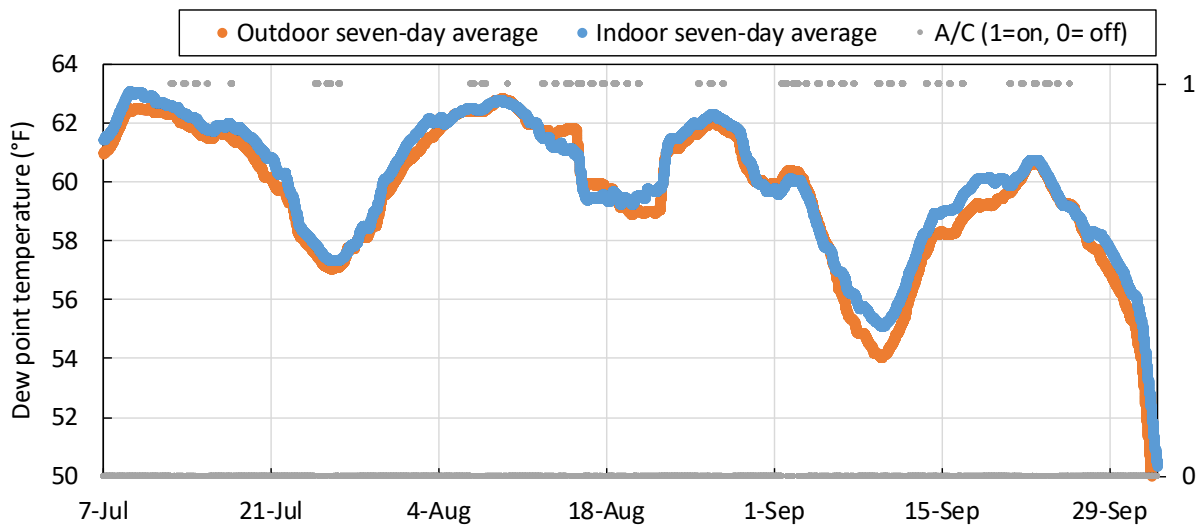


Figure 27: Seven-day moving average indoor (room) and outdoor dew point temperatures for CZ 8 Fullerton for summer. Air conditioner operation (on or off) is shown on the secondary axis.

Figure 28 shows the indoor and outdoor dew point temperatures from July 11 to 17. This includes the period during which the indoor dew point temperature is high and the air conditioner is on. It can be seen that the indoor dew point temperature is generally higher than that of the outdoor. When the air conditioner cycles on, the indoor dew point temperatures decrease below the outdoor dew point on each of the four occasions.

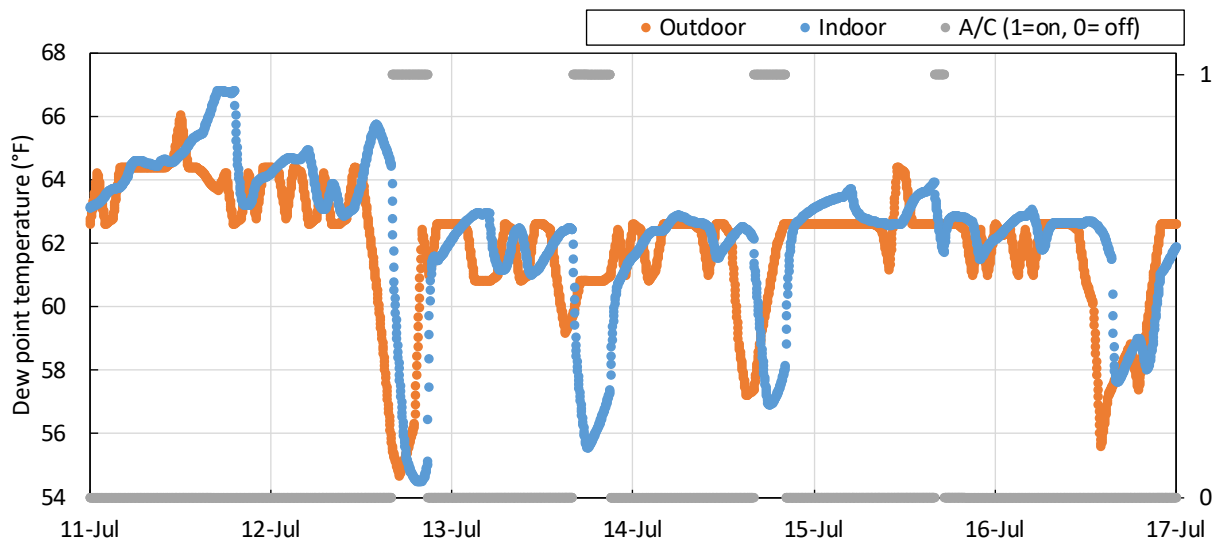


Figure 28: Indoor and outdoor dew point temperatures for CZ 8 Fullerton from July 11 to 17.

Figure 29 shows the distribution of hours for indoor and outdoor dew point temperatures for the month of July. The indoor distributions are similar to those of the outdoor except for the range 52.5°F to 57.5°F. The distribution for period with cooling is also shown.

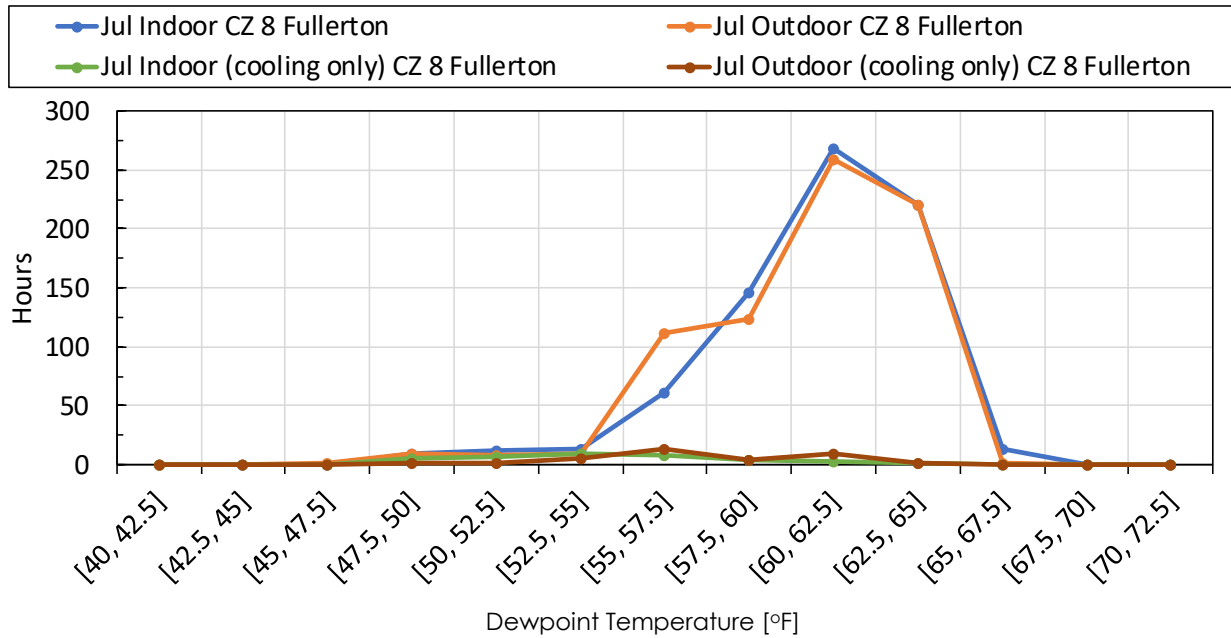


Figure 29: Distribution of hours for indoor and outdoor dew point temperatures for CZ 8 Fullerton for July. Distribution for periods with cooling also shown.

2.2.11. Climate Zone 9 - Burbank

The climate zone 9 CBECC-Res simulation results indicate that the air conditioner cooling period is from May 21, 6:27 PM to October 14, 9:12 PM. The total number of hours for which the air conditioner provides cooling is 454.

Figure 30 shows the seven-day moving average indoor and outdoor dew point temperatures for summer. The indoor is higher than the outdoor dew point temperature average except when the air conditioner runs continuously (e.g. after August 13 and before July 16).

The maximum seven-day average indoor dew point temperature is 64.3°F and occurs on July 9 at 3:18 AM (week: July 5 to 12 at 11:42 AM). The air conditioner also cycles on during this period.

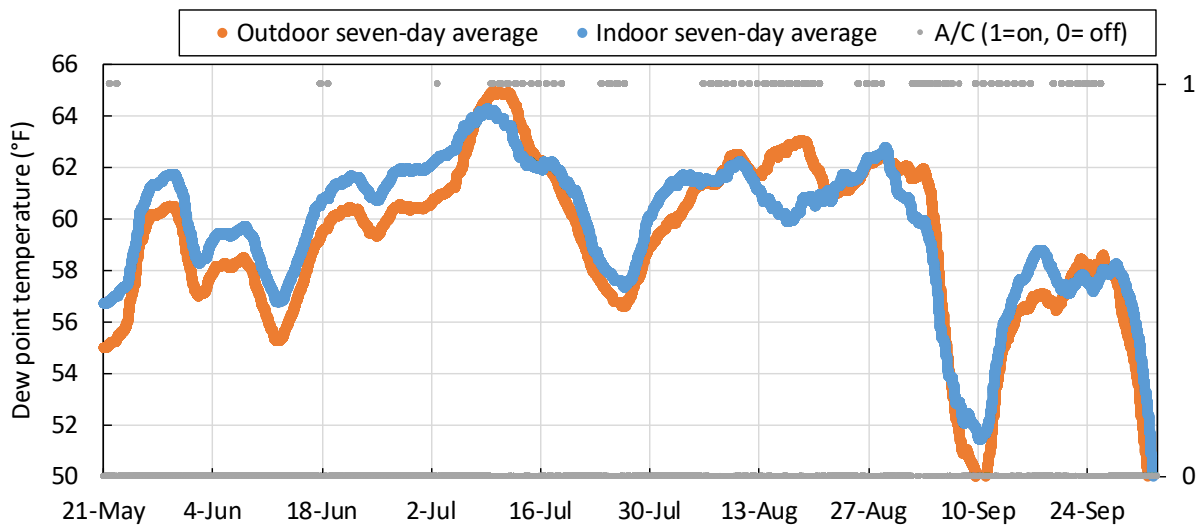


Figure 30: Seven-day moving average indoor (room) and outdoor dew point temperatures for CZ 9 Burbank for summer. Air conditioner operation (on or off) is shown on the secondary axis.

Figure 31 shows the indoor and outdoor dew point temperatures from July 7 to July 16. This includes the period during which the indoor dew point temperature is high and the air conditioner is on. Both indoor and outdoor dew point temperatures are quite high and exceed 67°F on several occasions. Furthermore, the indoor dew point temperature is generally higher than that the outdoor dew point temperature except when the air conditioner cycles on. On these occasions, the indoor dew point temperature rapidly decreases and becomes less than the outdoor dew point. Once the air conditioner cycles off, the indoor dew point rapidly rises.

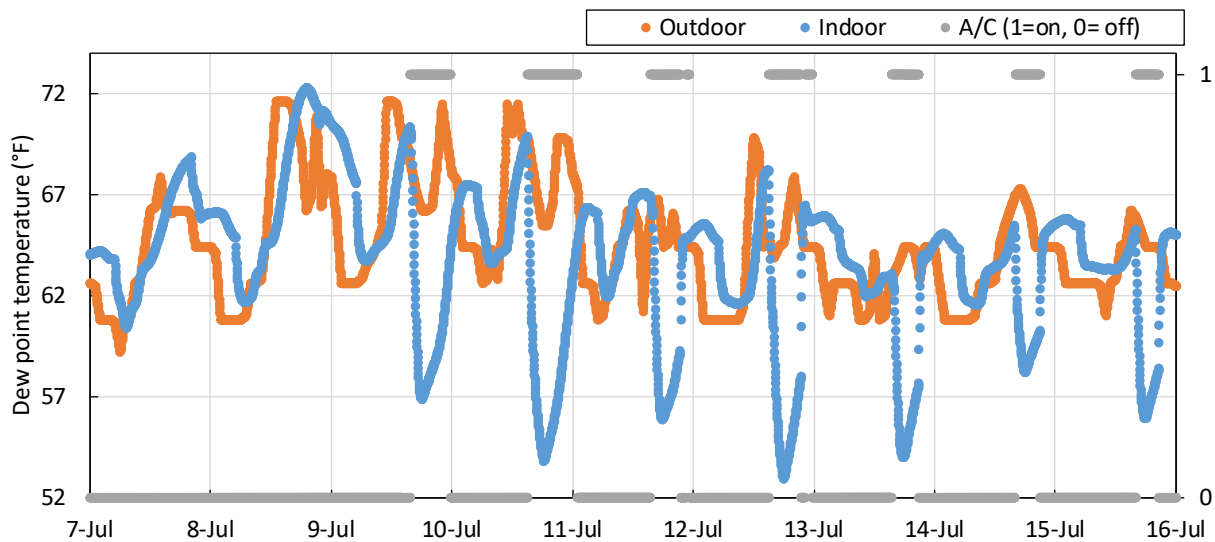


Figure 31: Indoor and outdoor dew point temperatures for CZ 9 Burbank from July 7 to 16.

Figure 32 shows the distribution of hours for indoor and outdoor dew point temperatures for the month of July. The distributions are similar except for the range 55 to 55.75°F. The distribution for periods with cooling are also shown. It can be seen that the indoor dew point temperatures are lower than outdoor temperatures when the air conditioner is on.

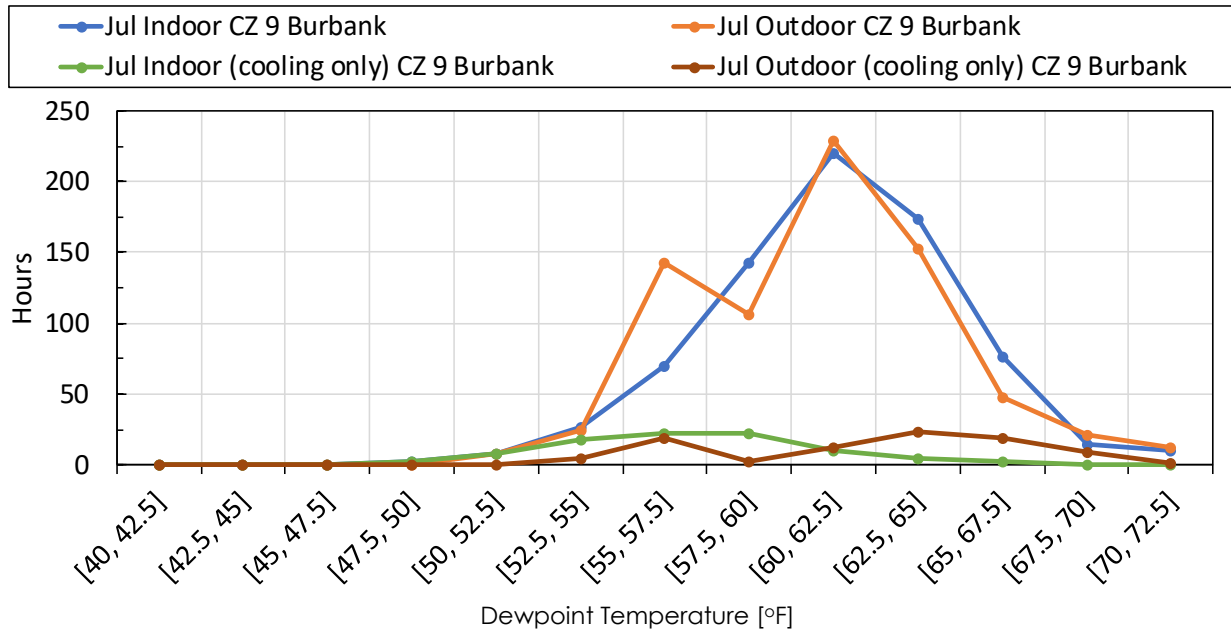


Figure 32: Distribution of hours for indoor and outdoor dew point temperatures for CZ 9 Burbank for July. Distribution for periods with cooling only also shown.

2.2.12. Climate Zone 10 - Riverside

The climate zone 10 CBECC-Res simulation results indicate that the air conditioner cooling period is from May 21, 5:24 PM to October 7, 7:39 PM. The air conditioner provides cooling for 692.

Figure 30 shows the seven-day moving average indoor and outdoor dew point temperatures for summer. For most the time, the indoor is higher than the outdoor dew point temperature average.

The maximum seven-day average indoor dew point temperature is 60.6°F and occurs on July 19 at 11:42 AM (week: July 15 to 22 at 11:42 PM). However, the air conditioner turns on very short duration during this period.

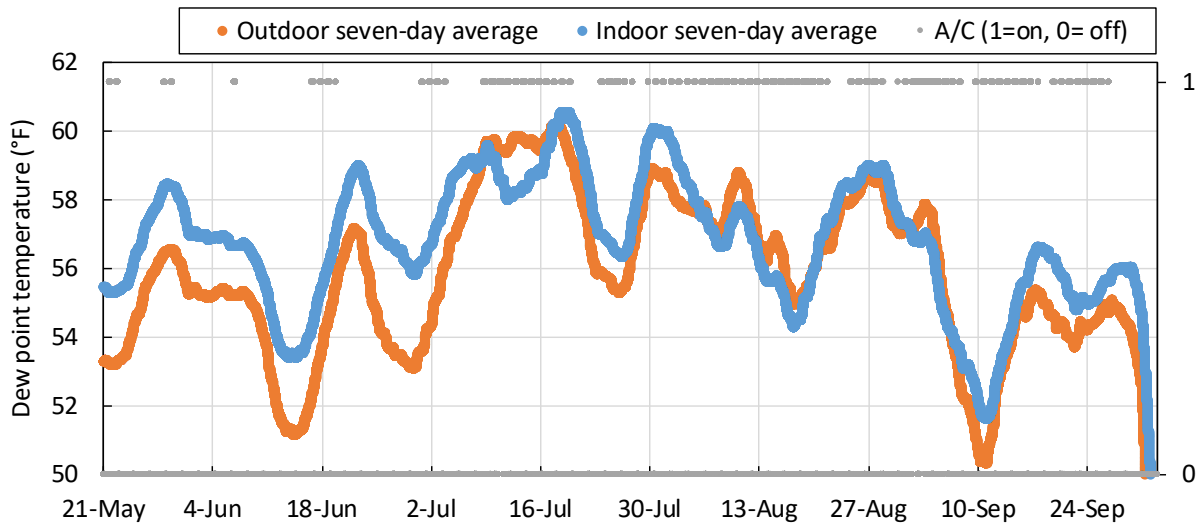


Figure 33: Seven-day moving average indoor (room) and outdoor dew point temperatures for CZ 10 Riverside for summer. Air conditioner operation (on or off) is shown on the secondary axis.

Figure 34 shows the indoor and outdoor dew point temperatures from July 7 to July 16. This includes the period during which the indoor dew point temperature is high and the air conditioner is on. It can be seen that the indoor dew point is higher than that of the outdoor except when the air conditioner cycles on. On these occasions, the indoor dew point temperature rapidly decreases below the outdoor dew point. Once the air conditioner cycles off, the indoor dew point rapidly rises.

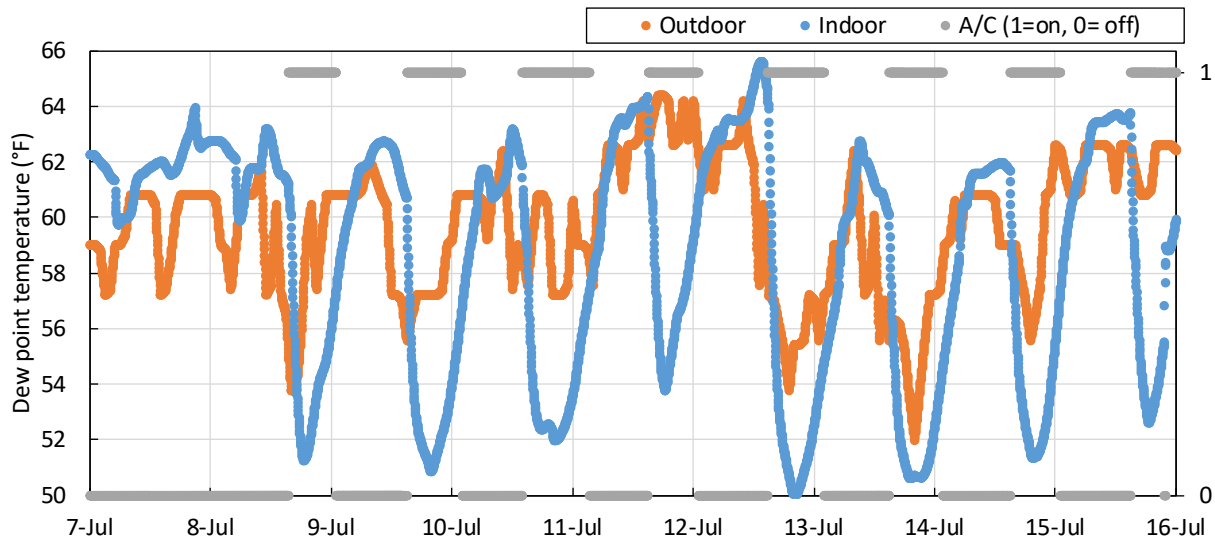


Figure 34: Indoor and outdoor dew point temperatures for CZ 10 Riverside from July 7 to 16.

Figure 35 shows the distribution of hours for indoor and outdoor dew point temperatures for the month of July. The outdoor temperature distribution is bimodal (i.e. has peaks). Overall, the distribution for indoor dew point temperatures correspond to higher range compared to the outdoor temperatures. However, for periods when the air conditioner is on, the indoor dew point temperatures are lower than outdoor temperatures.

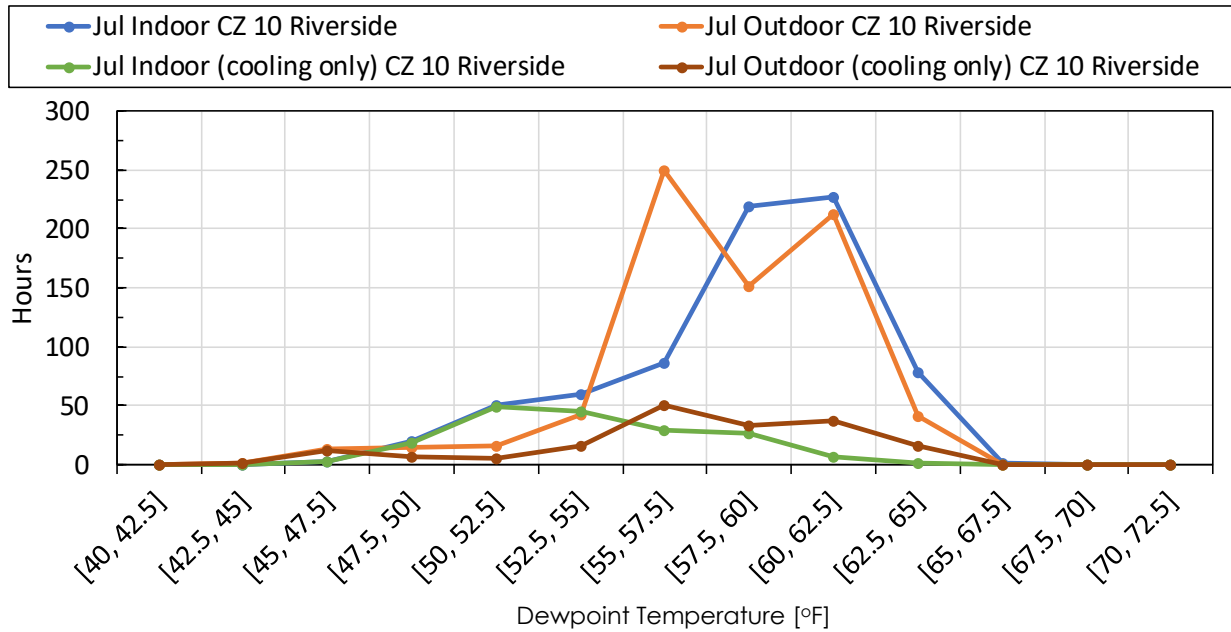


Figure 35: Distribution of hours for indoor and outdoor dew point temperatures for CZ 10 Riverside for July. Distribution for periods with cooling only also shown.

2.2.13. Climate Zone 11 - Red Bluff

The climate zone 11 CBECC-Res simulation results indicate that the air conditioner cooling period is from May 23, 4:00 PM to September 27, 12:57 AM. The air conditioner provides cooling for 1318 hours.

Figure 36 shows the seven-day moving average indoor and outdoor dew point temperatures for summer. Aside from June 10 to August 13, the indoor dew point temperature average is higher than the outdoor dew point temperature average.

The maximum seven-day average indoor dew point temperature is 59.3°F and occurs on June 23 at 11:42 PM (week: June 20 to 27 at 11:42 AM). The air conditioner also turns on during this period.

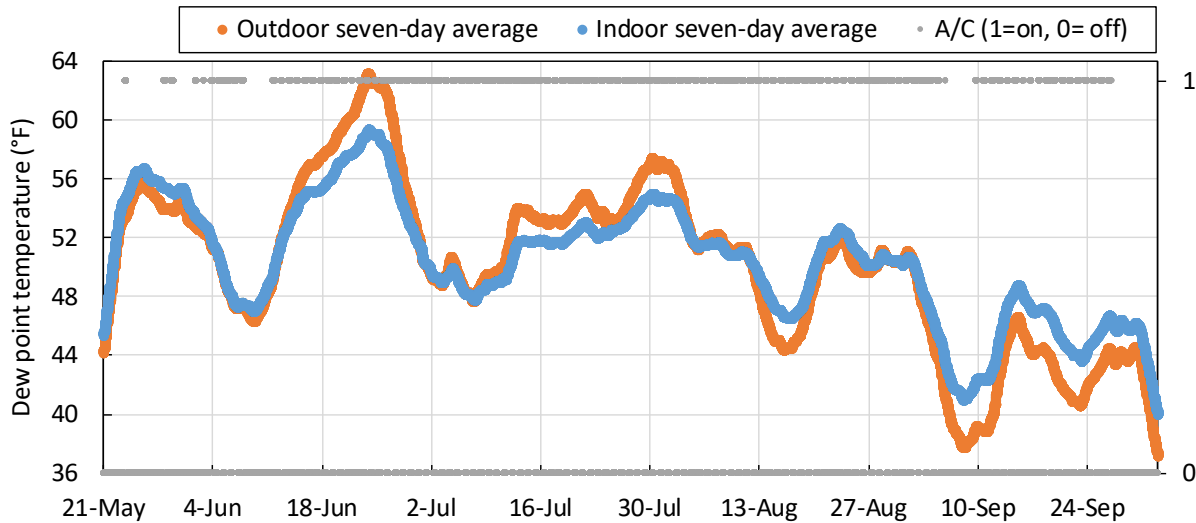


Figure 36: Seven-day moving average indoor (room) and outdoor dew point temperatures for CZ 11 Red Bluff for summer. Air conditioner operation (on or off) is shown on the secondary axis.

Figure 37 shows the indoor and outdoor dew point temperatures from June 23 to 29. This includes the period during which the indoor dew point temperature is high and the air conditioner is on. It can be seen that the air conditioner is on for considerably long periods and the indoor dew point is lower than that of the outdoor while the air conditioner is on.

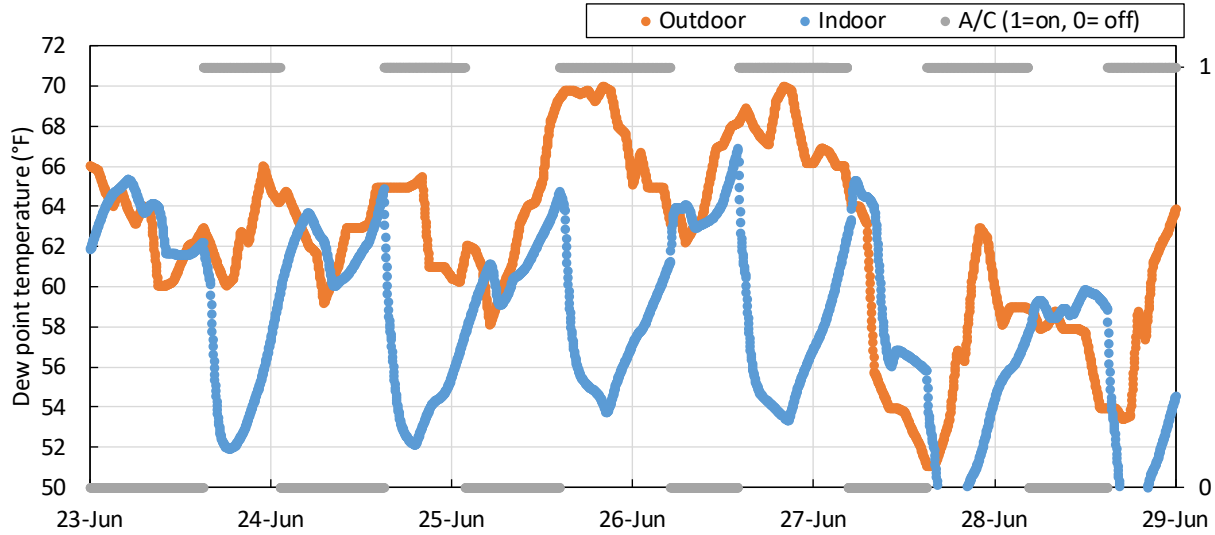


Figure 37: Indoor and outdoor dew point temperatures for CZ 11 Red Bluff from June 23 to 29.

Figure 38 shows the distribution of hours for indoor and outdoor dew point temperatures for the month of June. The distribution for indoor dew point temperatures correspond to a lower range compared to the outdoor temperatures due to extensive cooling. It should be noted that the lower limit had to be decreased in order to show all the points.

Unlike previous climate zones, in CZ 11, the distribution for periods with cooling is significant. As expected, for periods when the air conditioner is on, the indoor dew point temperatures are lower than outdoor temperatures.

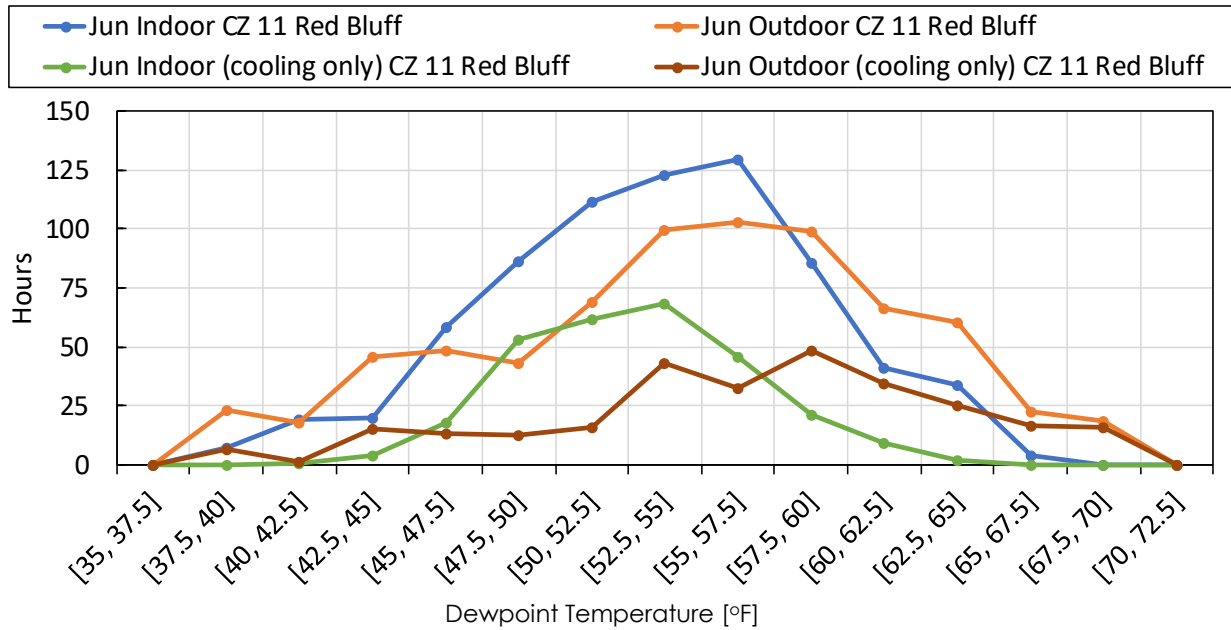


Figure 38: Distribution of hours for indoor and outdoor dew point temperatures for CZ 11 Red Bluff for June. Distribution for periods with cooling only also shown.

2.2.14. Climate Zone 14 - Palmdale

The climate zone 14 CBECC-Res simulation results indicate that the air conditioner cooling period is from May 22, 4:00 PM to September 27, 6:03 PM. The air conditioner provides cooling for 1296 hours.

Figure 39 shows the seven-day moving average indoor and outdoor dew point temperatures for summer. The indoor dew point temperature average is higher than the outdoor dew point temperature average throughout this period. It should be noted that the air conditioner does not remain on throughout but rather cycles on and off which gives multiple lines.

The maximum seven-day average indoor dew point temperature is 56.3°F and occurs on May 25 at 7:36 AM (week: May 21 to 28 at 7:36 PM). The air conditioner also turns on during this period.

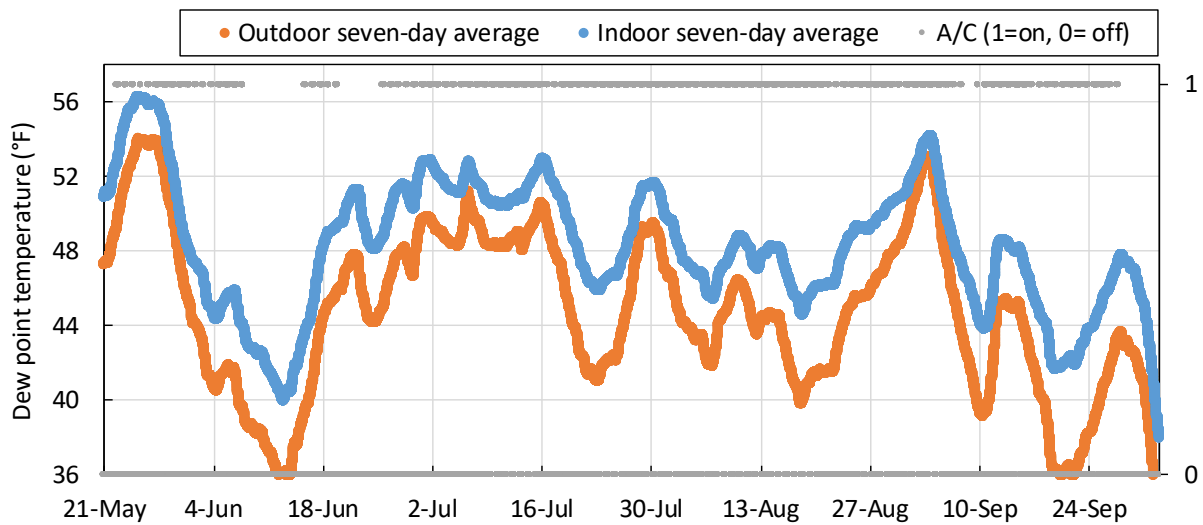


Figure 39: Seven-day moving average indoor (room) and outdoor dew point temperatures for CZ 14 Palmdale for summer. Air conditioner operation (on or off) is shown on the secondary axis.

Figure 40 shows the indoor and outdoor dew point temperatures from May 23 to 28. It can be seen that the indoor dew point temperature exceeds 64°F on four occasions. Furthermore, it can be seen that when the air conditioner turns on, the indoor dew point temperature decreases. However, on many occasions the air conditioner turns off while the indoor dew point temperature is still higher than outdoor dew point temperatures. For most of the period shown, the indoor dew point temperature is higher than that of the outdoor dew point temperature.

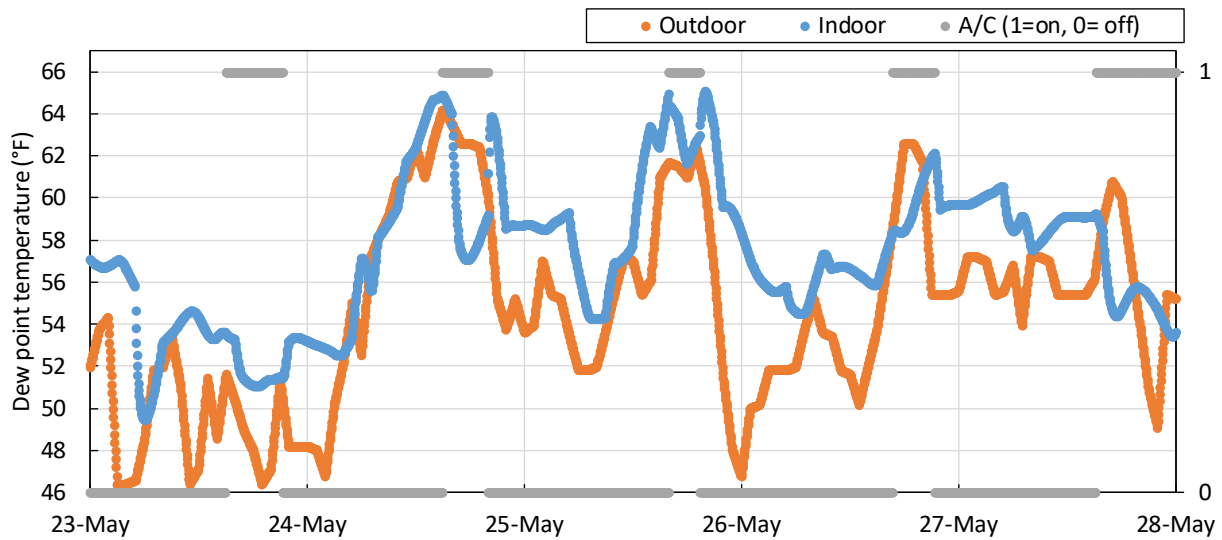


Figure 40: Indoor and outdoor dew point temperatures for CZ 14 Palmdale from May 23 to 28.

Figure 41 shows the distribution of hours for indoor and outdoor dew point temperatures for the month of May. The distribution for indoor dew point temperatures correspond to a higher range compared to the outdoor temperatures.

Unlike previous climate zones and similar to CZ 11, for CZ 14 the distribution for periods with cooling is significant. The indoor dew point temperatures are higher than outdoor temperatures, even for periods when the air conditioner is on.

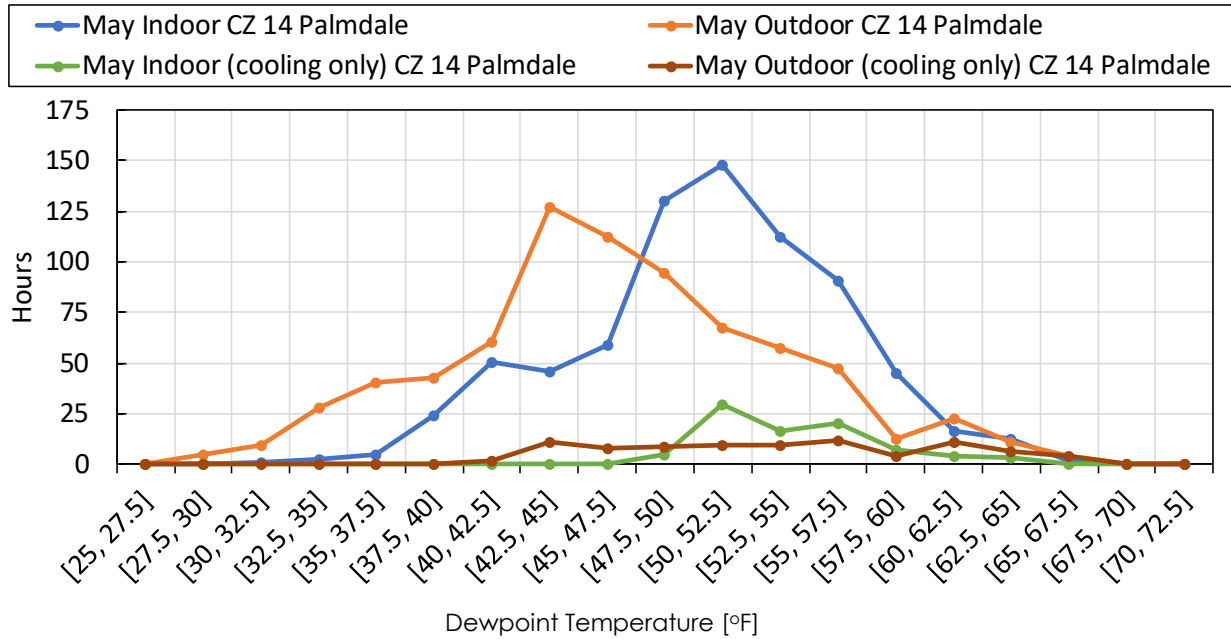


Figure 41: Distribution of hours for indoor and outdoor dew point temperatures for CZ 14 Palmdale for May. Distribution for periods with cooling only also shown.

2.2.15. Climate Zone 15 - Palm Springs

The climate zone 15 CBECC-Res simulation results indicate that the air conditioner cooling period is from March 15, 4:00 PM to October 31, 11:36 PM. Thus CZ 15 has the longest period for which cooling is required. The air conditioner provides cooling for 2783 hours.

Figure 42 shows the seven-day moving average indoor and outdoor dew point temperatures for summer. Aside from May 17 to September 15, the indoor dew point temperature average is higher than the outdoor dew point temperature average. There is a peak in both indoor and outdoor dew point temperatures towards the end of the season in November. The air conditioner also turns on close to this period.

The maximum seven-day average indoor dew point temperature is 55.0°F and occurs on August 16 at 1:09 AM (week: August 12 to 19 at 1:09 PM). The air conditioner also turns on during this period.

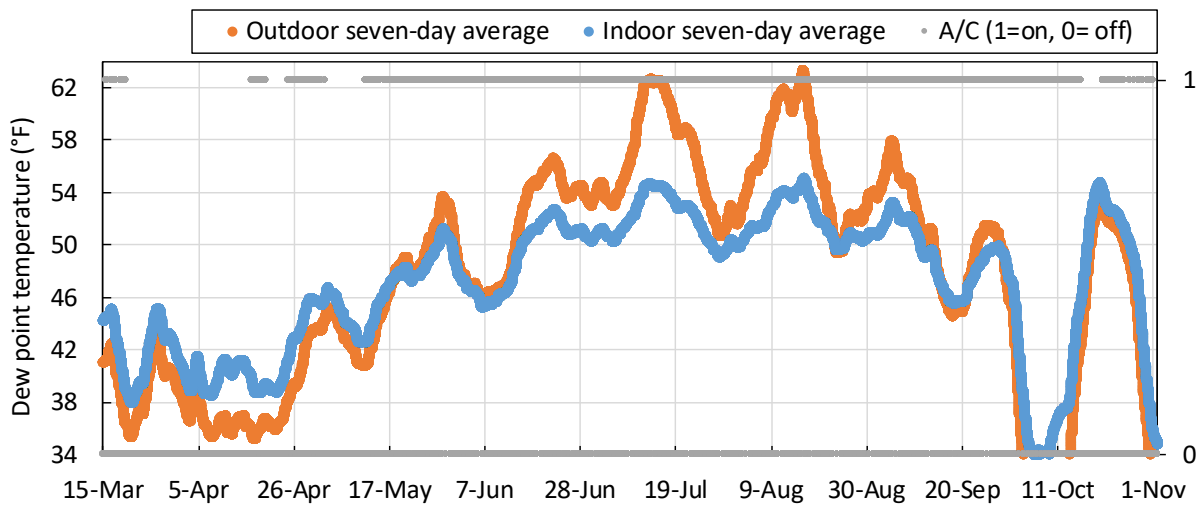


Figure 42: Seven-day moving average indoor (room) and outdoor dew point temperatures for CZ 15 Palm Springs for summer. Air conditioner operation (on or off) is shown on the secondary axis.

Figure 43 shows the indoor and outdoor dew point temperatures from August 14 to 18. It can be seen that the indoor dew point temperature exceeds 64°F on two occasions. However, on both occasions when the air conditioner turns on, the indoor dew point temperature decreases rapidly. For most of the period shown, the indoor dew point temperature is lower than the outdoor dew point temperature.

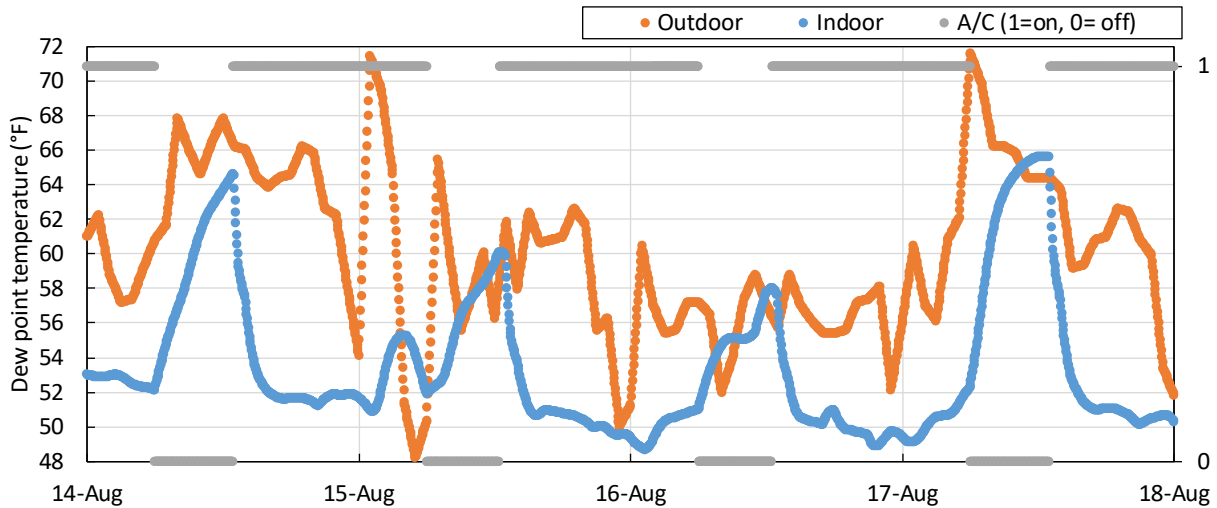


Figure 43: Indoor and outdoor dew point temperatures for CZ 15 Palm Springs from May 23 to 28.

Figure 44 shows the distribution of hours for indoor and outdoor dew point temperatures for the month of August. The distribution for indoor dew point temperatures correspond to a higher range compared to the outdoor temperatures.

For CZ 15, out of the total 744 hours of August, the air conditioner is on for 585 hours. This extensive cooling period is reflected in the figure and the distribution for periods with cooling appear similar to the total distribution. Due to the extensive cooling, the indoor dew point temperatures are lower than outdoor temperatures.

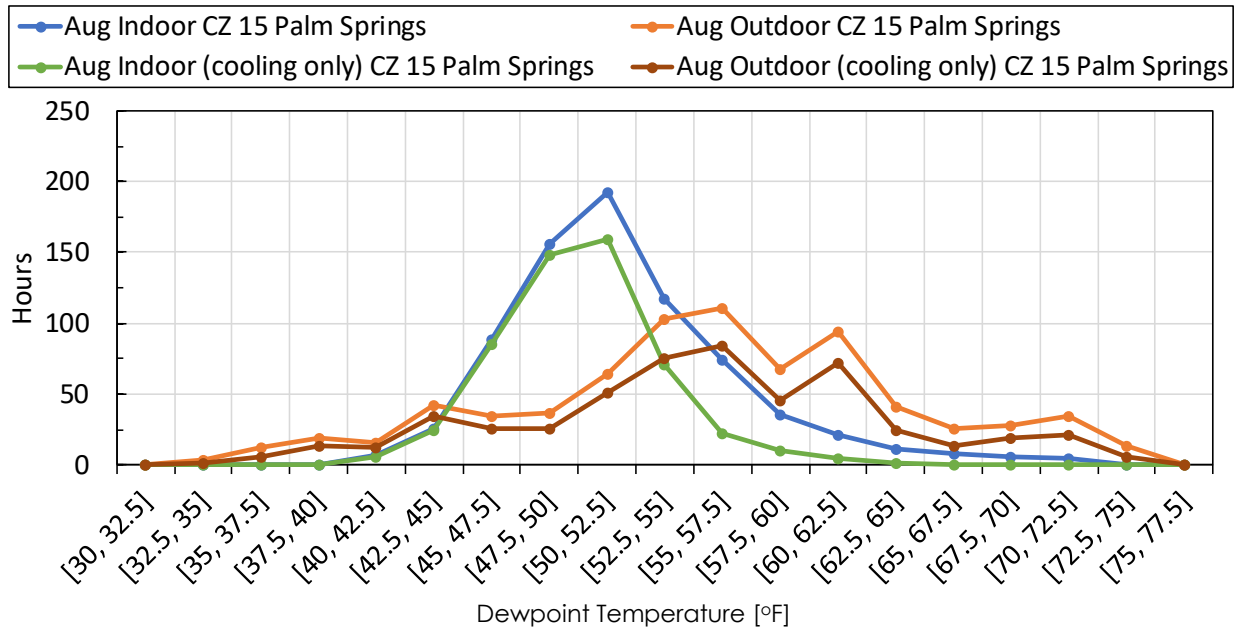


Figure 44: Distribution of hours for indoor and outdoor dew point temperatures for CZ 15 Palm Springs for August. Distribution for periods with cooling only also shown.

2.2.16. Climate Zone 16 - Blue Canyon

The climate zone 16 CBECC-Res simulation results indicate that the air conditioner cooling period is from July 1, 4:27 PM to September 25, 5:15 PM. The air conditioner provides cooling for 248 hours. Figure 45 shows the seven-day moving average indoor and outdoor dew point temperatures for summer. It is clear that the indoor dew point temperature average is 5°F to 8°F higher than the outdoor dew point temperature average.

The maximum seven-day average indoor dew point temperature is 55.2°F and occurs on July 29 at 11:30 PM (week: July 26 to August 2 at 11:30 AM). The air conditioner also turns on during this period.

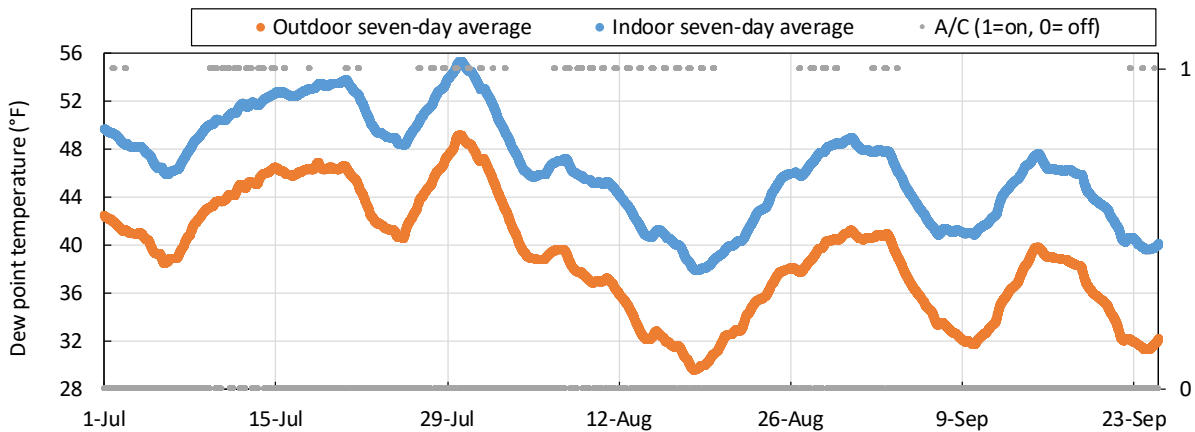


Figure 45: Seven-day moving average indoor (room) and outdoor dew point temperatures for CZ 16 Blue Canyon for summer. Air conditioner operation (on or off) is shown on the secondary axis.

Figure 46 shows the indoor and outdoor dew point temperatures from July 20 to August 2. It can be seen that the indoor dew point temperature exceeds 62°F on several occasions, however, the temperatures are low compared to previous climate zones. As expected when the air conditioner turns on, the indoor dew point temperature decreases rapidly. However, the air conditioner cycles on for very short durations and for almost the entire period shown, the indoor dew point temperature is higher than the outdoor dew point temperature.

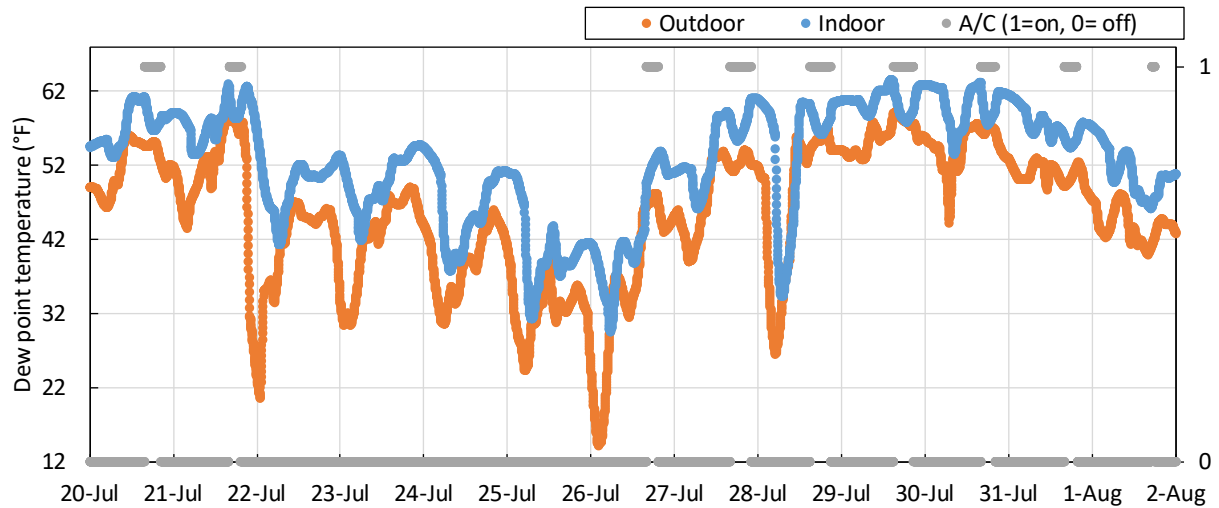


Figure 46: Indoor and outdoor dew point temperatures for CZ 16 Blue Canyon from July 20 to Aug 2.

Figure 47 shows the distribution of hours for indoor and outdoor dew point temperatures for the month of July. The distribution for indoor dew point temperatures correspond to a higher range compared to the outdoor temperatures. This is true even for the brief periods when the air conditioner is on although the difference between indoor and outdoor is less pronounced for the period when the air conditioner is on.

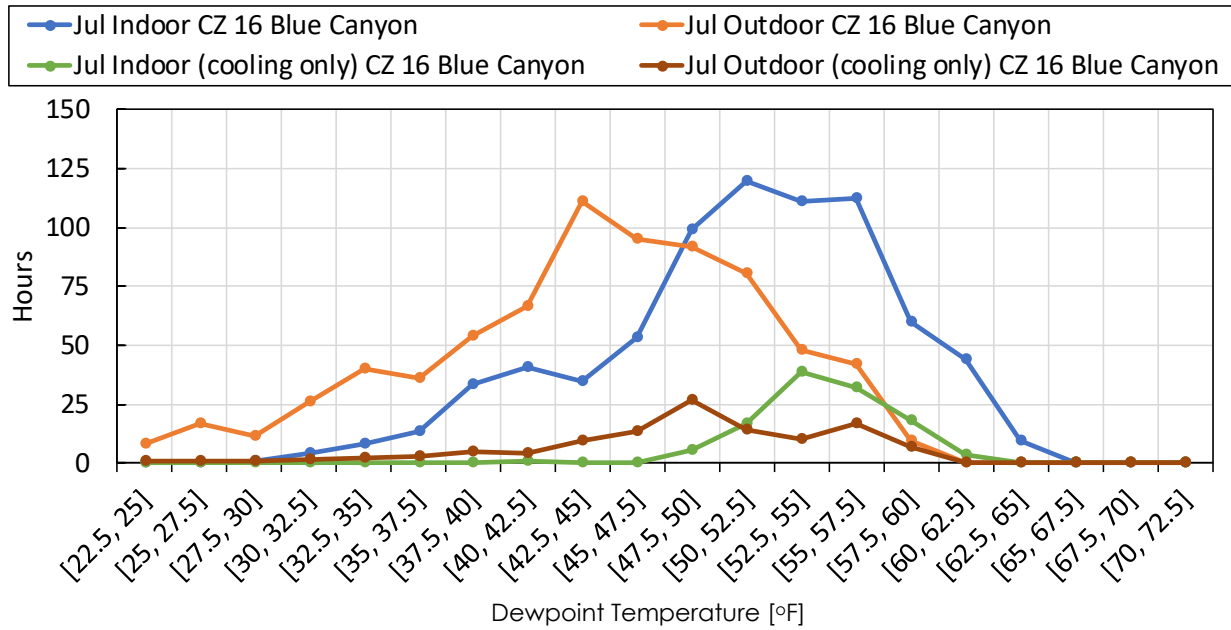


Figure 47: Distribution of hours for indoor and outdoor dew point temperatures for CZ 16 Blue Canyon for July. Distribution for periods with cooling only also shown.

2.2.17. Comparison: indoor CBECC-Res dew point temperatures and field measurements

In this section, the CBECC-Res model results are compared to the indoor CA humidity field data from a previous report (prepared by Proctor Engineering). The geographical distribution of the homes represented in the sample within that study was:

1. CZ 6, Los Angeles 68%
2. CZ 13, Fresno 27% (Central Valley)
3. CZ 15, Palm Springs 5% (Imperial Valley)

Figure 48 to Figure 52 illustrate the distribution of hours for indoor dew point temperatures from the CBECC-Res results for each of the three climate zones from May to September. In order to allow comparison to the field data, individual climate zone CBECC-Res results were used to calculate a weighted-average distribution. The weighting of each climate zone was set equal to the percentage of homes in the field study that were located in the given climate zone. Since 68% of the homes from the field data are located in LA, the CZ 6 results heavily influence the CBECC-Res weighted-average distribution. The results from the field data are also shown for comparison.

It can be seen that the CBECC-Res results for CZ 6, LA, indicate a very high indoor dew point temperature. This is because, according to the CBECC-Res model results, the air conditioner remains off for most of the year. From May to August, the CBECC-Res weighted average distributions indicate a much higher indoor dew point temperature distribution than the field study. For the month of September, the distributions are comparable (although the CBECC-Res results are still higher than field measurements). Possible reasons for the difference are differences in house type, occupant behavior and set-points.

For the given comparison, the CBECC-Res results would likely predict higher indoor dew point temperatures than those observed in the field. The CBECC-Res model results (indoor-air dry-bulb

temperature and dew point temperature) were used as an input for the condensation-evaporation model. It is likely that if actual field measurements were used, the predicted mass of water condensed on the duct surface would be lower.

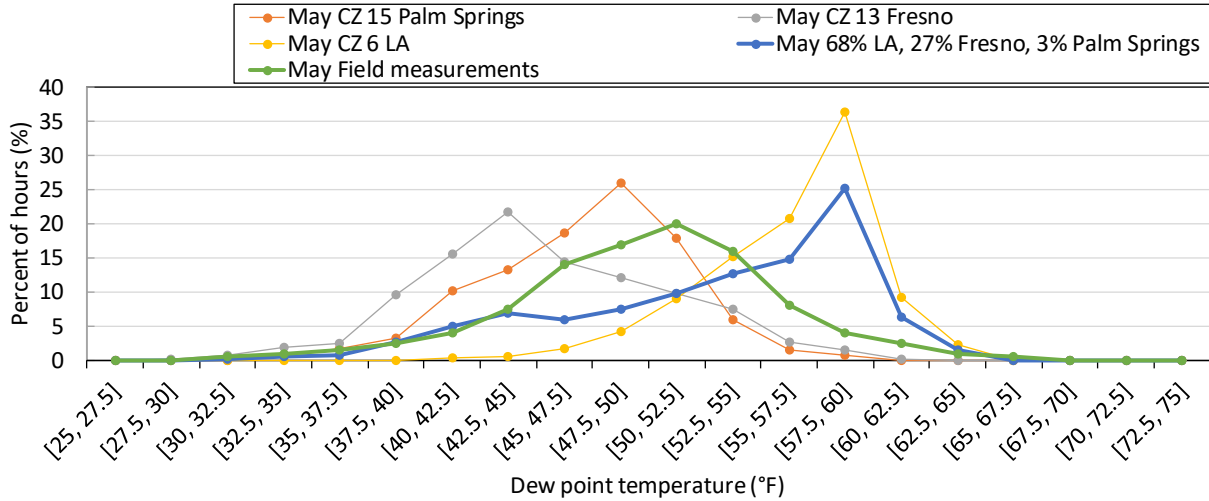


Figure 48: Percentage of hours for indoor dew point temperatures for the month of May for 68% CZ 6-LA, 27% CZ 13-Fresno and 3% CZ 15-Palm Springs from CBECC-Res simulations and from field measurements.

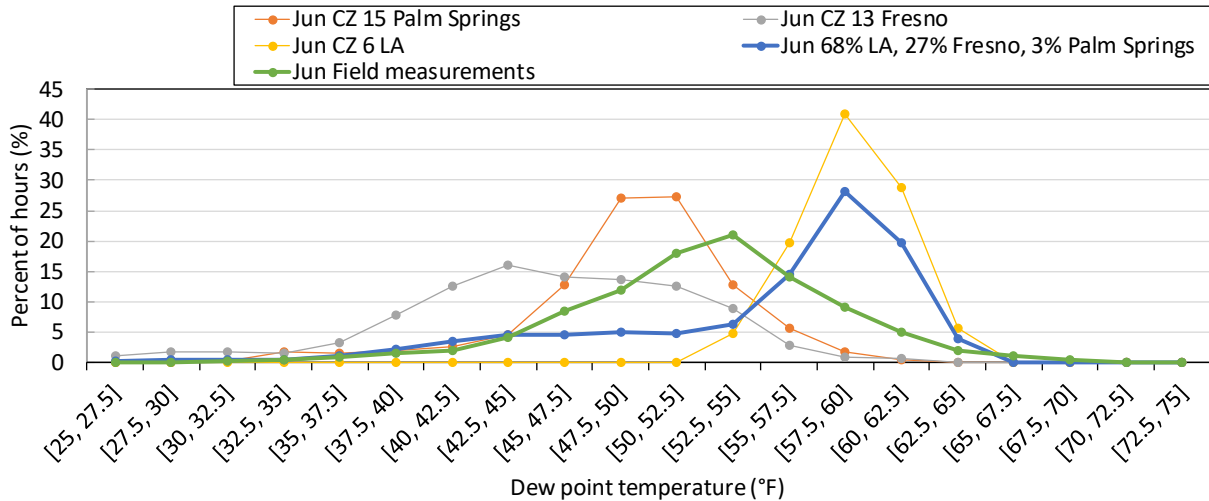


Figure 49: Percentage of hours for indoor dew point temperatures for the month of June for 68% CZ 6-LA, 27% CZ 13-Fresno and 3% CZ 15-Palm Springs from CBECC-Res simulations and from field measurements.

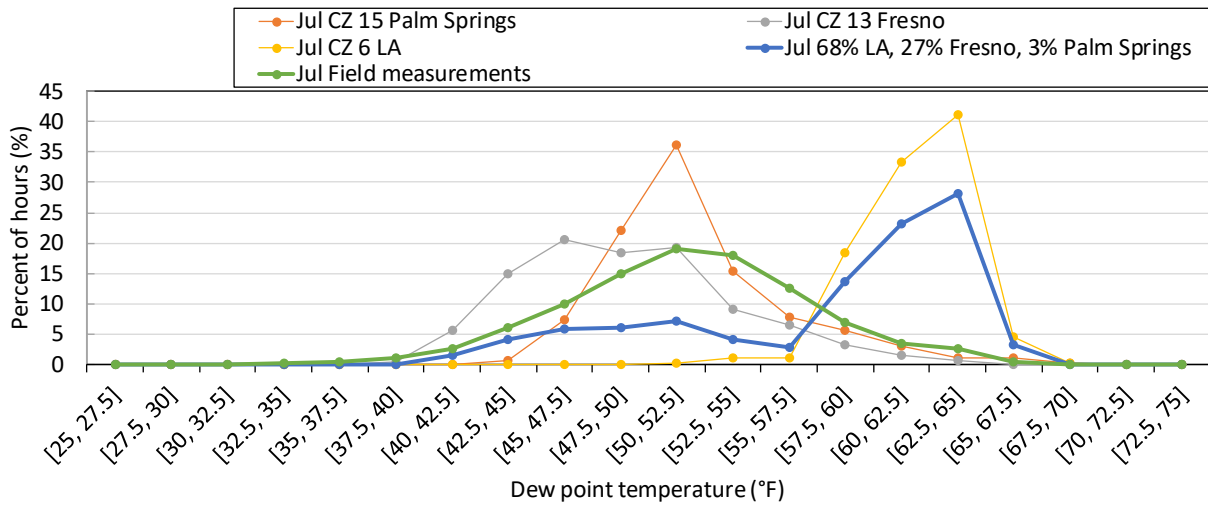


Figure 50: Percentage of hours for indoor dew point temperatures for the month of July for 68% CZ 6-LA, 27% CZ 13-Fresno and 3% CZ 15-Palm Springs from CBECC-Res simulations and from field measurements.

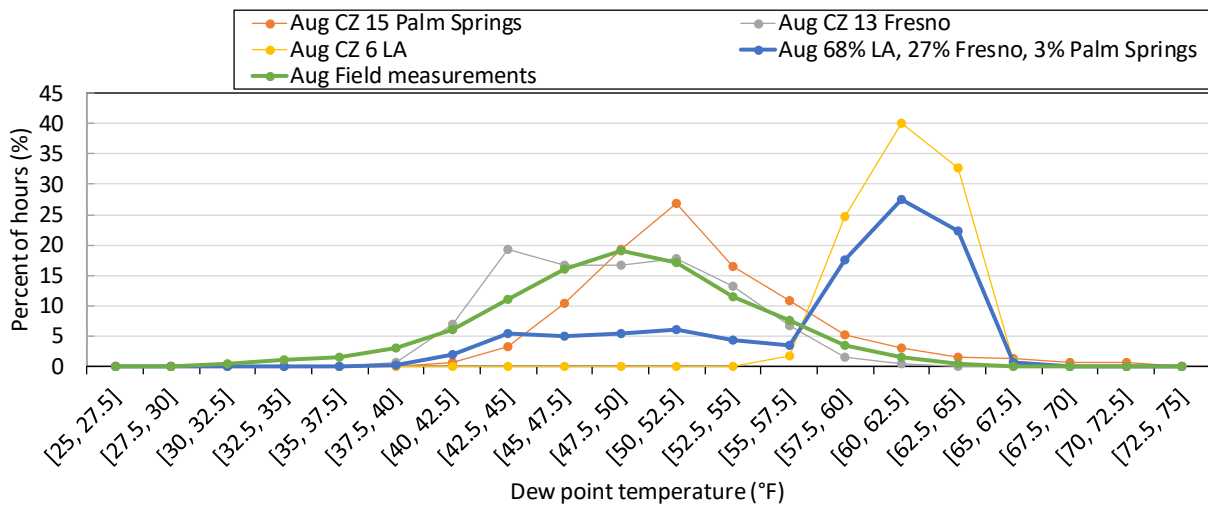


Figure 51: Percentage of hours for indoor dew point temperatures for the month of August for 68% CZ 6-LA, 27% CZ 13-Fresno and 3% CZ 15-Palm Springs from CBECC-Res simulations and from field measurements.

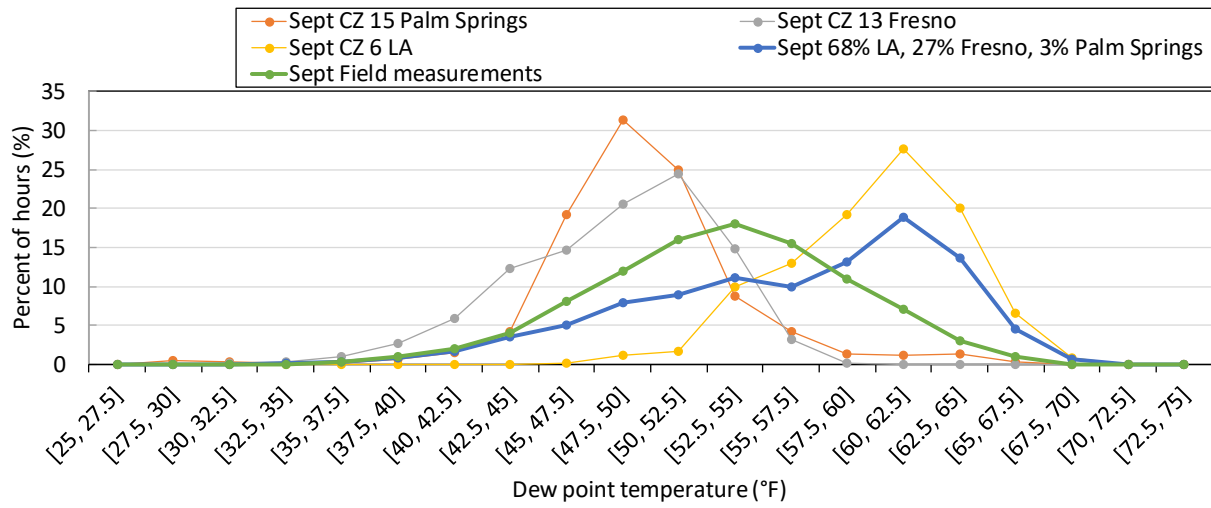


Figure 52: Percentage of hours for indoor dew point temperatures for the month of September for 68% CZ 6-LA, 27% CZ 13-Fresno and 3% CZ 15-Palm Springs from CBECC-Res simulations and from field measurements.

3. Modelling condensation/evaporation in vertical stud cavities with uninsulated ducts

3.1. Methodology

Figure 53 shows a simplified schematic of the cross-section of a duct in a vertical stud cavity. Only half of the cross section is shown and symmetry is assumed across the central plane. The convection coefficient for each surface is also shown.

When the air conditioner is turned on, cold air starts to flow inside the duct. Figure 54 shows the resistance-capacitance network diagram for the heat transfer process under these circumstances. The forced convection process inside the duct (coefficient represented as h_{di}) cools down the duct wall. The heat transfer is represented as q_{dai} while the capacitance of the duct wall is represented by C_d . At this stage, if the air inside the stud cavity is humid enough and duct surface is sufficiently cold, the moisture in the cavity air condenses on the duct surface. The resulting heat transfer is represented as $q_{condensation}$. At the same time heat is also transferred to the duct surface from the air in the cavity (q_{ca}) through natural convection (h_c). The capacitance of the air in the cavity is represented by C_c . When the air inside the stud cavity becomes colder than the air in the room, stack effect causes air to flow through any leaks at different heights in the vertical cavity. For the current analysis, the cavity is assumed to have 0.65-inch diameter holes both top and bottom, which means that the entire cavity leakage consists of top and bottom hole of 0.33 in² each.

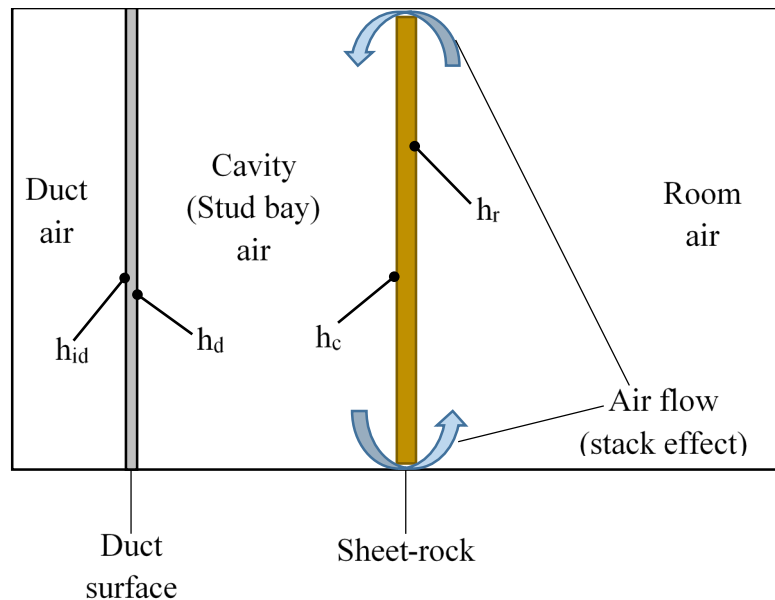


Figure 53: Cross-section of stud cavity (half section). The duct surface, sheetrock surface and room are also shown. The convection coefficients for each surface are also shown.

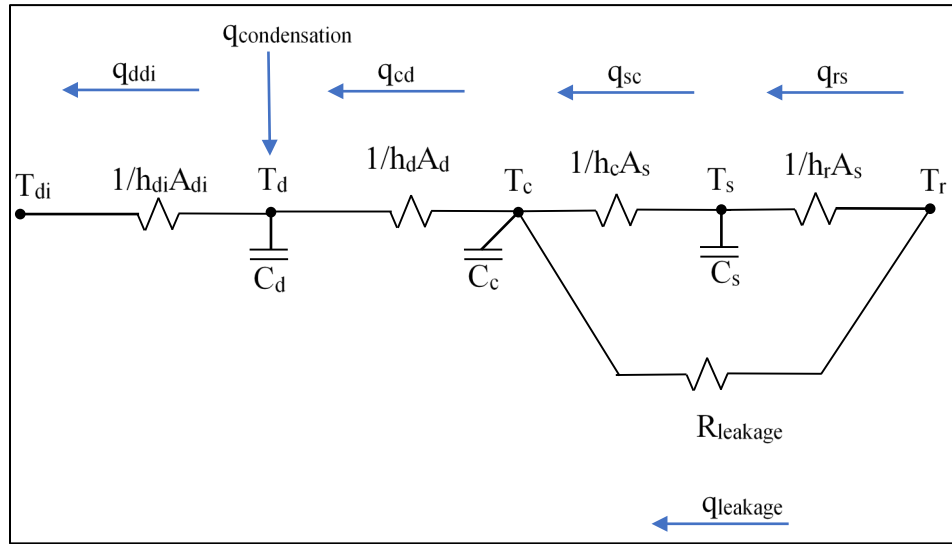


Figure 54: The resistance and capacitance diagram for the stud bay heat transfer process.

When the air inside the cavity is sufficiently cold, natural convection between the sheetrock inner surface and the cavity air is set up. With the passage of time, the sheetrock temperature also decreases and natural convection between the sheetrock outer surface and the room air is set up.

Needless to say, the model is based on certain approximations. The assumptions and approximations used to simplify the model are as follows:

1. Heat transfer along the vertical length of the sheetrock and the duct was neglected. Only heat transfer perpendicular to the thickness of the sheetrock and duct wall was modeled.
2. The natural convection coefficients depend on the temperature difference between the air and the surface. The surface and air temperatures depend on the heat transfer, which in turn depend on the convection coefficients. Therefore, an explicit formulation (using values from the previous time step) was used to develop the equations for the condensation-evaporation model.
3. The conduction resistance of the uninsulated duct wall was considered negligible compared to the convection resistances. Resistances due to the presence of condensed water on the duct surface was also ignored.
4. The conduction resistance of the sheetrock was considered negligible compared to the convection resistances.
5. The temperature of the air inside the duct (T_{di}) was assumed to be 55°F when the air conditioner is on, and is assumed to not change over the height of the duct. When the air conditioner turns off, heat transfer from the duct surface to the air inside the duct is neglected (i.e. the capacitance of the air inside the duct is ignored).
6. The latent heat of vaporization (h_{fg}) is 1048 BTU/lb. The air density, specific heat capacity etc. are also assumed to be constant.
7. The thermal capacitance and mass of the air inside the room is much larger than the cavity. Therefore, the cavity heat and mass transfer are assumed to have negligible impact on the room temperature and humidity. The indoor temperature and humidity from the CBECC-Res model results are used as an input for the condensation-evaporation model.

8. Initially (i.e. before the air conditioner is turned on for the first time), all the nodes are at room temperature for the first time-step. The humidity of the cavity air is also assumed to be initially equal to room humidity.

In order to derive the equations for the model, an energy balance is carried out at each node. The energy balance for duct surface is given below:

$$\dot{E}_{in} + \dot{E}_{gen} = \dot{E}_{out} + \dot{E}_{stored} \quad (1)$$

$$\therefore \dot{E}_{gen} = 0$$

$$q_{condensation} + q_{cd} = q_{ddi} + \frac{C_d(T_d^{+\Delta t} - T_d)}{\Delta t} \quad (2)$$

Rearranging:

$$T_d^{+\Delta t} = \frac{\Delta t (q_{condensation} + q_{cd} - q_{ddi})}{C_d} + T_d \quad (3)$$

where

Δt is the time-step, and

$T_d^{+\Delta t}$ is the duct temperature at the next time-step.

The heat transfer rates and capacitance in equation 3 are given as follows:

$$q_{condensation} = \dot{m}_{condensation} \times h_{fg} \quad (4)$$

$$q_{cd} = h_d A_d (T_c - T_d) \quad (5)$$

$$q_{ddi} = h_{di} A_{di} (T_d - T_{di}) \quad (6)$$

$$C_d = \rho_d V_d c_d \quad (7)$$

The convection coefficient between the duct and the air inside the duct (h_{di}) is calculated using the following Dittus-Boelter equations [3] for fully developed internal flow in a smooth circular pipe of diameter d :

$$h_{di} = \frac{k_{air} Nu}{d} \quad (8)$$

$$Nu = 0.023 Re^{0.8} Pr_{air}^{0.4} \quad (9)$$

$$Re = \frac{\rho_{air} v_{air} d}{\mu_{air}} \quad (10)$$

where

Pr_{air} is the Prandtl number of air.

The convection coefficient between the duct and the cavity air (h_d) is calculated using the following equations for natural convection from the ASHRAE Handbook of Fundamentals []:

$$h_d = 0.272 \left(\frac{T_d - T_c}{L} \right)^{1/4} \quad 10^5 < Ra < 10^9 \quad (11)$$

$$h_d = 0.182 (T_d - T_c)^{1/3} \quad Ra > 10^9 \quad (12)$$

where

L is the vertical height of the surface and

Ra is the Rayleigh number and is given as:

$$Ra = Gr Pr_{air} \quad (13)$$

$$Gr = \frac{g \beta (T_d - T_c) L^3}{\left(\frac{\mu}{\rho} \right)^2} \quad (14)$$

$$\beta = \frac{1}{T_c} \quad (15)$$

The other natural convection coefficients (h_r and h_c) are calculated using equations similar to equations 11 to 15.

The rate at which water is condensed ($\dot{m}_{condensation}$) on the duct depends on the mass transfer coefficient (h_{mc}) and the difference between the absolute humidity of the cavity (w_c) and saturation humidity that corresponds to the duct surface temperature ($w_{sat@T_d}$). The rate of condensation is given as:

$$\dot{m}_{condensation} = h_{mc} A_d (w_c - w_{sat@T_d}) \quad (16)$$

Since the transport mechanism governing the heat transfer from the air in the cavity to the duct surface is same mechanism that controls the mass transport of water from the cavity to the duct surface, the mass transfer coefficient (h_{mc}) can therefore be calculated using the following equation [4]:

$$h_{mc} = \frac{h_d}{c_c} \quad (17)$$

The energy balance for the air in the stud bay cavity gives the following equation:

$$q_{condensation} + q_{leakage} + q_{sc} = q_{cd} + \frac{C_c (T_c^{+\Delta t} - T_c)}{\Delta t} \quad (18)$$

$$T_c^{+\Delta t} = \frac{\Delta t (q_{condensation} + q_{leakage} + q_{sc} - q_{cd})}{C_c} + T_c \quad (19)$$

where

$q_{leakage}$ is the heat transfer due to the air flow between the cavity and the room and is calculated using the following set of equations [5]:

$$q_{leakage} = \dot{m}_{leakage} c_{air} (T_r - T_c) \quad (18)$$

$$\dot{m}_{leakage} = \rho_{air} A_{hole} \sqrt{\frac{2\Delta P}{\rho_{air}}} \quad (19)$$

$$\Delta P = \frac{g\rho_{air}L(T_r - T_c)}{2T_c} \quad (20)$$

q_{sc} represents the heat transfer between the sheetrock and the cavity air and is calculated as:

$$q_{sc} = h_c A_s (T_s - T_c) \quad (21)$$

The energy balance for the sheetrock results in the following equation:

$$q_{rs} = q_{sc} + \frac{C_s (T_s^{+\Delta t} - T_s)}{\Delta t} \quad (22)$$

$$T_s^{+\Delta t} = \frac{\Delta t (q_{rs} - q_{sc})}{C_s} + T_s \quad (23)$$

where

q_{rs} represents the heat transfer from the room air to the duct surface and is calculated as:

$$q_{rs} = h_r A_s (T_r - T_s) \quad (24)$$

Finally, a mass balance for water in the cavity air is carried out, and this yields the following equations:

$$\dot{m}_{in} = \dot{m}_{out} + \dot{m}_{stored} \quad (25)$$

$$\dot{m}_{leakage} (w_r - w_c) = \dot{m}_{condensation} + m_{air,c} (w_c^{+\Delta t} - w_c) \quad (26)$$

$$w_c^{+\Delta t} = \frac{\dot{m}_{leakage} (w_r - w_c) - \dot{m}_{condensation}}{m_{air,c}} + w_c \quad (27)$$

where

$m_{air,c}$ is the mass of air inside the cavity.

The equations used to model the evaporation process (when the air conditioner cycles off) are very similar to the equations presented thus far. The changes are:

1. $q_{condensation}$ is replaced by $q_{evaporation}$ and is opposite in direction
2. $\dot{m}_{condensation}$ is replaced by $\dot{m}_{evaporation}$ and is opposite in direction
3. In equation 3, q_{ddi} becomes zero
4. The temperature difference terms in the natural convection coefficients are reversed

Since the model is explicit, it was found that the time-step for the model needed to be 0.25 minutes in order to ensure convergence. The subsequent section presents the results from the condensation-evaporation model for various climate zones. The results for reference climate zone 13 Fresno are presented first and discussed extensively, after which the results for other climate zones are presented. As mentioned in section 2, there are three climate zones for which the air conditioner remains off

throughout the year. Obviously, condensation cannot take place in houses located in these climate zones, and thus condensation-evaporation was not modelled for these climate zones.

3.2. Detailed results for climate zone 13 - Fresno

The condensation-evaporation process was modelled for a house located in climate zone 13 (Fresno) for an entire year. The results indicate that out of 8760 hours of the year, condensed water is present on the duct surface for slightly less than 24.5 hours. The maximum mass of water present on the duct surface over a period of one year is 0.0013 lbs. (which is equal to a volume of 0.6 cm^3) and occurs on June 30 at 4:15 PM. The variation in the mass of water present on the duct for this day is shown in Figure 55. At 3:00 PM the air conditioner turns on. Condensation starts at 3:01 PM, continuing until 4:15 PM, after which evaporation starts. By 5:48 PM, all the water has evaporated.

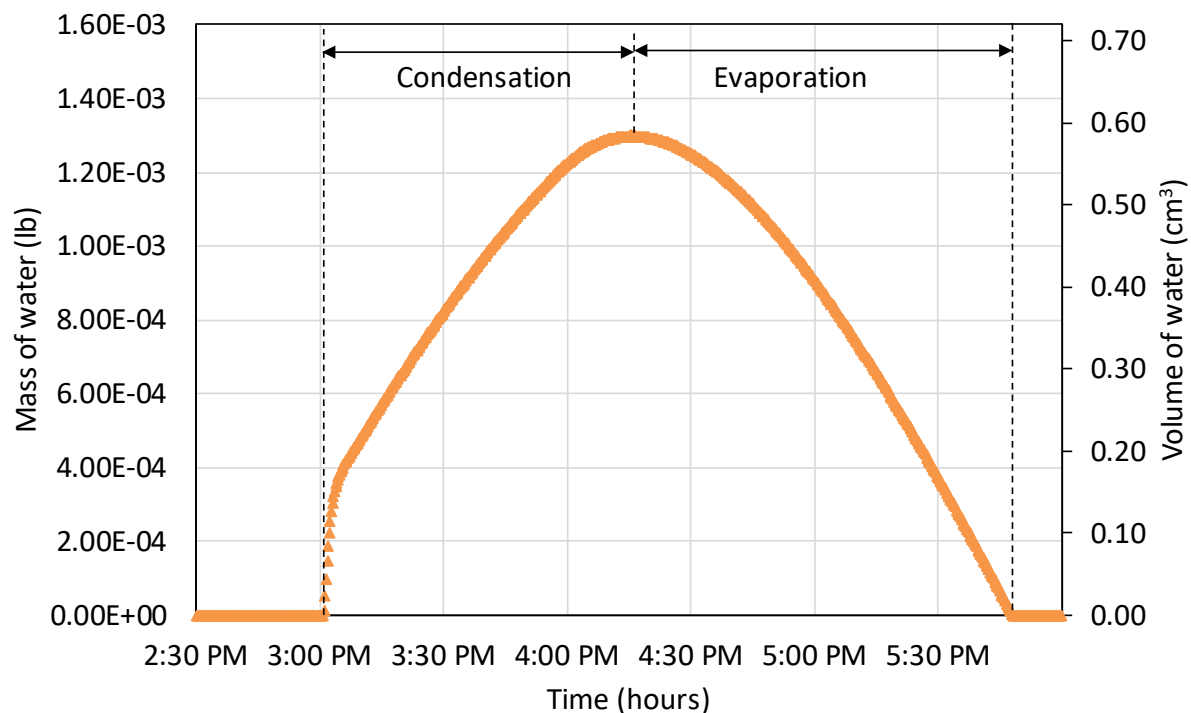


Figure 55: Mass of condensed water present on the duct surface in Climate Zone 13 for top and bottom leaks of 0.33 in^2 each (June 30). This date experiences the peak condensation of the year.

Figure 56 plots the temperatures for the center of the sheetrock, duct surface, room air, and cavity air for the same time period as Figure 55 (June 30, from 2:30 PM to 6:00 PM). Since the duct has a small thermal capacitance, it cools down rapidly when the air conditioner turns on at 3:00 PM. The thermal capacitance of the cavity air is lower than that of the duct (less than 1/10th of the duct capacitance). As a result, the cavity air also cools down rapidly. The cavity is not in direct contact with the air-conditioned room air, so its temperature is in between the duct and room temperatures due to the presence of resistances. Since the thermal capacitance of the sheetrock is much higher (more than 180 times that of the cavity air), it takes much longer to cool down. At 4:00 PM, the thermostat set point for the room air is reduced and the cooling provided by the air conditioner increases. As a result, the room air also starts to gradually cool down.

Whether condensation will take place depends on the difference between the saturated absolute humidity corresponding to the duct surface temperature and the absolute humidity of the air in the cavity. If the cavity absolute humidity is higher than the saturated absolute humidity of the duct, condensation will take place in that time step. When the cavity air is drier, if condensed water is present on the surface of the duct, evaporation will take place. As the duct temperature decreases (due to the cavity air getting colder), the saturated absolute humidity of the duct surface also decreases. Figure 57 shows the saturated absolute humidity at the duct surface temperature, the room-air absolute humidity and cavity-air absolute humidity. It can be seen that the room humidity drops below the cavity humidity at 4:15 PM, which is why the condensation stops at this time. Figure 57 also shows that the humidity of the cavity starts to decrease rapidly after 5:48 PM when all the water on the duct surface has evaporated.

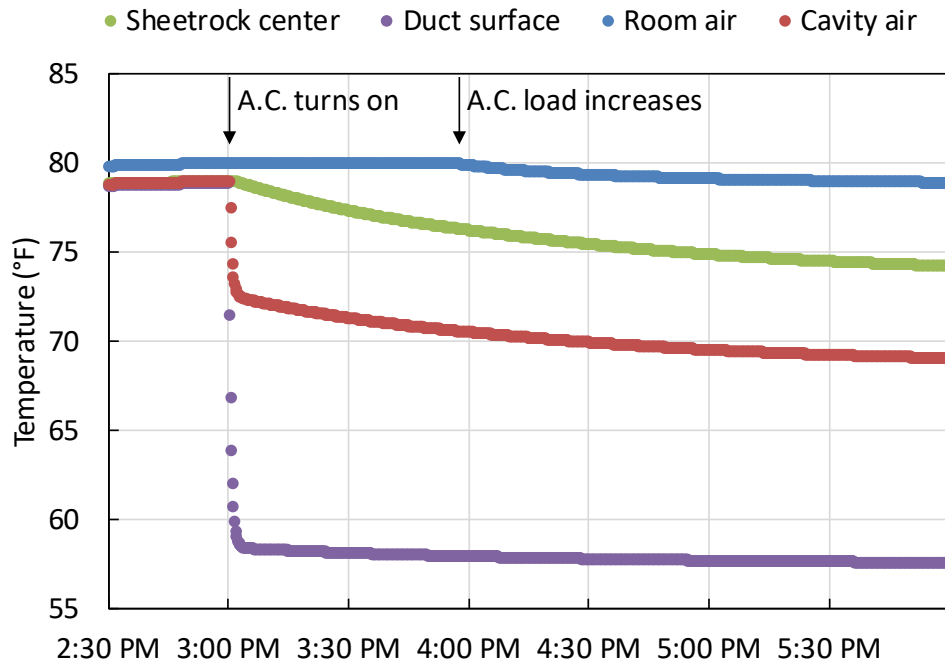


Figure 56: Sheetrock-center, duct surface, room-air and cavity-air temperatures on date with maximum duct-surface condensation in CZ 13 (June 30)

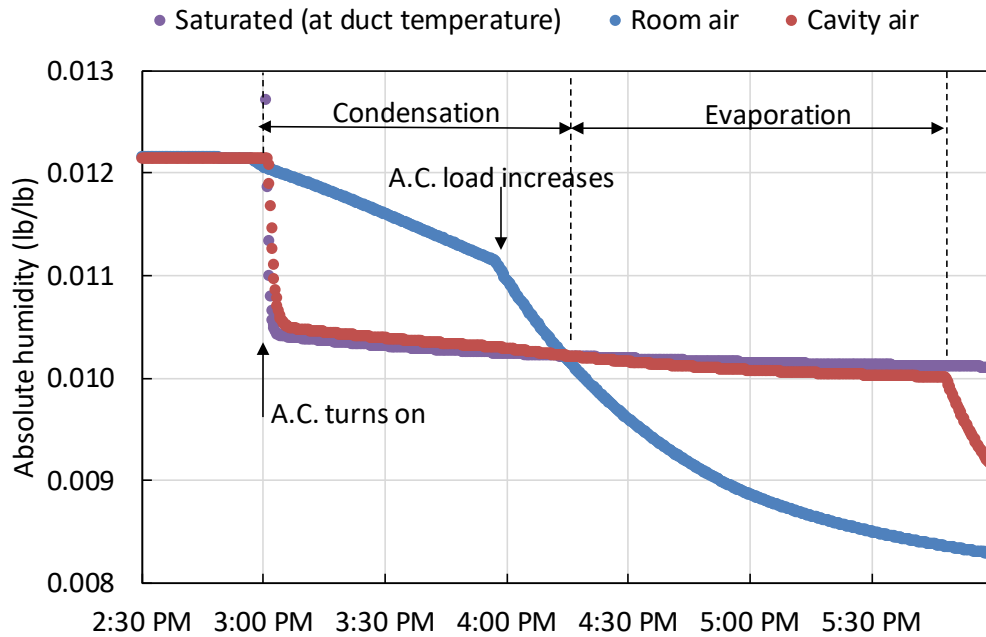


Figure 57: Saturated absolute humidity at duct surface temperature, room air absolute humidity and cavity air absolute humidity on day with maximum duct surface condensation in CZ 13 (June 30)

To understand why the room temperature and humidity fall after 4:00 PM, Figure 58 shows the sensible and latent cooling load for CZ 13, Fresno for June 30. The room dry-bulb temperature and the set-point temperatures are shown on the secondary axis (°F). After 4:00 PM the difference between the room temperature and the set-point becomes much higher than difference at 3:00 PM. As a result, the air conditioner runs at full capacity (meaning continuously). This is indicated by the sudden increase in the sensible and latent cooling load. The increased capacity cools down the room and removes moisture from the air inside the room.

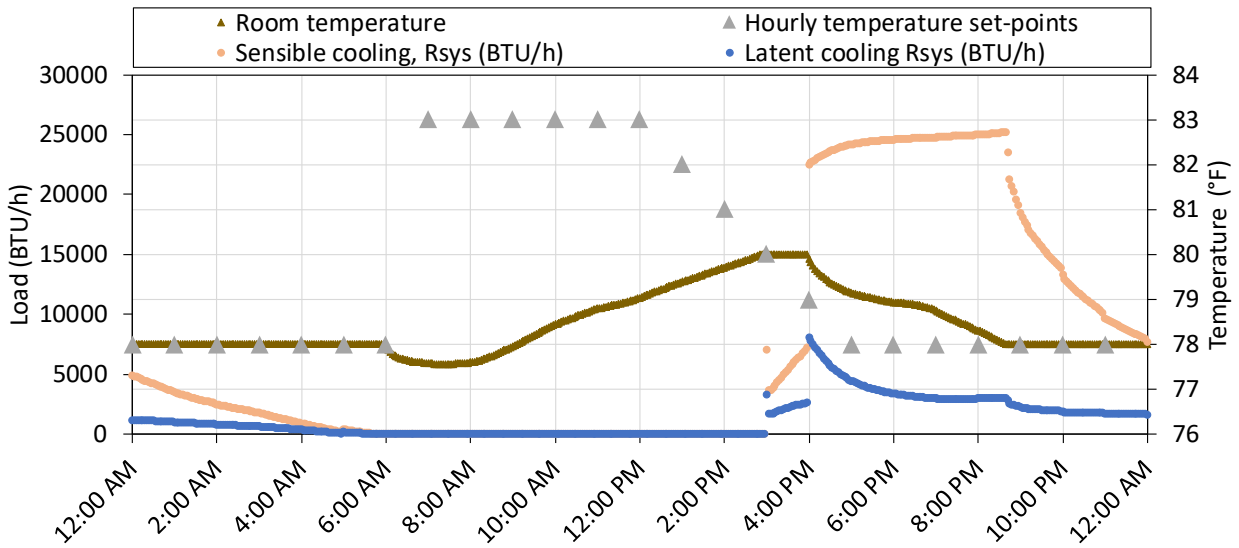


Figure 58: Sensible and latent cooling loads for June 30 in CZ 13 (Fresno). The room dry-bulb temperature and set-point temperature are plotted on secondary axis

As noted earlier, the results presented thus far are for holes at the top and bottom with an area of 0.33 in² each. Smaller holes would produce a lower air flow through the cavity, which would result in less condensed water during the period when the room air humidity is higher than the cavity humidity. To illustrate this, Figure 59 shows that for holes with an area of 0.08 in² (diameter of 0.32 inches) each, the maximum mass of water condensed decreases to 0.00061 lb which is 53% less than that for 0.33 in² holes. However, the smaller holes also lead to a prolonged evaporation process, as it takes longer for the moisture of the cavity to be removed by the air exchange between the cavity and the room. In this case, the evaporation continues up to 6:35 PM which means water is present on the duct for 42 minutes longer than for the 0.33 in² holes (evaporation ends at 5:48 PM).

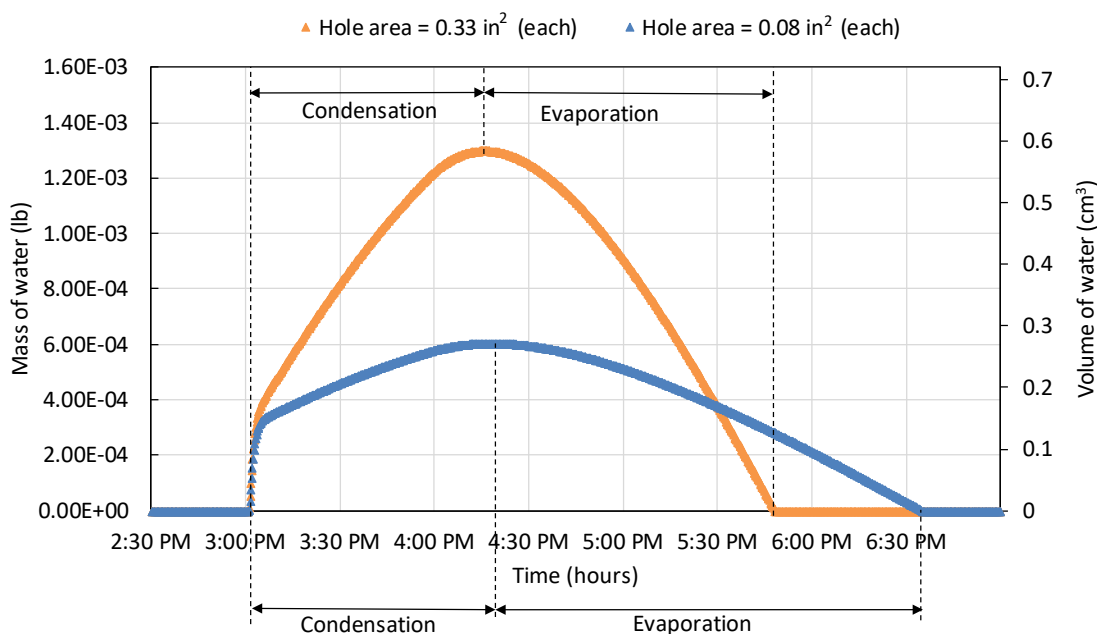


Figure 59: Mass of condensed water present on the duct surface for top and bottom leaks of 0.33 in² each and 0.08 in² each (CZ 13, June 30)

As noted above, all of these results are for ducts that have no radiative heat transfer from their surfaces, corresponding to a super low emissivity surface. This is a worst-case scenario, as this results in the coldest duct surface temperatures. The impact of surface emissivity is investigated in a subsequent section.

3.3. Results for other climate zones

The condensation-evaporation process was modelled for houses located in other climate zones for the months during which the mass of water condensed on the duct surface would be maximum. The indoor dew point temperature and air conditioner operation (from section 2) were used to identify these months.

Table 2 shows the maximum mass and volume of water condensed on the duct surface for each climate zone. The date and time at which this occurs is also tabulated. The maximum mass of water in the stud cavities will be discussed in a subsequent section.

The climate zone with the highest level of condensation is CZ 9 (Burbank) (0.0081 lb. or 3.7 cm³ of water), while the climate zone with the lowest level of condensation is CZ 2 (Santa Rosa). The average mass of water condensed on the duct surface for climate zones with less than 100 hours of cooling is 0.0015 lb while the average for climate zones with more than 100 hours of cooling is 0.0040 lb. It must be noted that these results are for duct surfaces with no radiative heat transfer (i.e. emissivity=0), which means that they represent an upper limit on condensation.

Furthermore, for all climate zones except CZ 4, CZ 7, CZ 14 and CZ 15, the maximum water condensation occurs either in the month of June or July. The implications of these results are discussed in a subsequent section.

Table 2 – Maximum mass of water on duct surface for different climate zones.

Climate zone	Maximum mass of water on duct (lb)	Maximum volume of water on duct (cm ³)	Mass of max water/mass of studs (%)	Date and time for maximum water on duct
Climate zones with less than 100 hours of cooling required				
CZ 2 Santa Rosa	0.000043	0.02	0.0003%	7/1/15 4:07 PM
CZ 4 San Jose	0.0017	0.76	0.012%	8/8/15 7:00 PM
CZ 6 Los Angeles	0.0026	1.2	0.019%	7/25/15 4:41 PM
CZ 7 San Diego	0.0018	0.79	0.013%	9/11/15 5:09 PM
Climate zones with more than 100 hours of cooling required				
CZ 8 Fullerton	0.0029	1.3	0.021%	7/17/15 6:00 PM
CZ 9 Burbank	0.0081	3.7	0.058%	7/9/15 11:48 PM
CZ 10 Riverside	0.0045	2.0	0.032%	7/19/15 8:21 PM
CZ 11 Red Bluff	0.0056	2.5	0.040%	6/22/15 11:45 PM
CZ 12 Sacramento	0.0015	0.70	0.011%	7/27/15 9:00 PM
CZ 13 Fresno	0.0013	0.59	0.0093%	6/30/15 4:15 PM
CZ 14 Palmdale	0.0061	2.7	0.043%	5/25/15 7:27 PM
CZ 15 Palm Springs	0.0028	1.3	0.02%	8/13/15 2:18 PM
CZ 16 Blue Canyon	0.0033	1.5	0.023%	7/29/15 8:45 PM

3.4. Condensation on ducts exposed directly to indoor air

Simulations of the condensation-evaporation model were also run to assess the mass of condensed water on ducts completely exposed to the room air (i.e. ducts in the room rather than in a building cavity). The simulations were run for the period corresponding to the maximum mass of water on the duct for Climate Zone 13. As before, it is assumed that the room air temperature and moisture are not affected by the heat and mass transfer to the duct surface since the mass of air inside the room is very large.

Figure 60 shows the mass and volume of water condensed on an uninsulated duct surface with an emissivity of 0.1 (i.e. low emissivity surface) when it is exposed directly to room air. It can be seen that the maximum moisture condensed for ducts directly exposed to indoor air (0.0017 lbs) is a bit higher than that for the same duct located in a cavity (0.0013 lbs in Figure 59). Unlike the cavity, where the condensation rate is limited by the air flow into the cavity, direct exposure to the indoor air causes moisture condensation to occur at a much higher rate, limited only by the mass transfer coefficient. This is somewhat counteracted by the cavity being cooler than the room (70°F in Figure 56 versus 78°F room temperature in Figure 61), which causes the duct surface to be cooler in the cavity (57.5°F in Figure 56 versus 61°F in Figure 61 for the duct in the room). The maximum condensation occurs at 3:36 PM for in-room ducts. This is earlier than for cavity ducts, for which the maximum occurs at 4:15 PM, due to the condensation stopping sooner for the warmer duct surface in the room. Correspondingly, direct exposure to the dry room air causes more rapid evaporation of the moisture

condensed on the duct in the room. Thus, the time duration of moisture being present on the duct is shorter for in-room ducts.

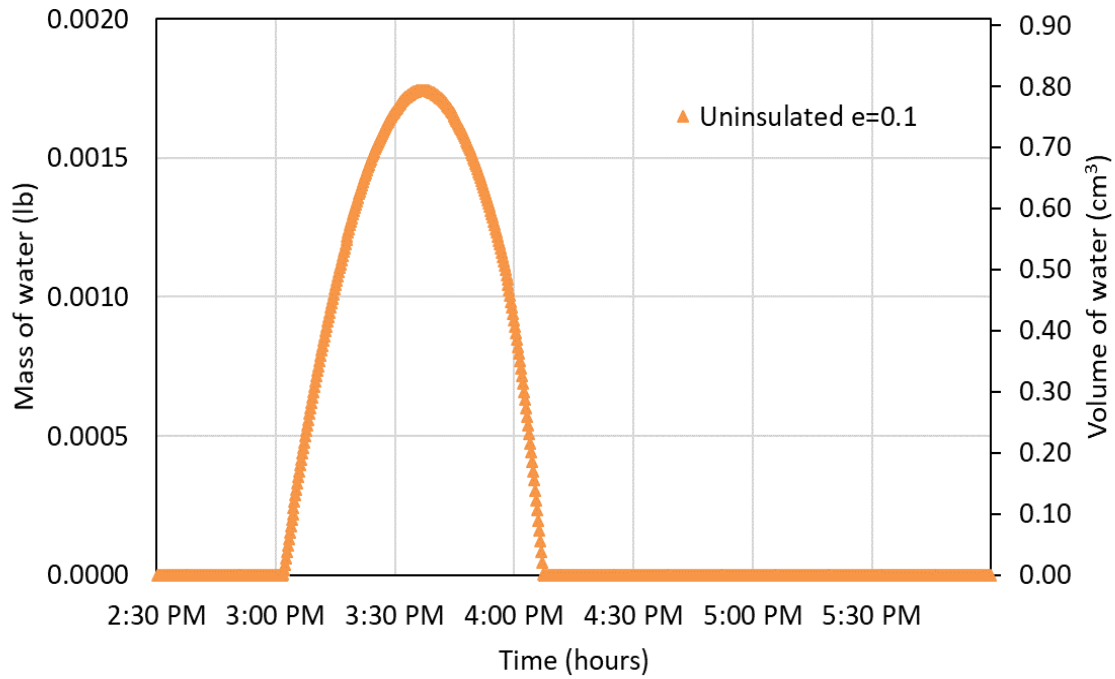


Figure 60: Mass and volume of water condensed on uninsulated duct surfaces with an emissivity of 0.1, and exposed completely to room air (June 30 in CZ 13).

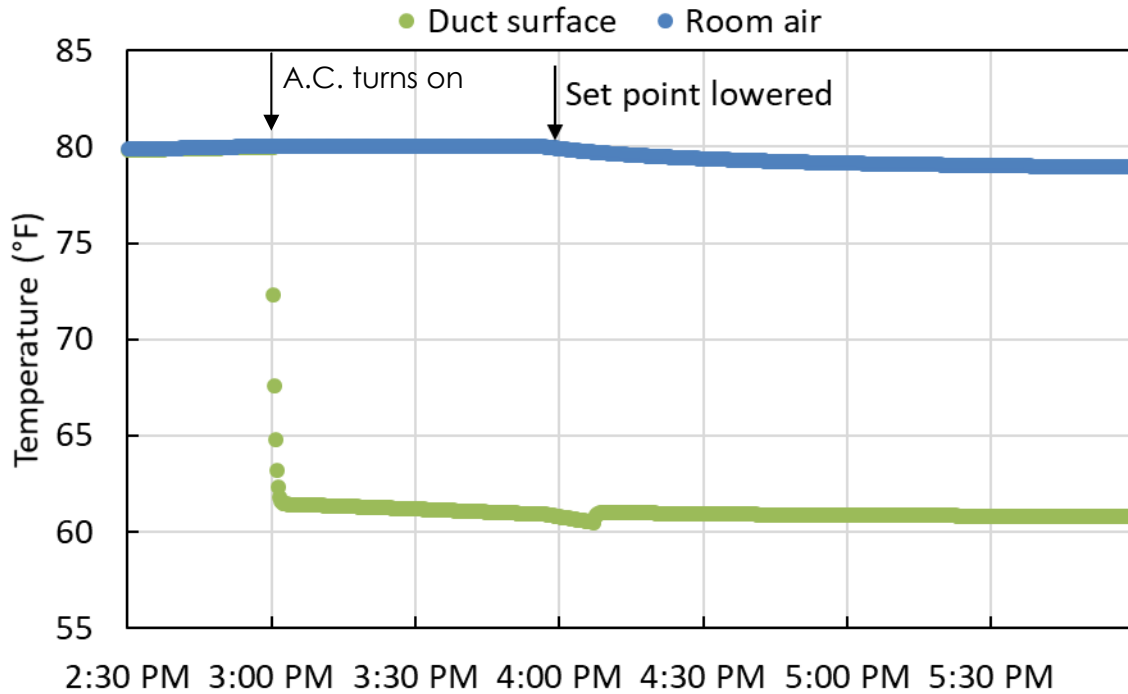


Figure 61: Surrounding air temperature and duct surface temperature for uninsulated duct surfaces with an emissivity of 0.1, and exposed completely to room air (June 30 in CZ 13).

3.5. Implications of Duct Surface Emissivity and Insulation for In-Room Ducts

The same simulation shown in Figures 60 and 61 was performed for uninsulated ducts with an emissivity of 0.9. For these ducts in Climate Zone 13 there was no condensation. The key parameter here is the surface temperature of that duct, which did not drop below 65 °F for the 0.9 emissivity case, which means that there would not be any condensation at room dewpoint temperatures below 65 °F. To determine whether there would be any condensation in any other climate zones, we need to look at the highest dewpoint temperature in those climate zones. The highest indoor dewpoint temperatures seen earlier in the report were in Burbank, which had dew point temperatures that were as high as 70°F.

In order to assess the effect of insulation on the moisture condensed, ducts with insulation were also modeled using a decoupled simplified approach. In addition to the aforementioned assumptions, it was also assumed that the surface area and dimensions of the ducts remain unchanged (not realistic, but likely okay for this simplified sensitivity analysis).

Based upon a series of additional simulations at different insulation levels, it was found the surface temperatures for in-room ducts with R-3 insulation and 0.1 emissivity, or in-space ducts with R-1

insulation and 0.9 emissivity, never dropped below 70°F, which means that any insulation level above those values would result in no condensation in any California climate.

3.6. Implications of Duct Surface Emissivity and Insulation on Cavity Ducts

The results in Table 2 were worst-case results, as they did not include any radiative heat exchange between the ducts and the cavity walls, which increases the duct surface temperature. This corresponds to assuming a surface emissivity of 0, which is not realistic in most situations. In order to assess the effects of emissivity and insulation on cavity ducts, they were modelled using the same decoupled simplified approach used for in-room ducts. As for the in-room ducts, it was also assumed that the surface area and dimensions of the ducts remain unchanged (not realistic, but likely okay for this simplified sensitivity analysis).

The results of the sensitivity runs performed at different surface emissivities, insulation levels and duct locations are summarized in Table 3. Table 3 also includes results for air-tight cavities, in which case the maximum condensation is that associated with having all of the air in the cavity reach a saturated condition at the duct surface temperature (i.e. pulling all of the moisture out of the air in the cavity, limited by that air coming into equilibrium with the duct surface).

Table 3 – Maximum mass of water on duct surface for different locations and duct characteristics for worst-case climate (Burbank – CZ-9)

Location	R-Value	Emissivity	Maximum Condensation			
			lbs	cm ³	Teaspoons	Thickness [thousandths]
In-Room	0	0.1	0.038	17	3.5	1.0
In-Room	0	0.9	0.011	4.9	1	0.3
In-Room	0.81	0.9	0	0	0	0
In-Room	3.1	0.1	0	0	0	0
Vertical Cavity	0	0.1	0.0076	3.4	0.7	0.2
Vertical Cavity	0	0.9	0.0053	2.4	0.5	0.1
Vert/Hor Cavity	3.7	0.9	0	0	0	0
Vert/Hor Cavity	7	0.1	0	0	0	0
Horizontal Cavity	0	0.1	0.0032	1.5	0.3	0.1
Horizontal Cavity	0	0.9	0.0021	1.0	0.2	0.06
Airtight Vert Cavity	Dewpoint 70°F		0.001	0.44	0.1	0.03
Airtight Vert Cavity	Dewpoint 65°F		0.0004	0.20	0.04	0.01

The results in Table 3 indicate that emissivity is an important factor with respect to the amount of condensation experienced. In all cases, lower emissivities result in larger amounts of condensation, as a higher emissivity decreases the resistance between the duct surface and its surroundings, thereby bringing the duct surface temperature closer to the warmer surroundings temperature. For in-room ducts, a low-emissivity surface increases condensation by a factor of 3.5. It therefore increases the insulation required to eliminate all condensation by about the same amount. For the vertical cavity, a low-emissivity surface only increases condensation by about 50%, the reason being that the surrounding surfaces are much colder than the room, and the amount of condensation is limited by

the flow of room air into the cavity. The low-emissivity surfaces increase the amount of insulation required to completely eliminate condensation by a factor of two in this case. Table 3 also includes results for a horizontal cavity, in which case the condensation is roughly 40% of that in a vertical cavity. This is due to the lower vertical height for the stack effect driving room air flow through the cavity, thereby reducing the total amount of room air available for condensation. Once again low surface emissivity increases condensation by roughly 50%. For the airtight cavity results in Table 3, emissivity was not considered, as in this case it is assumed that all of the moisture in the cavity air is condensed, limited by the starting dewpoint of that air. For airtight ducts with air starting out at a 70 °F dewpoint (similar to Burbank max value) the condensation is 15% to 20% of that in the vertical cavity.

4. Implications of duct surface condensation/evaporation results

Starting with the maximum mass of water condensed on the duct for the reference climate zone 13, Fresno, that condensation can be compared with other metrics in order to appreciate the magnitude of this condensation. One way to do this is to imagine that the 0.0013 lb of condensed water is absorbed by the studs surrounding the duct. The total length of 2-inch by 4-inch studs surrounding each duct that is available to absorb the moisture is 122 inches (vertical stud = 93 inches, top and bottom stud = 14.5 +14.5 in.). As the two vertical studs surrounding the cavity are shared with the adjacent cavities, the 93 inches represents half the mass of the two vertical studs enclosing the cavity ($0.5 * 2 = 1$ complete vertical stud). The calculation includes all of the mass of the top and bottom plates, which are not shared. If an eight-foot-long 2-inch by 4-inch kiln dry stud weighs 11 lb. [6], this means the full length of studs surrounding each duct weigh 14 lbs. Thus if 0.0013 lbs of water is absorbed, it would increase the gravimetric moisture content by 0.0093%. According to the American Softwood Lumber Standard [7], dry lumber has a maximum moisture content of 19% while for industry grade KD 15, 15% moisture content is generally permitted. To provide additional perspective, for 48-inch by 96-inch oriented strand board, a 1/8-inch gap is provided for expansion due to moisture absorption, and a moisture content change of up to 10% is permitted [8]. Thus, in comparison, an increase of 0.0093% is negligible.

It should also be noted that for these results the diameter of the holes at the top and bottom that allow air to leak from the room to the cavity was assumed to be 0.65 inches each, which means the area of the holes is 0.33 in² each, which is very much on the high side for stud-cavity leakage. As noted above, smaller leakage would translate to less condensation.

Even for CZ 9, Burbank, which has the highest condensation, the percentage increase in the gravimetric moisture content would be 0.058% (using data from Table 2). Although this value is much higher than that for CZ 13 Fresno, it is still negligible.

Another way to put the simulated condensation levels in perspective is to calculate the thickness of the condensed water layer on the duct surfaces. Table 3 shows that the maximum thickness of this water layer is 1 thousandth of an inch, for uninsulated ducts with a low emissivity surface, located entirely within the occupied space, and this thickness is reduced by at least a factor of 5 when the duct is in a cavity. This can be compared to the layer of water condensation on the interior surface of windows in the winter.

Yet another way to put our results in perspective would be to compare them to the interior surfaces of uninsulated exterior walls *in the winter*, which would also be exposed to warm humid indoor air due to leakage to/from the cavity and indoors. These surfaces are likely to be considerably colder than the 55°F temperatures in the ducts, and therefore experience more condensation.

Finally, it seems that although putting the ducts in the occupied space instead of in cavities increases condensation, the increase is more modest than might be predicted. Moreover, that condensation issue can be addressed by adding a modest amount of insulation, which is much easier when the duct size is not constrained by the cavity. Simply avoiding the use of low-emissivity duct surfaces eliminates condensation in CZ13 (or any other climate zone with dewpoints less than 65°F). In the worst climates (e.g. Burbank) with dew point temperatures as high as 70°F, condensation can be eliminated by using ducts with R-3 insulation and 0.1 emissivity, or ducts with R-1 insulation and 0.9 emissivity.

5. Modelling variation in thermal losses and duct delivery effectiveness for different duct insulation levels

The model used to analyze the thermal performance of uninsulated and insulated ducts was developed by the WCEC under contract to EPRI for the CEC [9] [10]. This model determines duct delivery efficiency (ratio of cooling (enthalpy) delivered at a grille to the cooling (enthalpy) entering the duct serving that grille) as a function of duct dimensions (length, diameter), duct flow, duct insulation level, the enthalpy of the air entering the duct, and the temperature of the air surrounding the duct. The model also calculates the conduction effectiveness of each duct, which only looks at the temperature of the air entering and leaving the duct, thereby providing a clearer picture of what happens to sensible cooling when capacity and flow are modified. The principal application of the model in this study was to a duct system using 3.5" diameter ducts to serve each zone/room, connected to a variable capacity heat pump. The system was modeled with four different length ducts (corresponding to four different zones to be cooled, located at different distances from the space-conditioning equipment). For the primary simulations, each zone is served by three separate equal-length ducts of 3.5" diameter, all exposed to indoor air that is entrained into vertical wall cavities (see Figure 62). It should be noted that this is a very conservative assumption, as the cavities are in this analysis assumed to be at room temperature, whereas the condensation analyses above clearly indicate that the cavity temperatures are roughly halfway between room temperature and duct temperature.

One set of simulations was performed with the same flowrate through all ducts, and another set was performed with the flowrate being determined by the length of the duct (i.e. assuming the same pressure drop across all ducts). The duct-system designs are summarized in Table 4. Simulations were performed for four different capacities (100%, 80%, 60%, 40%) and three different fan flow settings at each capacity: (a) flow scaled directly with capacity (e.g. 40% fan flow at 40% capacity), (b) 120% of direct-scaling flow, and (c) 80% of direct-scaling flow.

In addition to analyzing the overall delivery performance, the performance of the ducts serving different zones were compared, focusing on the ratio of the worst performing duct to the best performing duct. The ratio serves as a metric for how well the duct system is meeting its design intent.

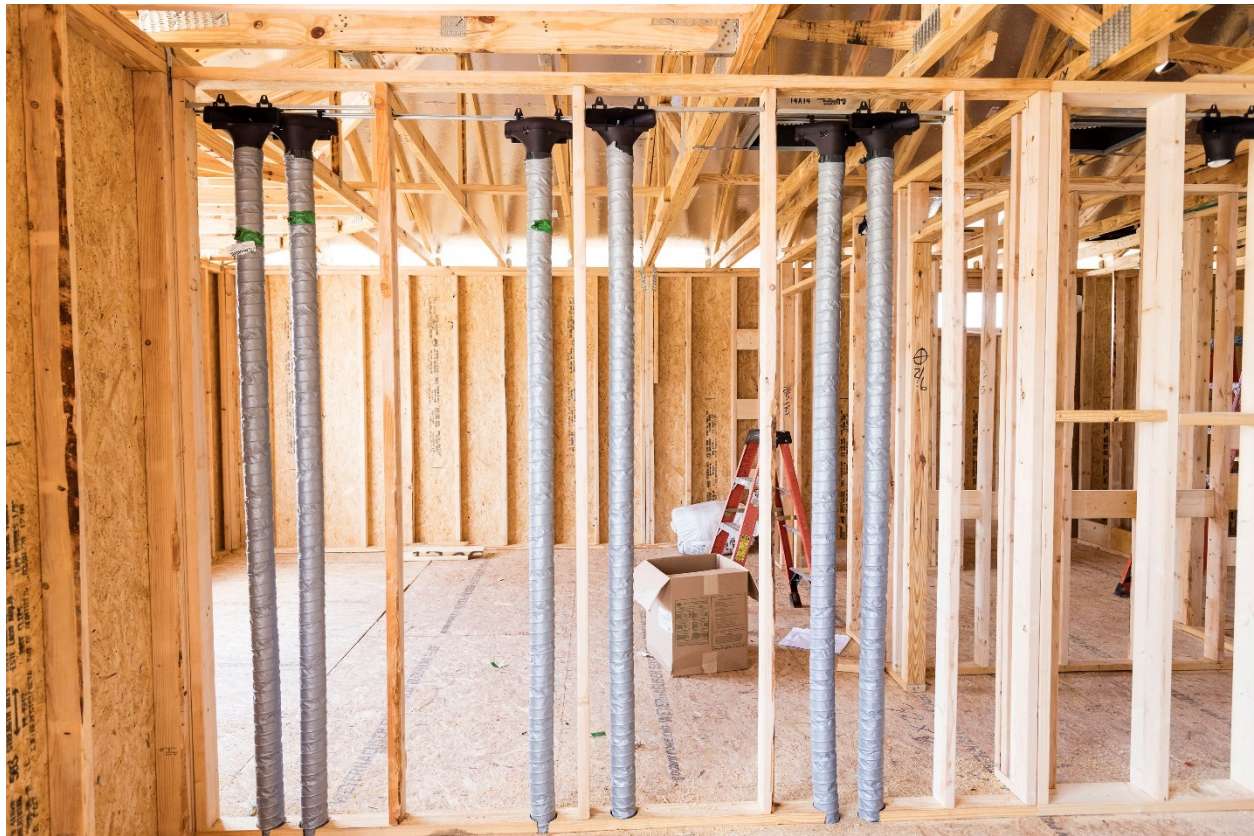


Figure 62: 3.5" diameter ducts located in vertical stud bays.

Table 4 – Duct system designs for duct delivery effectiveness simulations.

Zone	Duct	Duct Length [ft]	Nominal Flow at 100% Capacity [cfm] Equal Duct Flows	Nominal Flow at 100% Capacity [cfm] Equal Duct Pressure Differentials
1	1	15	33	48
1	2	15	33	48
1	3	15	33	48
2	1	30	33	34
2	2	30	33	34
2	3	30	33	34
3	1	45	33	28
3	2	45	33	28
3	3	45	33	28
4	1	60	33	24
4	2	60	33	24
4	3	60	33	24

A similar simulation was conducted using one 6-inch diameter instead of three 3.5-inch diameter ducts to serve the needs of each zone. From an air velocity perspective, using three small ducts with a cross-sectional area of $3 \times \pi / 4 \times 3.5^2 = 28.9 \text{ in}^2$, versus using one 6-inch diameter duct with a 28.3 in^2 cross section, these two designs are effectively equivalent. In addition, to provide a reference point, an additional simulation was performed using a traditional R-6 ducts located in a zone at $105 \text{ }^\circ\text{F}$ (mimicking a duct system in an attic during cooling).

6. Implications of thermal losses and duct delivery effectiveness for different duct insulation levels.

The average delivery effectiveness for a duct system consisting of the twelve 3.5” diameter ducts all moving the same air flow is plotted as a function of individual duct flow in Figure 63. As expected, the overall delivery effectiveness decreases as the capacity decreases, and as the duct flow decreases. This is consistent with results previously published for insulated attic ductwork [9,10].

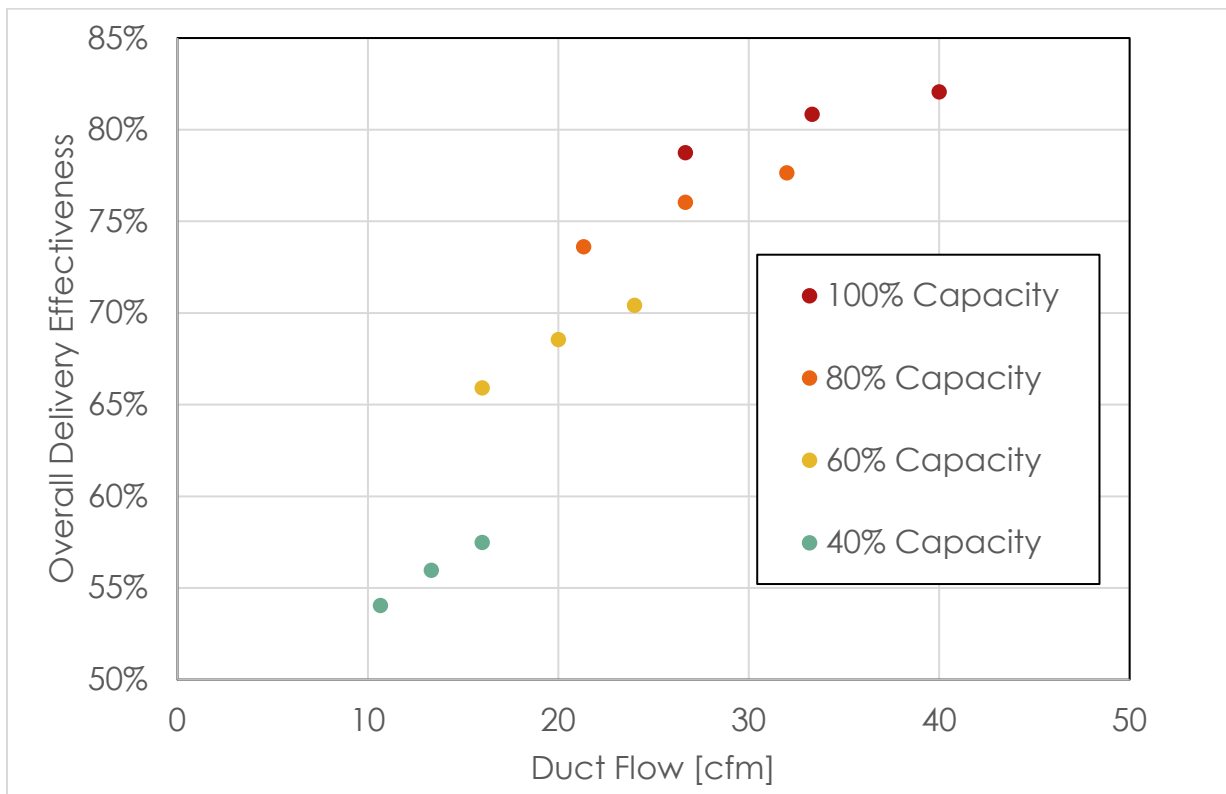


Figure 63: Overall duct system effectiveness versus individual duct flow at different levels of compressor capacity - equal flows in three 3.5” diameter ducts (in conditioned space) serving each of four zones

Figure 64 shows similar results for the conduction effectiveness for the same ductwork, in this case comparing the results for equal duct flows with equal duct pressure drops (i.e. fixed plenum pressure and no dampers). There are three key takeaways from Figure 64: a) unlike the system effectiveness, the conduction effectiveness scales smoothly with duct flow (i.e., no discontinuities), b) the conduction effectiveness is somewhat lower than the system effectiveness, and c) equal duct flows

and equal duct pressures show the same behavior (with the equal-flow values being somewhat lower), The first two takeaways are due to the fact that the system effectiveness includes latent capacity, which is not impacted by conduction losses. The third takeaway can be explained by more air being moved through longer ducts when assuming equal flow through all ducts.

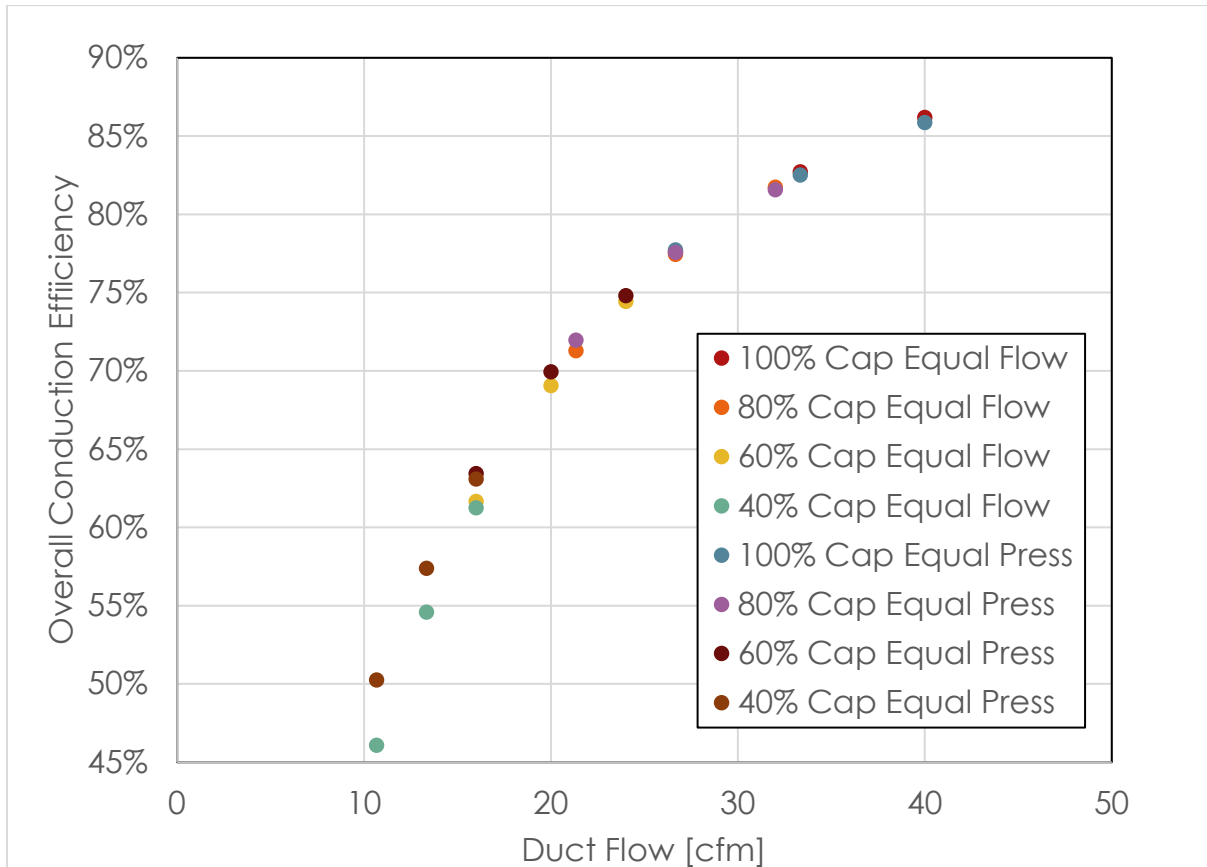


Figure 64: Overall duct system conduction effectiveness versus individual duct flow at different levels of compressor capacity - equal flows and equal pressure drops (length-based flows) in 3.5" diameter ducts in conditioned space

Figure 65 compares simulation results for 3.5" diameter uninsulated ducts with the performance of uninsulated 6-inch diameter ducts. As expected, having one six-inch diameter duct per zone results in better cooling delivery as compared to running three 3.5" diameter ducts for each zone. Although the duct lengths are the same in both cases, the duct surface area is considerably larger for the 3.5-inch ducts (total circumference of $3 \times \pi \times 3.5 = 33$ inches versus $\pi \times 6 = 19$ inches), thereby leading to larger conduction losses for the 3.5-inch ducts. It should be noted that all of these results are based upon the ducts being fully exposed to indoor air conditions, despite the fact that the 3.5" diameter ducts would be located in vertical stud cavities, and that the 6" diameter ducts would not fit in vertical stud cavities. Modelling the effect of the stud cavities would on balance decrease the thermal losses for the 3.5-inch ducts. The cooler temperatures in the cavities would decrease thermal losses,

however the fin effect associated with the ducts being in direct contact with the sheetrock would increase losses. On balance, the performance of ducts in cavities should be better than what is calculated for ducts completely within the occupied space. It should be noted that Figure 65 utilizes zone flow instead of duct flow (used in Figure 64). Zone flows are used to allow for direct comparison of 3.5 inch and 6-inch ducts.

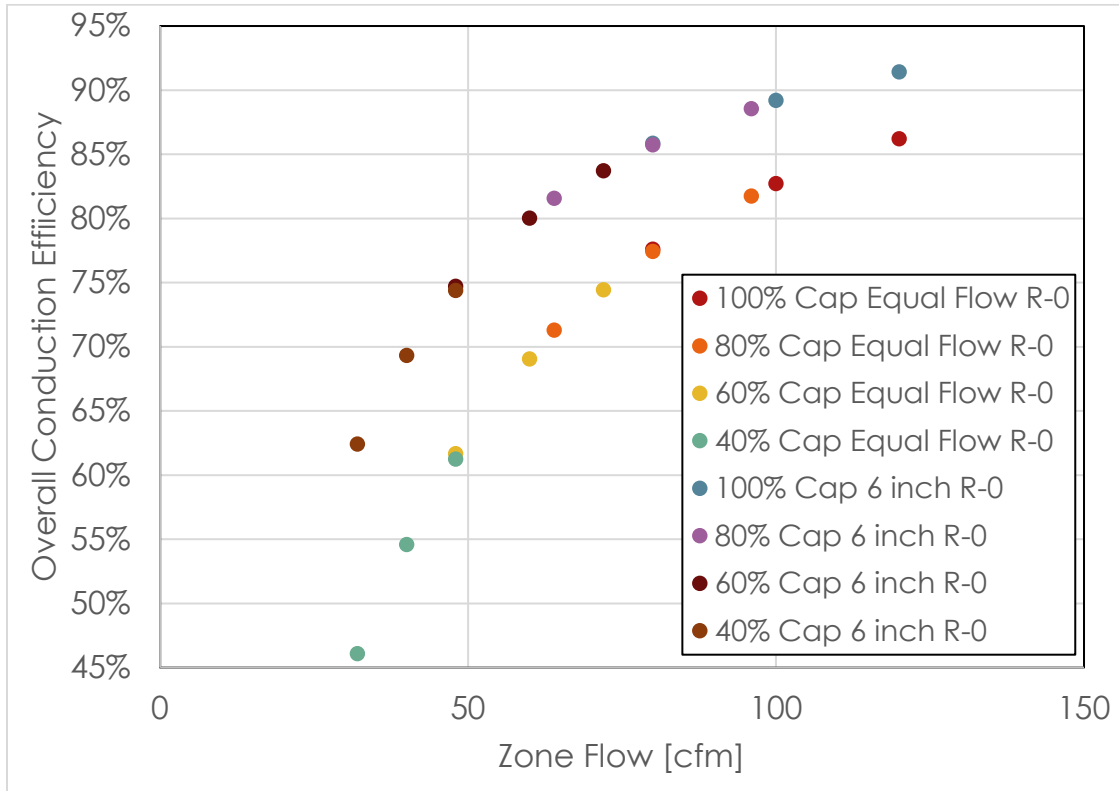


Figure 65: Overall duct system conduction effectiveness versus individual zone flow at different levels of compressor capacity - equal flows in three 3.5" diameter ducts per zone, and equal flows in single 6" ducts for each zone

It needs to be emphasized that the duct losses in Figures 63 through 65 are to conditioned spaces, and therefore do not represent losses of energy from the house. That said, the purpose of a duct system is to distribute heating or cooling to each zone in a house according to the load calculated for that zone., as if the duct system does not distribute well, there will be comfort problems, which can turn into energy inefficiencies depending upon how those comfort problems are addressed. For example, if the thermostat setting needs to be lowered to keep the far rooms cool, the other zones will be over-cooled, and energy use will increase. To this end, we need to characterize how well a duct system distributes heating/cooling. For this report, that effect is characterized by the ratio of the performance of the longest duct to the performance of the shortest duct.

Figure 66 shows the ratio of the worst-performing to best-performing ducts for different operating conditions for uninsulated 3.5-inch diameter ducts (at different equipment capacities and zone flow rates). Figure 66 clearly demonstrates that both duct flow and equipment capacity have dramatic impacts on the degree to which a duct system distributes heating and cooling uniformly to the zones. A ratio of one would correspond to perfectly uniform cooling distribution. As expected, the non-

uniformity is worse at low flowrates and capacities, dropping as low as 15% at 40% equipment capacity and 32% of maximum duct flow.

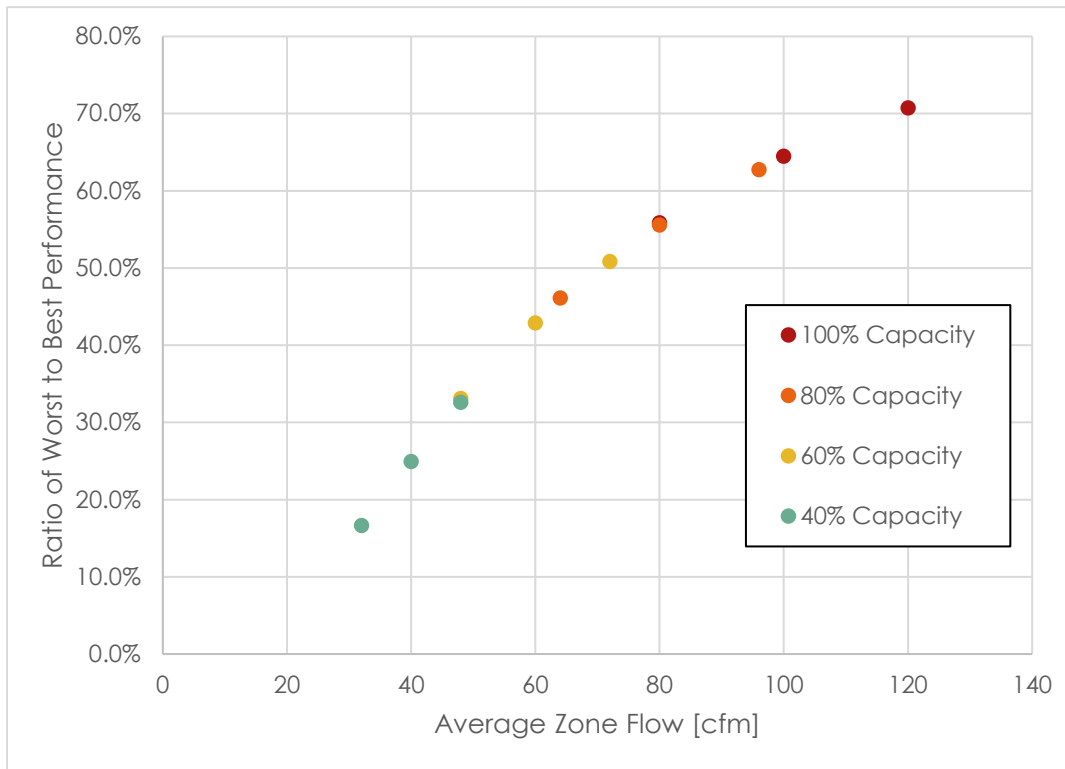


Figure 66: Ratio of worst duct performance to best duct performance versus individual duct flow at different levels of compressor capacity and length-based flows in uninsulated 3.5" diameter ducts

To examine the impact of adding insulation, the worst-to-best ratio impacts of adding R-2 insulation to 3.5-inch diameter ducts are shown in Figure 67. For comparison purposes, the performance of uninsulated 6-inch diameter ducts is also shown in that figure. In brief, adding R-2 insulation does improve performance, but not by as much as using one 6-inch diameter duct instead of three 3.5-inch diameter ducts. Once again, 3.5-inch ducts located in a cavity will perform better than if those ducts are completely in the room.

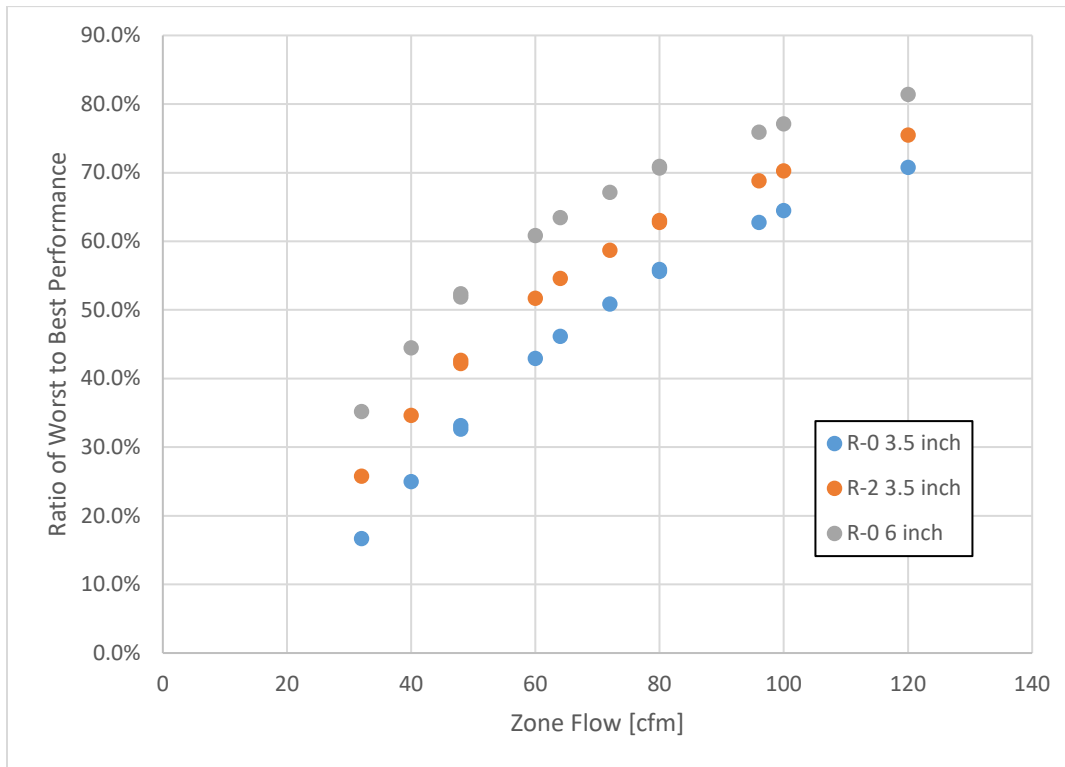


Figure 67: Ratio of worst duct performance to best duct performance versus average zone flow at different levels of compressor capacity (length-based flows in uninsulated 3.5" diameter ducts, 3.5" diameter ducts with R-2 insulation, and uninsulated 6" diameter ducts)

Finally, to put the performance of uninsulated interior duct systems into perspective, the performance of a similarly designed and controlled 6-inch diameter R-6 duct system located in an attic was also simulated. The results of that simulation are compared with the simulation results for two types of uninsulated ducts located in the conditioned space in Figure 68. In brief, the worst-to-best performance of the uninsulated interior ducts is comparable to a typical R-6 duct system located in an attic.

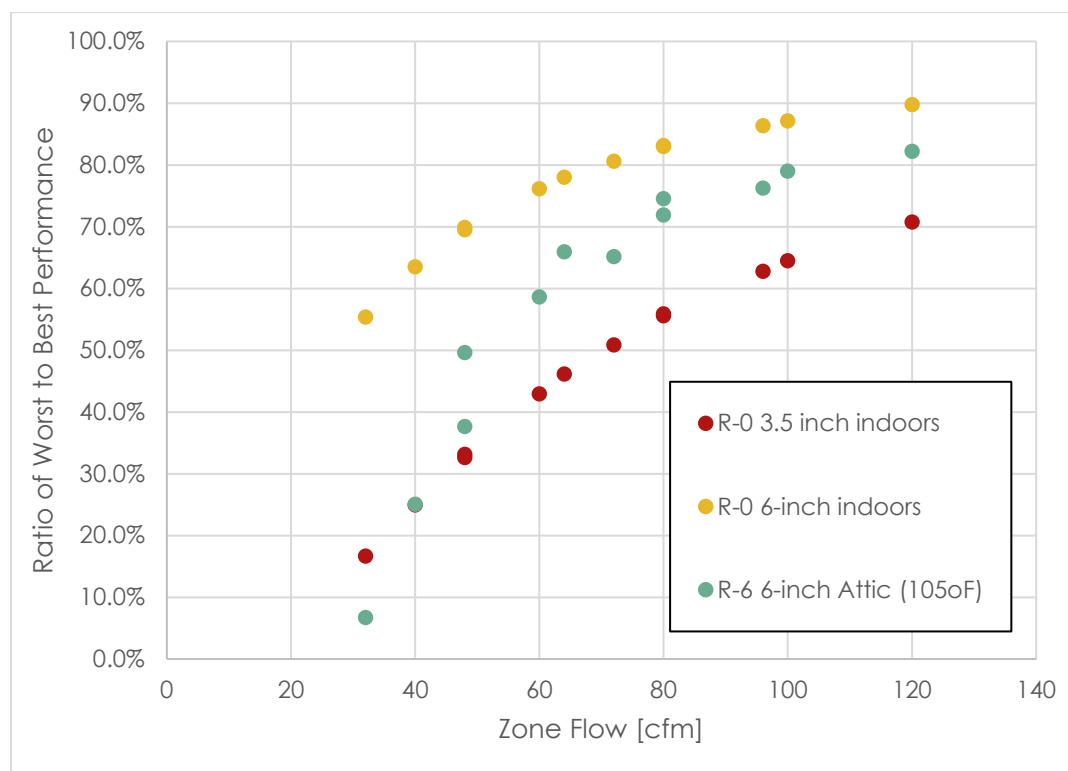


Figure 68: Ratio of worst duct performance to best duct performance versus average zone flow at different levels of compressor capacity for different duct systems - length-based flows in uninsulated indoor 3.5" diameter ducts, uninsulated indoor 6" diameter ducts, R-6 6" diameter ducts in an attic (105°F)

7. Conclusions and Recommendations

Based on the analyses performed the authors conclude that condensation of water on duct surfaces is not likely to be a major issue for uninsulated ducts located in wall cavities in California homes. The worst-case maximum condensation of water on a duct in a relatively leaky vertical stud cavity (5/8th inch diameter holes top and bottom) was 3.4 cubic centimeters of water in Burbank, California for a duct surface emissivity of 0.1. This condensation corresponds to 0.0076 lbs of water (0.7 teaspoons) in a vertical stud cavity, or a 0.06% change in the moisture content of the wood in that stud cavity, whose moisture content typically ranges between 7% and 15%. Putting this into perspective, the maximum thickness of condensation on the duct surface is 0.2 thousandths of an inch, and all condensation evaporates within 5 hours. Another way to put this amount of condensation in perspective is to compare it to condensation on windows in the winter. Yet another relevant comparison is with the interior surfaces of uninsulated exterior walls in the winter, which would also be exposed to warm humid indoor air. These surfaces are likely to be considerably colder than the 55°F temperatures in the ducts, and therefore experience more condensation.

Turning to our sensitivity analysis, simply using ducts with a standard emissivity of 0.9 reduces this maximum condensation by 30%. In addition, this condensation is reduced by roughly another factor

of two for horizontal cavities (due to less height for driving room air through the cavity). Finally, since the moisture available for condensation comes from air being brought into the cavity from the room, the total condensation is controlled by the flowrate of room air into the cavity, which means that there will be less condensation in tighter cavities. In the limit, for an airtight cavity the maximum 0.0076 lbs of water condensation is reduced by roughly 90%. One recommendation might be to forbid low-emissivity surfaces on ducts in cavities.

Relative to the condensation issue, the impact of locating the ducts in the occupied space rather than in cavities was also examined. The simulations indicate that the quantity of water condensed on uninsulated in-space ducts with low emissivity surfaces ($\epsilon=0.1$) was five times higher than that for cavity ducts. For ducts with standard emissivity surfaces ($\epsilon=0.9$) the condensation was only twice as high in-space, suggesting that emissivity has a larger impact on in-space ducts. This level of condensation might or might not be acceptable, as it might be visible and/or dripping might occur in wetter climates (e.g. Burbank). That said, simply avoiding low-emissivity surfaces eliminated the possibility of condensation in Climate Zone 13 (Fresno). Going to R-3.1 insulation for low-emissivity ducts ($\epsilon=0.1$), or going to R-0.8 insulation for normal-emissivity ducts ($\epsilon=0.9$) in the occupied space avoids the possibility of condensation in any climate zone (including Burbank), due to duct surfaces never being cooler than 70°F.

Turning to the thermal performance of uninsulated ducts in conditioned spaces, it appears that they exhibit thermal-distribution inefficiencies similar to insulated ducts running through an attic, although the performance of uninsulated interior ducts may be somewhat worse at full capacity. In both cases, slowing down the fan and reducing cooling capacity result in significant degradation of distribution performance. It should be noted however that the losses for the interior ducts wind up in the conditioned space, although not necessarily where intended.

8. Acknowledgements

We would like to thank Kelly Cunningham and Pacific Gas and Electric for funding this research.

9. Nomenclature

L: vertical length (ft) (SI units: m)

d: diameter (ft) (SI units: m)

A: area (ft²) (SI units: m²)

h: heat transfer convection coefficient (BTU h⁻¹°F⁻¹ft⁻²) (SI units: Wm⁻²K⁻¹)

h_m: mass transfer coefficient (lb. h⁻¹ ft⁻²) (SI units: kg m⁻²s⁻¹)

h_{fg}: latent heat of vaporization (BTU lb⁻¹) (SI units: J kg⁻¹)

R: thermal resistance (°F h BTU⁻¹) (SI units: KW⁻¹)

c: specific heat capacity (BTU lb⁻¹ °F⁻¹) (SI units: J kg⁻¹ K⁻¹)

C: heat capacity (BTU °F⁻¹) (SI units: J K⁻¹)

ρ: density (lb ft⁻³) (SI units: kg m⁻³)

T: Temperature (°F) (SI units: K)

Δt: time-step (h) (SI unit: s)

ṁ: mass flow rate (lb. h⁻¹) (SI unit: kg s⁻¹)

q: heat transfer rate (BTU h⁻¹) (SI units: W)

μ: viscosity (lb. ft⁻¹ h⁻¹) (SI units: Pa s)

v: velocity (ft h⁻¹) (SI units: m s⁻¹)

Re: Reynolds number (dimensionless)

Pr: Prandtl number (dimensionless)

Ra: Rayleigh number (dimensionless)

Gr: Grashof number (dimensionless)

Subscripts:

d: duct surface

di: air inside the duct

c: air inside the stud bay cavity

s: sheet-rock

r: air inside the room

10. References

- [1] California Energy Commission, "CBECC-Res Compliance Software Project," [Online]. Available: <http://www.bwilcox.com/BEES/cbecc2013.html>. [Accessed November 2020].
- [2] California Energy Commission, "2013 Residential Alternative Calculation Method- Approval Manual," California Energy Commission, Sacramento, 2012.
- [3] F. P. Incropera, A. S. Lavine, T. L. Bergman and D. P. Dewitt, *Fundamentals of Heat and Mass Transfer*, 7th Edition ed., Jefferson City: John Wiley & Sons, 2011.
- [4] Stoecker and Jones, *Refrigeration and Air Conditioning*, New York: McGraw-Hill, 1982.
- [5] u.-y. Yu, K.-d. Song and a. D.-w. Cho, "Resolving Stack Effect Problems in a High-Rise Office Building by Mechanical Pressurization," September 2017. [Online]. Available: <http://www.mdpi.com/2071-1050/9/10/1731/pdf>. [Accessed September 2020].
- [6] The Engineering Toolbox, "Lumber weights," [Online]. Available: https://www.engineeringtoolbox.com/green-kiln-dried-pressure-treated-lumber-weights-d_1860.html. [Accessed 5 November 2020].
- [7] U.S. Department of Commerce, "American Softwood Lumber Sandard," pp. 20-70, 1970.
- [8] J. Wiehagen and V. Kochkin, "High-R Walls for Remodeling: Wall Cavity Moisture Monitoring," U.S. Department of Energy, Oak Ridge, 2012.
- [9] S. Krishnamoorthy, M. Modera and C. Harrington, "Efficiency Optimization of a Variable-Capacity/Variable-Blower-Speed Residential Heat-Pump System with Ductwork," *Energy and Buildings*, vol. 150, no. (1), pp. 294-306, 2017.
- [10] S. Krishnamoorthy, M. Modera and C. Harrington, "Improving System Efficiency for a Variable-Capacity / Variable-Blower-Speed Residential Heat-Pump System with Multi-zone Ductwork," *Science and Technology for the Built Environment*, 2018.